University of Sussex

A field theoretical description of quantum black holes

Dionysios Fragkakis

Submitted for the degree of Doctor of Philosophy

University of Sussex

May 2013

Declaration

I hereby declare that this thesis has not been and will not be submitted in whole or in part to another University for the award of any other degree.

Signature:

Dionysios Fragkakis

UNIVERSITY OF SUSSEX

Dionysios Fragkakis, Doctor of Philosophy

A field theoretical description of quantum black holes

Summary

The subject of this thesis is the description of quantum black holes as a way to probe quantum gravity. Scenarios of a lower Planck scale make quantum gravity experimentally approachable, therefore a theoretical framework is needed in order to be able to probe quantum gravitational effects. We present a field theoretical formalism for the treatment of quantum black holes and their interactions with particles of the Standard Model. We examine the properties and assumptions governing quantum black holes and develop a methodology to examine their behavior using quantum field theory language. We apply our formalism in several different cases and calculate the cross sections for the production of quantum black holes. We use our results to gain phenomenological insights to quantum gravity, such as the derivation of bounds for the Planck mass from Standard Model processes. The distinction between a continuous and a discrete mass spectrum, for a quantum black hole, is discussed and the relevant cross sections presented. Finally, we use quantum black holes as a gateway to supersymmetry and calculate the branching ratios for the decay of quantum black holes into supersymmetric particles.

Acknowledgements

I would like to thank my supervisor Xavier Calmet for his guidance during this DPhil project. I would also like to thank the members of the TPP group: Mark Hindmarsh, Daniel Litim, Stephan Huber, Sebastian Jaeger, David Bailin and Norman Dombey for their direct or indirect support and inspiration. I express my gratitude towards my colleagues: Nina Gausmann, Ting-Cheng Yang, Michael Atkins, Kostas Nikolakopoulos, Kevin Falls, Edouard Marchais, Ippokratis Saltas and Dimitris Skliros for useful discussions and for sharing their knowledge. Finally, I thank my friends and family for their encouragement during the writing of this thesis.

Contents

List of Tables

List of Figures

Chapter 1

Introduction

An important problem of theoretical physics is the unification of quantum mechanics and general relativity. Quantum mechanics typically describes physics in the microscopic level, which is the scale where we examine elementary particles and their interactions. General relativity on the other hand deals with massive energy scales and describes objects such as black holes and other astronomical phenomena. For the most part these two theories have little to do with each other, each focusing on an entirely different regime than the other. However, there are instances where both theories are called into action simultaneously, at an energy scale typically associated with the Planck scale. Specifically, situations such as the earliest stages of the universe or singularities demand a treatment that doesn't ignore either theory. Thus we are inclined to develop a theory that accurately describes the quantum behavior of gravity.

Towards this effort we focus our research on the study of quantum black holes, one of the most fascinating aspects of quantum gravity. We will discuss extensively what quantum black holes are, but one can define them as small black holes where quantum effects have to be taken into account. By their definition, they are objects with a strong gravitational field and a quantum behavior. Therefore, they are considered the ideal paradigm to study aspects of quantum gravity. One of the driving forces behind our work is the fact that they could be experimentally relevant, a condition that until recently was deemed impossible. Particle accelerators such as the Large Hadron Collider and cosmic rays entering the atmosphere could now be the environment where quantum black holes form and decay.

This thesis is organized according to the projects undertaken during the DPhil program from 2010 to 2013. They roughly follow a chronological order.

- We start with a short review of the theoretical background on which we expanded to

produce our work. We present the basic concepts and tools of general relativity and quantum field theory. We proceed with the classical and semiclassical production of black holes which paves the way for the quantum case. We note the similarities and differences and examine the necessary assumptions to produce meaningful results. We briefly review the literature on quantum black holes, their characteristics and the phenomenology produced thus far. Lastly, we discuss the ways used to lower the Planck scale to a more approachable value, an essential step in making predictions for the detection of quantum black holes in experiments like the ones taking place at the Large Hadron Collider.

- In chapter 3 we develop our methodology and discuss how we produce an effective way of describing quantum black holes and their interactions with particles of the Standard Model. Using our formalism, we calculate the cross section for the production of quantum black holes from the collisions of fermions. We use our framework to derive bounds for the Planck scale by considering flavor physics phenomena in the domain of quantum black holes. These include the anomalous magnetic moment of the muon, lepton flavor violation, electric dipole moment and finally proton decay.

- In chapter 4 we briefly review research on the fundamental nature of space, whether it is continuous or not. Our interest in this is connected to the nature of the mass spectrum of a quantum black hole. We present arguments made in favor of the existence of a minimal length and how this is connected to a discrete mass spectrum for a quantum black hole. Our expansion on the literature is to produce cross sections for the production of a quantum black hole in both the continuous and discrete case for the Large Hadron Collider.

- We continue our work in chapter 5, where we examine quantum black holes with spin and color created from the collisions of quarks and gluons. We further develop our methodology and illustrate its advantages and its possible applications. The effective nature of our formalism is made evident as is the practical use of our results.

- Finally, in chapter 6 we delve more into the phenomenology of quantum black holes, specifically their possible connection to supersymmetric particles. We argue that quantum black holes can serve as a gateway to supersymmetry. We calculate branching ratios for the decay of quantum black holes to supersymmetric particles, that interact gravitationally with the Standard Model, and in fact find an enhancement for the production of superpartners via quantum black holes.

- The thesis ends with a concluding chapter, summarizing our work and highlighting our results.

The purpose of this thesis, apart from presenting the results of our research, is to inspire creative thinking when facing the many problems of quantum gravity and hopefully serve as a step towards the next level of understanding the fundamental properties of nature, both in theory and experiment.

Chapter 2

Theoretical Background

In this section we present the literature on which our research is based. We aim to describe quantum black holes and their interactions in order to probe aspects of quantum gravity. Therefore we review the basics of general relativity and classical black holes as well as quantum field theory as the language we will use in our analysis. We discuss small black holes created from the collision of energetic particles in the classical, semiclassical and finally quantum case and review the phenomenology of quantum black hole production. We also present bounds on the Planck mass from the literature which can act as a basis for comparison with our results in chapter 3.

2.1 General Relativity

2.1.1 Einstein's field equations

General relativity is a theory first proposed by Albert Einstein in 1916 as an effort to unify his special theory of relativity with gravity. It introduced the groundbreaking viewpoint of gravity as a geometric property of spacetime and describes how the curvature of spacetime is affected by the presence of energy and matter. The main mathematical result of general relativity is Einstein's field equations, which can be derived from the Einstein-Hilbert action[1] :

$$S = \int \left(\frac{1}{2\kappa} R + L_M \right) \sqrt{-g} d^4x, \tag{2.1}$$

where $\kappa = 8\pi G c^{-4}$, R is the Ricci scalar, g is the determinant of the metric tensor and L_M is the term for any appropriate matter fields. We vary the action with respect to the inverse metric and demand that the variation is zero from the action principle.

$$\delta S = \int \left[\frac{1}{2\kappa} \frac{\delta(\sqrt{-g}R)}{\delta g^{\mu\nu}} + \frac{\delta(\sqrt{-g}L_M)}{\delta g^{\mu\nu}} \right] \delta g^{\mu\nu} d^4x = \tag{2.2}$$

$$= \int \left[\frac{1}{2\kappa} \left(\frac{\delta R}{\delta g^{\mu\nu}} + \frac{R}{\sqrt{-g}} \frac{\delta\sqrt{-g}}{\delta g^{\mu\nu}} \right) + \frac{1}{\sqrt{-g}} \frac{\delta(\sqrt{-g}L_M)}{\delta g^{\mu\nu}} \right] \delta g^{\mu\nu} \sqrt{-g} d^4x = 0 \tag{2.3}$$

This is true for any variation of the inverse metric, therefore we can deduce that:

$$\frac{\delta R}{\delta g^{\mu\nu}} + \frac{R}{\sqrt{-g}} \frac{\delta\sqrt{-g}}{\delta g^{\mu\nu}} = -2\kappa \frac{1}{\sqrt{-g}} \frac{\delta(\sqrt{-g}L_M)}{\delta g^{\mu\nu}}, \tag{2.4}$$

where

$$-2\kappa \frac{1}{\sqrt{-g}} \frac{\delta(\sqrt{-g}L_M)}{\delta g^{\mu\nu}} \propto T_{\mu\nu}, \tag{2.5}$$

is the stress-energy tensor. We still need the variation of the Ricci scalar and the determinant of the metric, which are given by:

$$\frac{\delta R}{\delta g^{\mu\nu}} = R_{\mu\nu} \tag{2.6}$$

$$\frac{1}{\sqrt{-g}} \frac{\delta(\sqrt{-g})}{\delta g^{\mu\nu}} = -\frac{1}{2} g_{\mu\nu}. \tag{2.7}$$

Adding up all the components we get Einstein's field equations [1]:

$$R_{\mu\nu} - \frac{1}{2} g_{\mu\nu} R = \frac{8\pi G}{c^4} T_{\mu\nu}. \tag{2.8}$$

They are more commonly written as:

$$G_{\mu\nu} + g_{\mu\nu}\Lambda = 8\pi T_{\mu\nu}, \tag{2.9}$$

where we have input the Einstein tensor

$$G_{\mu\nu} = R_{\mu\nu} - \frac{1}{2} R g_{\mu\nu}, \tag{2.10}$$

introduced a cosmological constant Λ and chose units where $G = c = 1$.

2.1.2 Basic properties

General relativity redefined fundamental concepts of physics. Instead of considering a gravitational force as the responsible mechanism for acceleration, we now perceive the apparent acceleration as an inertial motion in a curved spacetime [1]. At the same time the curvature is caused by the energy-momentum of the matter. To coin John Archibald Wheeler "spacetime tells matter how to move, matter tells spacetime how to curve" [2]. With that in mind, phenomena such as the deflection of light near a massive object are easily explained. Light doesn't need to have mass to experience gravity. Instead, it follows a curved path determined by the presence of matter.

A great advantage of general relativity is its strong mathematical foundations. Since it is a theory built using tensors, it satisfies general covariance, meaning that all laws derived in the theory are independent of the choice of coordinate systems. Additionally, since the theory is background independent all laws are the same for all frames of reference, a requirement which is called the general principle of relativity [1]. Lastly one of the most important properties of general relativity is Einstein's equivalence principle which states that "The outcome of any local non-gravitational experiment in a freely falling laboratory is independent of the velocity of the laboratory and its location in spacetime" [3].

2.1.3 Effects of general relativity

General relativity has predicted a plethora of phenomena, some of which we have already observed or tested experimentally, while others are still under investigation. We list the most important ones [1].

- Apsidal precession: One of the first triumphs of general relativity was the explanation of the anomalous perihelion shift of the planet Mercury. According to general relativity the apsides of any orbit will precess within its orbital frame.

- Gravitational time dilation: In general relativity gravity changes the passage of time. Specifically, time slows down when we examine a process near a massive object compared with the same process taking place in an empty background. A direct result of this is the gravitational frequency shift. Light approaching a gravity well is blueshifted, while light leaving a gravity well is redshifted.

- Light Deflection: As mentioned earlier light is subject to gravity and will be deflected when in the area of a massive object. A direct consequence of light deflection is the

gravitational time delay, which describes how light will take longer to traverse an area with a gravitational field than an area without one.

- Gravitational waves: An important prediction of general relativity, that hasn't been directly observed yet, gravitational waves are ripples in the curvature of spacetime that propagate at the speed of light.

- Orbital Decay: If we examine a binary system, we expect to see the distance between the two bodies decrease due to loss of energy from the emission of gravitational waves. This was the first indirect observation of gravitational waves in 1974, from the study of the binary pulsar PSR1913+16.

- Gravitational Lensing: A consequence of light deflection, gravitational lensing is the phenomenon we observe when a massive object blocks from our line of sight a source of light. The deflection of light will have as a result the appearance of multiple copies of the hidden source. Due to the curvature of spacetime light will travel around the massive object and appear at different places.

- Black Holes: One of the most fascinating predictions of general relativity, and the one we are interested in, is the formation of black holes from the gravitational collapse of matter.

2.2 Black Holes

The prediction of black holes is perhaps the most intriguing result of general relativity. There has been extensive research associated with black holes and their behavior. Although not directly visible, there are strong signs from observations that they exist, based on the study of phenomena that take place in their vicinity, such as the accretion of gas clouds or the orbits of stars or bigger stelar formations around them. In fact, supermassive black holes are believed to exist in the center of galaxies like our own Milky Way [1]. They could be simply described as a region of space, or more accurately spacetime, where gravity is so strong that not even light can escape. The first solution of Einstein's field equations to indicate a black hole was derived by Karl Schwarzschild in 1916 [1].

2.2.1 The Schwarzschild solution

The Schwarzschild solution constitutes the first exact solution of Einstein's field equations (apart from the trivial flat space solution) [1]. It assumes a spherically symmet-

ric and static spacetime and postulates a vacuum solution. The solution describes the gravitational field outside a spherical, non-rotating mass with no electric charge and no cosmological constant.

In Schwarzschild coordinates, the line element for the Schwarzschild metric is given by [1]:

$$c^2 d\tau^2 = \left(1 - \frac{r_s}{r}\right) c^2 dt^2 - \left(1 - \frac{r_s}{r}\right)^{-1} dr^2 - r^2(d\theta^2 + sin^2\theta d\phi^2), \tag{2.11}$$

where τ is the proper time, c is the speed of light, t is the time coordinate, r_s is the Schwarzschild radius ($r_s = 2Gm/c^2$) and r, θ, ϕ are the usual spherical coordinates. This solution is called a Schwarzschild black hole, with the Schwarzschild radius defining the event horizon, the surface boundary of a black hole. The problematic value $r = 0$ defines a gravitational singularity and will be discussed in the next section. The Schwarzschild solution is strengthened by Birkhoff's theorem which states that "any spherically symmetric solution of the vacuum field equations must be static and asymptotically flat" [4]. There are other solutions of Einstein's field equations describing more complicated black holes. For instance, there is the Kerr metric for a rotating black hole, while charged black holes are described by the Reissner-Nordstrom metric. The aspect we are interested in is that Einstein's field equations can be solved in ways that predict the existence of black holes.

2.2.2 Properties of black holes

Black holes are characterized by their mass, electric charge and angular momentum. This is due to the no-hair theorem [1], which implies that all other information regarding the formation or the contents of a black hole disappears inside the black hole and is irretrievable. It was once again John Archibald Wheeler that coined the phrase "black holes have no hair" [2]. A direct consequence of this statement is that any two black holes that have the same mass, charge and angular momentum are indistinguishable. It is advantageous that these three properties can all be determined from outside the black hole by analyzing the interactions of the black hole with its surroundings otherwise such a statement wouldn't be very useful.

As we mentioned earlier black holes are defined by the fact that past a certain point nothing can escape their gravitational field, not event light. The surface around the black hole that determines the point of no return is called the event horizon [1]. The name implies that any events that take place inside the black hole will be contained there and

no information about them will ever reach us. For a non-rotating black hole the event horizon is the surface of a sphere of radius r_s, while for a rotating black hole the surface is an oblate spheroid. Classically the event horizon is an absolute barrier, in the sense that nothing comes out. As we will see later on with the introduction of quantum effects the event horizon becomes quite an interesting area.

The most exotic property of black holes is the gravitational singularity [1], which according to general relativity lies at the center of black holes. Even describing what happens there doesn't make physical sense since general relativity (and quantum mechanics) breaks down and we can't discuss any meaningful physics. The spacetime curvature becomes infinite, the metric blows up and we are left with a point of infinite density since all the mass is concentrated at an area of zero volume. In Schwarzschild black holes the singularity is a space-like surface in spacetime, while in rotating black holes it takes the shape of a ring. Physically it can be said that singularities at the center of black holes are similar to the supposed singularity at the very beginning of the universe. Our current understanding dictates that neither general relativity or quantum mechanics is enough to describe a singularity and the circumstances call for a theory of quantum gravity. This makes sense since the energy scale of what we perceive as a singularity is that of quantum gravity. Therefore, we believe that such a treatment of the problem will cure the shortcomings when describing the center of black holes and eliminate singularities.

Black holes are also characterized by other surfaces with interesting effects. We briefly mention the photon sphere [1], which is defined as the surface around the black hole where photons tend to travel in unstable orbits. Photons crossing the photon sphere with an inbound trajectory will be captured by the black hole, while photons crossing it with an outbound trajectory will escape its gravitational well. It has a spherical shape with a characteristic radius 1.5 times the Schwarzschild radius. In rotating black holes there is also a region called the ergosphere [1], which is defined as a region of spacetime in which it is impossible to stand still, with respect to infinity. It has an oblate spheroidal shape and connects with the event horizon at the poles defined by the rotation.

2.2.3 Formation of black holes

Now that we have given an overview of the main properties of black holes, we can discuss the physics behind their formation. Einstein's field equations predict their existence but we still have to address how they come to be. Depending on their mass and size black holes can form from astronomical gravitational collapse or high energy collision of particles.

Gravitational collapse is the end result of the battle between pressure and gravity of a star [1]. Typically, it is a process with several stages. As soon as gravity dominates it forces the mass of the object to become more condensed. This leads to an increase in temperature and pressure which could initiate new processes, that until then didn't have the required conditions to begin. This can then lead to an explosion as big as a supernova. If the remaining parts are massive enough, gravity will eventually dominate again and the process will repeat. The end result is a compact star that depending on the initial mass could be a white dwarf, a neutron star or a black hole. The whole journey towards a black hole can be more complicated. For instance after an explosion, where the star has lost a significant portion of its mass, it is possible that the star replenishes its mass supply by accreting mass from a nearby gas cloud. That could be enough to change the fate of the star from a neutron star to a black hole. The cutoff for the creation of a black hole after such an event is the Tolman-Oppenheimer-Volkoff limit [1] and has a value of about 3 to 4 solar masses. Despite their exotic nature, the method behind the creation of black holes is not very special. Essentially, a sufficiently massive star collapses under its own gravity.

A more spectacular, albeit speculative, way of creating black holes is the collision of two very energetic particles [6]. We should note that these would take place at a very different scale. Instead of solar masses we are now talking about subatomic particles. The main principle stays the same though. The density has to be high enough for a black hole to form. One would expect quantum effects to play an important role and indeed that is the case. These are the black holes discussed in this thesis, but before we explore them we will briefly review the necessary tools for their analysis, the language of quantum field theory.

2.3 Quantum field theory

Quantum field theory is one of the pillars of modern physics. It is not a theory by itself, but a theoretical framework for constructing theories combining quantum mechanics with principles of relativity. In quantum field theory, particles are treated as excited states of fields. These fields are quantum superpositions of states and the interactions between particles correspond to interactions between the underlying fields [5]. Since fields are continuous over space, there can be a large number of particles in the excited states, which has as a result the emergence of infinite degrees of freedom. These tend to be problematic by leading to divergences in calculations. We usually employ tools like renormalization and discretization of spacetime to cure these divergences and produce meaningful results.

The language of quantum field theory has been used to produce theories such as quantum electrodynamics (with an electron and a photon field), quantum chromodynamics (with one field for each type of quark) and of course the Standard Model. Using perturbative methods we are able to identify the fundamental forces and the mediating particles. For instance, in quantum electrodynamics, the particle responsible for the electromagnetic force between two electrons is the photon. For the weak force we have the W and Z bosons and for the strong force, in quantum chromodynamics, we have the gluons. Despite the great success of quantum field theory, it has been unable to produce a theory for gravity, for which the mediating particle would be the graviton.

There are mainly two methods of constructing a quantum field theory, canonical quantization and the path integral approach. We will point out their main points, without going into a full analysis, which would be quite lengthy.

2.3.1 Canonical quantization

Quantization is the process of quantizing a classical theory. The term canonical has to do with the Hamiltonian approach to classical mechanics, wherein variables (typically position and momentum) can be inserted in Poisson brackets. Historically we define the first quantization as the stage where particles are treated as quantum objects, while background fields are treated clasically. Quantum field theories use the second quantization in order to describe many-particle systems where the fields are also quantized.

The first fields to be quantized were free fields (not interacting), such as the Dirac field. While useful in developing tools for quantum field theory, the analysis of free fields was just a prelude to interacting fields, like the ones found in quantum electrodynamics or Yukawa theory. Since no interacting field theory is exactly solvable (at least in more than two spacetime dimensions), we invoke perturbation theory to help us come close to exact results. The methodology is quite simple and it essentially treats the interaction term H_{int} in the Hamiltonian as a perturbation.

We begin by considering a simple two-point correlation function [5]:

$$\langle \Omega | T\phi(x)\phi(y) | \Omega \rangle \,, \tag{2.12}$$

where $|\Omega\rangle$ is the ground state of the interacting thory and T is a time-ordering symbol. The physical meaning of a correlation function is simply the amplitude for the propagation of a particle between x and y. Through rigorous analysis the above expression can be reduced to [5]:

$$\langle 0|T\phi(x)\phi(y)|0\rangle\,, \tag{2.13}$$

where $|0\rangle$ is the ground state of the free theory. Wick's theorem allows us to turn such an expression into a sum of products of Feynman propagators [5], typically illustrated in Feynman diagrams. Therefore, for a n-point correlation function we can write [5]:

$$\langle\Omega|T[\phi(x_1)\cdots\phi(x_n)]|\Omega\rangle = (\text{sum of all connected diagrams with n external points}) \tag{2.14}$$

What we ultimately want is a way to calculate cross sections and decay rates, which can then be applied to collider events. The cross section is a way to express the probability of getting any particular final state from the interaction of initial states. To do that we identify the initial particles as wavepackets, evolve the initial state with the time-evolution operator of the interacting field $exp(-iHt)$, and overlap the final states with wavepackets for the desired final-state particles [5]. We want to calculate the following probability:

$$P = |\,\langle\phi_1\phi_2\cdots|\phi_A\phi_B\rangle\,|^2, \tag{2.15}$$

where $\phi_{A,B}$ represent the initial states and $\phi_{1,2}$ the final states. This expression is related to a set of transition amplitudes between the *in* and *out* states of definite momentum [5],

$$\langle p_1p_2\cdots|k_Ak_B\rangle\,. \tag{2.16}$$

To calculate the overlap of *in* and *out* states we write:

$$\langle p_1p_2\cdots|k_Ak_B\rangle = \lim_{T\to\infty}\left\langle p_1p_2\cdots|e^{-iH(2T)}|k_Ak_B\right\rangle = \langle p_1p_2\cdots|S|k_Ak_B\rangle\,, \tag{2.17}$$

where S is the S-matrix. If we impose momentum conservation we get [5]:

$$\langle p_1p_2\cdots|iT|k_Ak_B\rangle = (2\pi)^4\delta^{(4)}(k_A+k_B-\Sigma p_f)\dot{i}M(k_A,k_B\to p_f), \tag{2.18}$$

where M the invariant matrix element is defined by the above expression. The matrix element is used for the calculation of cross sections. The symbol T can be thought as the non-trivial interacting part of the S-matrix. After further analysis we get an expression for cross sections:

$$d\sigma = \frac{1}{2E_A 2E_B |u_A - u_B|} \left(\Pi \frac{d^3 p_f}{(2\pi)^3} \frac{1}{2E_f} \right) \times |M|^2 (2\pi)^4 \delta^{(4)}(p_A + p_B - \Sigma p_f), \tag{2.19}$$

where p_A, p_B, E_A and E_B are the momenta and energies of the initial wavepackets, p_f and E_f represent *out* states of definite momentum formed in the asymptotic future and $|u_A - u_B|$ is the relative velocity of the two beams that carry the wavepackets.

The above expression simplifies considerably. What is important is the relation between the cross section and the matrix element. Using equation 2.14 and a bit of algebra, we reach the conclusion that the matrix element can be calculated from Feynman Diagrams. One has just to look up the Feynman rules for the specific setup and that's it. The above discussion is obviously very short, but it should illustrate the main line of thought for calculating cross sections, something that is done repeatedly in this thesis.

2.3.2 Path integral formulation

The path integral approach is a very important tool of quantum field theory. It generalizes the action principle for quantum mechanics and uses the Lagrangian (instead of the Hamiltonian) as the fundamental quantity, preserving all symmetries of the theory. The name stems from the functional integral used to calculate a quantum amplitude. Instead of the classical view of a particle following a single trajectory to go from one set of coordinates to another, we now sum all the possible trajectories between the two points. If we define the coordinates as q^i and the conjugate momenta p^i we can write the transition amplitude [5]:

$$U(q_a, q_b; T) = \left\langle q_b | e^{-iHT} | q_a \right\rangle, \tag{2.20}$$

where U is the amplitude for a transition from q_a to q_b in time T. We split the time interval into N parts of duration ϵ,

$$e^{-iHT} = e^{-iH\epsilon} e^{-iH\epsilon} \cdots e^{-iH\epsilon} \tag{2.21}$$

and insert a complete set of intermediate states between these factors,

$$\mathbf{1} = \left(\Pi \int dq_k^i \right) |q_k\rangle \langle q_k|. \tag{2.22}$$

Doing that for $k = 1 \ldots (N-1)$ and taking $\epsilon \to 0$ we get [5]

$$\langle q_{k+1}|e^{-iH\epsilon}|q_k\rangle \to \langle q_{k+1}|(1-iH\epsilon+\cdots)|q_k\rangle \tag{2.23}$$

Assuming that H is Weyl ordered [5] the above expression changes to:

$$\langle q_{k+1}|e^{-i\epsilon H}|q_k\rangle = \left(\Pi\int\frac{dp_k^i}{2\pi}\right)exp\left[-i\epsilon H\left(\frac{q_{k+1}+q_k}{2},p_k\right)\right]\times exp\left[i\Sigma p_k^i(q_{k+1}^i-q_k^i)\right] \tag{2.24}$$

If we multiply for N factors and integrate over the intermediate coordinates q_k we get:

$$U(q_a,q_b;T)=\left(\Pi\int Dq(t)Dp(t)\right)exp\left[i\int_0^T dt\left(\Sigma p^i q^i-H(q,p)\right)\right], \tag{2.25}$$

where $\int Dq(t)$ and $\int Dp(t)$ are the path integrals. As in the canonical quantization case this can be related to the two-point correlation function. Then one can proceed and rederive Feynman rules for any theory. The expression that connects path integrals to correlation functions is:

$$\langle\Omega|T\phi_H(x_1)\phi_H(x_2)|\Omega\rangle=\lim_{T\to\infty(1-i\epsilon)}\frac{\int D\phi\phi(x_1)\phi(x_2)exp\left[i\int_{-T}^T d^4xL\right]}{\int D\phi exp\left[i\int_{-T}^T d^4xL\right]}. \tag{2.26}$$

Another useful relation in the path integral formulation is the generating functional of correlation functions [5]:

$$Z[J]=\int D\phi exp\left[i\int d^4x(L+J\phi)\right], \tag{2.27}$$

which changes the previous expression into:

$$\langle 0|T\phi(x_1)\phi(x_2)|0\rangle = Z[J]^{-1}\left(-i\frac{\delta}{\delta J(x_1)}\right)\left(-i\frac{\delta}{\delta J(x_2)}\right)Z[J]|_{J=0} \tag{2.28}$$

Although the presentation of the basic formulae of quantum field theory in this section was rather short, it nevertheless illustrates the main tools for constructing a quantum field theory. Depending on the theory, one needs only to construct the appropriate Feynman rules, with methods like the path integral formulation, and then we are able to calculate quantities that are more realistic (closer to experiments), such as cross sections and decay rates. In turn the results of such calculations can be applied phenomenologically to test the theory or improve it.

After reviewing the basics of general relativity, black holes and quantum field theory, we will now focus more on the production of small black holes from particle collisions. Having started from classical astronomical black holes we will review the literature for classical small black holes (which is essentially general relativity for small black holes), continue with semiclassical black holes, where we start to take quantum effects into consideration, and conclude with quantum black holes, black holes for which a theory of quantum gravity is required in order to accurately describe them.

2.4 Classical production of small black holes

The prospect of forming a black hole in a high energy collision of two particles has been thoroughly studied [6, 7, 8, 9, 10, 11] . In particular Eardley and Giddings have calculated estimates of the classical cross-section for black hole production in a D-dimensional spacetime and the black hole mass [6], used both in the semiclassical and quantum cases. The first estimate of the cross section for black hole production given in [12, 13] is

$$\sigma \sim \pi r_h^2(\sqrt{s}), \tag{2.29}$$

where r_h is the horizon radius corresponding to center of mass energy $\sqrt{s}$. D'Eath and Payne [8, 9, 10, 11] considered the case of zero impact parameter b and went on to find a closed trapped surface, necessary for the creation of a black hole. Their calculations produced a lower bound of $M > \sqrt{s/2}$ and an estimate of $M \approx 0.84\sqrt{s}$ for the mass of the black hole. Eardley and Giddings used the same methods as D'Eath and Payne, [8, 9, 10, 11] but extended the analysis for $b \neq 0$. Penrose [7] examined both cases, $b = 0$ and $b \neq 0$, but never published his results.

Each incoming particle is treated as a point particle that carries along with it a gravitational shock wave. These shock waves are arranged in such a way as to simulate two colliding surfaces. When they collide the two shock waves pass through one another and interact nonlinearly by shearing and focusing [6]. For the purpose of simplicity the high-energy collisons are taking place in a D-dimensional flat space, which turns out to be a good approximation. It should be noted that Eardley and Giddings discuss TeV-scale gravity scenarios with the usual assumptions they entail, in order to talk about realistic detection of black holes. These will be presented in detail in the relevant section.

A coordinate system is defined $(\overline{u}, \overline{v}, \overline{x}^i)$ where retarded and advanced times $(\overline{u}, \overline{v})$ are $(\overline{t} - \overline{z}, \overline{t} + \overline{z})$ in terms of Minkowski coordinates, where $\overline{z}$ is the direction of motion and $\overline{x}^i$

are the transverse coordinates, where $i = 1...D-2$ [6]. As stated previously the impact parameter is b and the particles are initially incoming along $\overline{x}^i = (\pm b/2, 0, ..., 0)$. In order to derive a solution, the rest-frame solution is boosted, taking the limit of large boost and small mass with fixed total energy μ, where $\mu = \sqrt{s}/2$, the energy of each of the high-energy particles in the center of mass frame. The D-dimensional Schwarzschild solution with mass M is

$$ds^2 = -\left(1 - \frac{16\pi GM}{(D-2)\Omega_{D-2}}\frac{1}{r^{D-3}}\right)dt^2 + \left(1 - \frac{16\pi GM}{(D-2)\Omega_{D-2}}\frac{1}{r^{D-3}}\right)^{-1} dr^2 + r^2 d\Omega_{D-2}^2, \tag{2.30}$$

where $d\Omega_{D-2}^2$ is the line element and Ω_{D-2} is the volume of the unit $D-2$ sphere. The Aichelburg-Sexl solution [14] for a particle moving in the $+z$ direction is

$$ds^2 = -d\overline{u}d\overline{v} + d(\overline{x}^i)^2 + \Phi(\overline{x}^i)\delta(\overline{u})d\overline{u}^2, \tag{2.31}$$

where Φ takes the form:

$$\Phi = -8G\mu ln(\overline{\rho}), D = 4 \tag{2.32}$$

$$\Phi = \frac{16\pi G\mu}{\Omega_{D-3}(D-4)\overline{\rho}^{D-4}}, D > 4 \tag{2.33}$$

where $\overline{\rho} = \sqrt{\overline{x}^i\overline{x}_i}$ is the transverse radius.

It is noteworthy that Φ satisfies Poisson's equation:

$$\nabla^2\Phi = -16\pi G\mu\delta^{D-2}(\overline{x}^i). \tag{2.34}$$

The construction of a solution for $D = 4$ is rigorous and is presented in detail in [6]. The main results are outlined below. The maximum value for the impact parameter for which a black hole is produced is:

$$b_{max} \approx 3.219\mu. \tag{2.35}$$

For that value, the lower limit of the cross section is

$$\sigma_{bhproduction} \geq \pi b_{max}^2 \approx 32.552(G\mu)^2. \tag{2.36}$$

Finally, a lower bound for the mass of the black hole is calculated as a function of the impact parameter b

$$M \approx 0.71\sqrt{s}, b = 0 \tag{2.37}$$

$$M \approx 0.45\sqrt{s}, b = b_{max}. \tag{2.38}$$

These results, stemming from the classical treatment of the problem, will be the basis for the next step in the process, the semiclassical production of black holes.

2.5 Semiclassical black hole production

The discussion of Eardley and Giddings treats the problem of the collision of two high-energy particles in the context of general relativity. In the process of going from the classical to the quantum environment, one has to introduce the language of quantum field theory. This was done by Stephen D. H. Hsu, when he applied a path integral formalism to black hole production [15] . This method was first introduced in [16, 17] and was used in addressing baryon number violation in the electroweak theory. In [16] T. M. Gould, S. D. Hsu and E. R. Poppitz calculate the expression for the S-matrix describing the transition from an initial two particle state to a final state, in other words what we try to simulate as two particles creating a black hole. In [17] Stephen D. H. Hsu estimated the amplitude for the process $|i\rangle \rightarrow |f\rangle$ to be

$$\langle f|S|i\rangle \sim \int d\phi_i d\phi_j D\phi \Psi_i[\phi(T_i)]\Psi_f^*[\phi(T_f)]e^{iS[\phi]}, \tag{2.39}$$

where $d\phi_i d\phi_j$ represent the path integrals, $T_{i,f}$ indicate the fluctuations of the fields in the asymptotic past and future and the wave-functionals $\Psi_{i,f}$ measure the overlap of the initial and final states with $\hat{\phi}$ eigenstates at asymptotic times. If we take the limit $T_{i,f} \rightarrow \pm\infty$, the above expression reduces to just the S-matrix. The process of calculating the S-matrix semiclassically, while considering the initial and final states in the extremization, was dubbed the GHP procedure (from the initials of the authors), and it boils down to a

boundary value problem with the boundary conditions fixed by the initial and final states with the usual equations of motion.

The modifications to the path integral formalism in order to describe the production of a black hole are minimal. Specifically, following [15] we replace ϕ with the metric $g_{\mu\nu}$ along with the appropriate matter fields. The gravitational action $S_g = \int d^4x\sqrt{-g}R$ is still valid and the action could be expressed in terms of a surface integral over Bondi masses [18]. For the S-matrix to be meaningful we have to assume asymptotically flat spacetimes in the far past and future and consider black holes as excitations. In order to do that we define semiclassical black hole states as those with a strong resemblence with the trajectories of classical black holes. This way the issue of creating a black hole from a two-particle initial state is connected to the solution of the boundary problem. Not surprisingly the cross section for the production of a black hole closely matches that of the geometrical case πr^2, a result that will prove useful in the quantum analysis of the problem.

It is now well established that semiclassical black holes are not very similar to their quantum analogs, nevertheless it is useful to point out their main characteristics and see later on how these change at the quantum level. One thing they have in common is that in order to realistically produce them, the presence of extra dimensions is required [19]. This will be discussed in the following section explicitly, for now we list it as a requirement needed for the observation of small black holes. Semiclassical black holes typically have a mass a few times larger (from 5 to to 20 times as large) than the scale of quantum gravity, where we can no longer ignore their quantum behaviour. We treat semiclassical black holes as thermal objects that emit Hawking radiation [20]. They decay in a relatively large number of particles and evaporate completely. It is evident that trying to treat this process with the language of quantum field theory would be rather difficult, since the number of final states would complicate things. Fortunately that is not the case for quantum black holes as we will see later on. Unfortunately, it has now been estimated that semiclassical black holes will not be produced at the Large Hadron Collider, due to the fact that the center of mass energy is not high enough [27]. While this is disheartening, the same is not true for quantum black holes, which we hope to observe at collider events or in cosmic rays.

2.6 Quantum production of black holes

2.6.1 What are quantum black holes

In the simplest sense, quantum black holes are very small black holes, for which quantum effects have to be taken into account. In the microscopic world of particle physics they could be described as gravitationally bound states and have little in common with astronomical black holes. Under a set of assumptions, they are expected to form in high energy particle collisions that take place in particle accelerators or when cosmic rays enter the atmosphere. As in the classical case, in order for a quantum black hole to form, there has to be a sufficient concentration of matter or energy to create a region, defined by the Schwarzschild radius, from which the escape velocity exceeds the speed of light. The classical analog of this requirement, for general relativity is the hoop conjecture [22]. Ideally, quantum black holes and their behaviour would be described by a theory of quantum gravity, a theory that would accurately describe gravity at the microscopic level. Since a complete theory of quantum gravity is a work in progress we take an alternate route. We extrapolate from the classical case to the quantum environment and try to gain insight into their phenomenological implications, which in turn can be used to help develop a full quantum gravity theory.

2.6.2 Lowering the Planck scale

As we pointed out in the previous sections a necessary requirement for the production and possible observation of quantum black holes is lowering the Planck scale to the order of a few TeV which is the energy scale probed by the Large Hadron Collider and cosmic rays observations. Normally the Planck scale is of the order 10^{18} GeV which makes it impossible to conduct any sort of meaningful experiment or observation. The Planck scale is the energy regime where quantum gravitational effects become dominant and where a theory of quantum gravity, whatever that may be, operates. However, in their seminal papers [24] Nima Arkani-Hamed, Savas Dimopoulos, Gia Dvali and in a slightly different and refined version Lisa Randall and Raman Sundrum [25] proposed a radical way to achieve a Planck scale comparable to the weak scale., by introducing large extra dimensions. There has also been an interesting approach on the same issue without the use of extra dimensions proposed by Xavier Calmet, Stephen D. H. Hsu and David Reeb that instead makes use of the renormalization of Newton's constant [26, 27], achieving the same result, making quantum gravity accesible by current technology. What follows is a

brief review of this very important work that makes it possible for us to discuss quantum black hole phenomenology and probe gravity at the quantum level.

Arkani-Hamed et al. first considered large extra dimensions in order to address the hierarchy problem, specifically why the electroweak scale is so much smaller than the Planck scale. The troublesome relation $m_{EW}/M_{Pl} \sim 10^{-17}$ has greatly troubled physicists and has been one of the main focus points of theories beyond the Standar Model. The authors proposed the idea that there are n extra spatial dimensions of radius $\sim R$, arranged in such a way that $M_{Pl(4+n)} \sim m_{EW}$. The first result produced by this hypothesis is a modified gravitaional potential, derived from Gauss's law in $(4+n)$ dimensions

$$V(r) \sim \frac{m_1 m_2}{M_{Pl(4+n)}^{n+2}} \frac{1}{r^{n+1}}, (r \ll R) \tag{2.40}$$

$$V(r) \sim \frac{m_1 m_2}{M_{Pl(4+n)}^{n+2} R^n} \frac{1}{r}, (r \gg R) \tag{2.41}$$

so the effective 4 dimensional M_{Pl} is

$$M_{Pl}^2 \sim M_{Pl(4+n)}^{2+n} R^n \tag{2.42}$$

Demanding $M_{Pl(4+n)} \sim m_{EW}$ gives

$$R \sim 10^{\frac{30}{n}-17} \text{ cm } \times \left(\frac{1 \text{ TeV}}{m_{EW}} \right)^{1+\frac{2}{n}} \tag{2.43}$$

In this setup the Standard Model particles cannot propagate in the extra dimensions and have to remain localized to a 4 dimensional manifold. This is a result of the fact that the Standard Model gauge forces have been studied sufficiently at weak scale distances while gravity has not. The only fields propagating freely in the $(4+n)$ bulk are the $(4+n)$ dimensional gravitons. The 4-dimensional M_{Pl} is not considered a fundamental scale any more and the electroweak scale emerges as the only fundamental scale. In this framework, gravity is comparable to the gauge forces at the electroweak scale. This was the first proposal that made quantum gravity approachable with current means and methods and opened up a torrent of exciting new prospects.

When the novel idea of introducing extra dimensions to solve the hierarchy problem (and coincidentally make the detection of quantum black holes possible) came out, there was a huge interest from the scientific community and a lot of physicists used it as the

basis for their research. Lisa Randall and Raman Sundrum on the other hand presented a refined version [25] of the same idea with a different setup in order to improve it. Starting from the hypothesis that spacetime is higher dimensional with $4+n$ spacetime dimensions the 4-dimensional M_{Pl} is given by

$$M_{Pl}^2 = M^{n+2} V_n, \tag{2.44}$$

where V_n is the volume of the compact space attributed to the extra dimensions. Their main argument for changing the setup provided by [24] was that although in that setup the hierarchy between the weak scale v and the Planck scale M_{Pl} is cured, a new hierarchy between v and the compactification scale $\mu_c \sim 1/V_n^{1/n}$ is introduced. They instead proposed [25] that the metric is not factorizable, but rather the four-dimensional metric is multiplied by a "warp" factor which is a rapidly changing function of an additional dimension. This can be written as

$$ds^2 = e^{-2kr_c\phi}\eta_{\mu\nu}dx^\mu dx^\nu + r_c^2 d\phi^2, \tag{2.45}$$

where k is a scale of order the Planck scale, x^μ are coordinates for the familiar four dimensions and $0 \leq \phi \leq \pi$ is the coordinate for an extra dimension, which is a finite interval whose size is set by r_c. The "warp" factor $e^{-2kr_c\phi}$ is an exponential function of the compactification radius, therefore there is no need for a very large r_c. The main difference from [24] is that the hierarchy between the five-dimensional Planck scale and the compactification scale, $\mu \equiv 1/r_c$ is only of order 50, instead of $(M_{Pl}/TeV)^{2/n}$. Also there is only one extra dimension introduced instead of $n \geq 2$. The result of this spacetime configuration is that the scale at which gravity becomes strong can be quite low.

The previous paradigms depend exclusively on the existence of extra dimensions, large or otherwise, to lower the Planck scale at the TeV range. An alternative method was developed by Xavier Calmet, Stephen D. H. Hsu and David Reeb which examines the renormalization of Newton's constant as a way to achieve the same result. In this scenario no extra dimensions are required. The authors argue that Newton's constant G ($G = M_{Pl}^{-2}$ in natural units $\hbar = c = 1$) could be scale dependent [26]. With that assumption, the scale μ_* at which quantum gravity effects become important is one at which

$$G(\mu_*) \sim \mu_*^{-2}. \tag{2.46}$$

Since gravity has only been tested at distances greater than that corresponding to an energy scale of 10^{-3}eV, it can be argued that theories consinsting of particles with masses greater than this scale or theories of modified gravity could result in the running of Newton's constant. As in the case of extra dimensions scenarios, the hierarchy problem is solved and quantum gravity becomes an experimental reality. Following [27] , if we start from the action

$$S = \int d^4x\sqrt{-g}\left(-\frac{1}{16\pi G}R + \frac{1}{2}g^{\mu\nu}\partial_\mu\phi\partial_\nu\phi\right) \tag{2.47}$$

and consider the gravitational potential between two heavy, non-relativistic sources due to graviton exchange, the leading term in the gravitational Lagrangian is $G^{-1}R \sim G^{-1}h\Box h$ with $g_{\mu\nu} = \eta_{\mu\nu} + h_{\mu\nu}$. By keeping G out of the small fluctuations h we can interpret quantum corrections to the graviton propagator as a renormalization of G. The graviton propagator with one-loop correction is

$$D_h(q) \sim \frac{iG}{q^2} + \frac{iG}{q^2}\Sigma\frac{iG}{q^2} + \ldots, \tag{2.48}$$

where q is the momentum carried by the graviton. The term in Σ proportional to q^2 can be interpreted as a renormalization of G and is given from the Feynman diagram

$$\Sigma \sim -iq^2\int^{\Lambda} d^4pD(p)^2p^2 + \ldots, \tag{2.49}$$

where $D(p)$ is the propagator of the particle in the loop. If we consider a scalar field for the calculation the loop integral is quadratically divergent so we redefine G to absorb this and using the heat kernel method we get the expression

$$\frac{1}{G_{ren}} = \frac{1}{G_{bare}} + c\Lambda^2, \tag{2.50}$$

where Λ is the ultraviolet cutoff of the loop and $c \sim 1/16\pi^2$.

The running of the reduced Planck mass due to scalar fields, Weyl fermions and vector bosons can be deduced from the running of Newton's constant to be

$$\bar{M}(\mu)^2 = \bar{M}(0)^2 - \frac{1}{16\pi^2}\left(\frac{1}{6}N_l + 2\xi N_\xi\right)\mu^2, \tag{2.51}$$

where μ is the renormalization scale and $N_l = N_S + N_F - 4N_V$ where N_S,N_F and N_V are the numbers of real, minimally coupled, scalar fields, Weyl fermions and vector bosons

in the model and N_ξ is the number of real scalar fields in the model with a non-minimal coupling to gravity.

The scale at which quantum gravitational effects become important, μ_* is given by the requirement that the reduced Planck mass at this scale be comparable to $\bar{M}(\mu_*) \sim \mu_*$. This leads to

$$\mu_* = \frac{\bar{M}(0)}{\sqrt{1 + \frac{1}{16\pi^2}\left(\frac{1}{6}N_l + 2\xi N_\xi\right)}}. \tag{2.52}$$

In order to obtain $\mu_* = 1\text{TeV}$ there has to be a large hidden sector of scalars and Weyl fermions with approximately 10^{33}particles. Alternatively, we could consider a real scalar field than is non-minimally coupled with $\xi \sim 10^{32}$. It is noteworthy that the mumber of degrees of freedom introduced in this scenario is similar to that in the theories with extra dimensions.

2.6.3 Characteristics of quantum black holes

After giving a short review of the necessary requirements for the production of quantum black holes, we will now discuss the properties of these black holes and their general behaviour. We will talk about what parameters we use to define them, certain core assumptions for their creation, their expected cross section, the group theory setup and finally their decay widths.

As we already mentioned, quantum black holes are treated as non-thermal objects, meaning they decay into only a few particles not following Hawking decay [20] and typical black hole thermodynamics. This is an important deviation from the semiclassical case, where black holes are expected to decay isotropically to many energetic particles. If we consider inelasticity and black hole entropy, the multiparticle final states are very suppresed due to the fact that only black holes that are produced well above threshold have sufficient entropy [28]. And while black hole production increases with energy, the falling parton distribution functions overcompensate for that increase. Therefore, almost all events where gravity is strong will occur at the lowest possible energy scale. Quantum black holes will decay to a few particles, each with Compton wavelength of order the size of the black hole.

We define quantum black holes using three main quantities: their mass, spin and gauge charges and list two central assumptions [29].

I) “Processes involving quantum black holes conserve QCD and U(1) charges since

local gauge symmetries are not violated by gravity".

We should note that this assumption does not extend to global charges. To better understand why we make this assumption and believe it to be true, imagine a large Gaussian 2-sphere surrounding the spatial region where quantum black holes are created and then decay. By causality, the total flux through this sphere is constant, which implies a conservation of charge. An immediate consequence of this assumption is that quantum black holes can be classified according to representations of $SU(3)_c$ and $U(1)_{em}$.

II) "Quantum black hole coupling to long wavelength and highly off-shell perturbative modes is supressed".

We require this assumption in order to prohibit the quantum gravity scale to be much larger than the TeV range in precision measurements such as the anomalous magnetic moment of the muon [30] or proton decay. It is likely that a nonperturbative quantum black hole state couples weakly to long distance or highly off-shell modes and strongly to modes of similar energy to that of the black hole. We should note that Lorentz invariance is not listed as a central assumption. In the case where quantum gravity violates Lorentz invariance we expect assumption (II) to suppress such effects. Our results will depend on whether we require that quantum black hole processes correspond to Lorentz invariant, local effective field theory operators.

2.6.4 Phenomenology

As we mentioned earlier one of the great advantages of quantum black holes is that they are expected to form at energies of a few TeV. Such energies are accessible at experiments taking place at the Large Hadron Collider and in cosmic rays entering the atmosphere. The detection of quantum black holes would give us a unique opportunity to study aspects of quantum gravity, as well as validate theories that lower the Planck scale.

Large Hadron Collider

We assume that the cross section for the production of quantum black holes can be extrapolated by the cross-section for semiclassical black holes [31]

$$\begin{aligned}\sigma^{pp}(s, x_{min}, n, M_D) &= \int_0^1 2zdz \int_{\frac{(x_{min}M_D)^2}{y(z)^2 s}}^1 du \int_u^1 \frac{dv}{v} \\ &\times F(n)\pi r_s^2(us, n, M_D) \sum_{i,j} f_i(v, Q) f_j(u/v, Q)\end{aligned} \tag{2.53}$$

where $z = b/b_{max}$, $x_{min} = M_{BH,min}/M_D$, n is the number of extra dimensions, u and v are dummy variables that represent the fractions of momenta carried by each parton, s is a Mandelstam variable, $F(n)$ and $y(z)$ are the factors inroduced by Eardley and Giddings, $f_i(v,Q), f_j(u/v,Q)$ are the parton distribution factors and

$$r_s(us, n, M_D) = k(n) M_D^{-1} [\sqrt{us}/M_D]^{1/(1+n)} \tag{2.54}$$

is the n dimensional Schwarzschild radius, where

$$k(n) = \left[2^n \sqrt{\pi}^{n-3} \frac{\Gamma((3+n)/2)}{2+n} \right]^{1/(1+n)}, \tag{2.55}$$

M_D is the reduced Planck mass and $M_{BH,min}$ is defined as the minimal value of black hole mass for which the semiclassical extrapolation is valid. Since we will be referring to Mandelstam variables throughout this thesis we should quickly define them. In a particle interaction where p_1, p_2 and p_3, p_4 are the momenta of the incoming and outgoing particles respectively, the Mandelstam variables are defined by the following formulae:

$$s = (p_1 + p_2)^2 = (p_3 + p_4)^2 \tag{2.56}$$

$$t = (p_1 - p_3)^2 = (p_2 - p_4)^2 \tag{2.57}$$

$$u = (p_1 - p_4)^2 = (p_2 - p_3)^2 \tag{2.58}$$

Calmet et al. argue that quantum black holes are not expected to have high angular momentum [29] . According to [29] the incoming partons are effectively objects, which are extended in space-time and their typical size is fixed by M_D^{-1} due to a minimal length imposed by quantum gravity [32] . At impact parameter M_D^{-1} the classical angular momentum of the black hole would be of order one at most, therefore the impact parameter and angular momentum of the quantum black hole are small. If one considered a classical black hole of this size with large angular momentum, it would have to spin faster than the speed of light. With that in mind, the spin down process before the final explosion that occurs in semiclassical black holes does not take place here. As we stated before, quantum black holes decay immediately to a small number of final states.

Quantum black holes form representations of $\mathrm{SU}(3)_c$ and carry a QED charge. The process of two partons p_i, p_j forming a quantum black hole in the c representation of $\mathrm{SU}(3)_c$ and charge q can be written as: $p_i + p_j \to \mathrm{QBH}_c^q$. The following different transitions are possible at a proton collider:

a) $\mathbf{3} \times \overline{\mathbf{3}} = \mathbf{8} + \mathbf{1}$

b) $\mathbf{3} \times \mathbf{3} = \mathbf{6} + \overline{\mathbf{3}}$

c) $\mathbf{3} \times \mathbf{8} = \mathbf{3} + \overline{\mathbf{6}} + \mathbf{15}$

d) $\mathbf{8} \times \mathbf{8} = \mathbf{1}_S + \mathbf{8}_S + \mathbf{8}_A + \mathbf{10} + \overline{\mathbf{10}}_A + \mathbf{27}_S$

Most of the time the black holes which are created carry a $\mathrm{SU}(3)_c$ charge and come in different representations of $\mathrm{SU}(3)_c$ as well as QED charges. An example of the cross section for the production of a QBH_1^0 is given by

$$\begin{aligned} \sigma^{pp}(s, x_{min}, n, M_D) &= \int_0^1 2zdz \int_{\frac{(x_{min}M_D)^2}{y(z)^2 s}}^1 du \int_u^1 \frac{dv}{v} \\ &\times F(n)\pi r_s^2(us, n, M_D) \\ &\left(\frac{1}{9} \sum_{i,j=q,\bar{q}} f_i(v,Q) f_{\bar{j}}(u/v,Q) + \frac{1}{64} f_g(v,Q) f_g(u/v,Q) \right) \end{aligned} \tag{2.59}$$

where i, j runs over all the quarks and anti-quarks subject to the constraint of QED charge neutrality, and f_q, f_g are the quark and gluon parton distribution functions.

The next logical step, since we have an expression for the cross section is to estimate the decay width, given by

$$\Gamma(QBH_c^q \to p_1 \dots p_f) \sim \left(2\pi \left(\frac{1}{(2\pi)^2} \right)^{(n_f-1)} \left(\frac{1}{2} \right)^{(n_f-1)} \right) \pi r_s^2 M_{BH}^3. \tag{2.60}$$

If we assume a two particle final state the decay width simplifies to

$$\Gamma = \frac{1}{4\pi} \frac{M_{BH}^5}{M_D^4}, \tag{2.61}$$

which for a quantum black hole of one TeV is of the order of $M_{BH}/4\pi \sim 80GeV$.

Regarding the phenomenology of quantum black holes at the Large Hadron Collider, we should note the work of Gingrich [35], who has produced a set of cross sections and decay topologies for quantum black holes. In the work presented in [35] a model is built for quantum black holes that requires the conservation of local charges, such as color, electric charge and spin, but not the conservation of global charges, such as baryon and lepton numbers. Lastly, Lorentz invariance is required. The main assumptions for the environment where these black holes operate are similar to the ones discussed in this chapter. The black holes have a mass comparable to the Planck mass so they will not behave semiclassically and they will decay into a few particles. The presence of a mechanism for lowering the Planck scale is obviously required and the author posits that even the most pessimistic scenarios will allow for quantum black hole detection at the Large Hadron Collider, assuming the assumptions are correct. For a detailed presentation see [35].

Cosmic Rays

Apart from the Large Hadron Collider, quantum black holes are expected to be observed in cosmic ray observatories [36], [37], [38] , neutrino telescopes [39] and space-based experiments [40] . Cosmic particles entering Earth's atmosphere can easily achieve energies in the TeV scale, which under the assumption of extra dimensions or a large hidden sector is the energy scale where quantum gravity emerges. These projects could very well provide the first evidence for the validity of our assmptions, opening the door for quantum gravity physics that is in accordance with observations. On the other hand, failure to detect any meaningful signature would help develop stricter bounds on the scale of quantum gravity.

If black holes are to be observed in cosmic rays it won't be from cosmic rays of hadronic nature, rather we are likely to observe black holes created from incoming neutrinos. The reason for this is that QCD cross sections are 10^9 times more likely than cross sections for black holes, making black holes virtually undetectable. In the neutrino case however, the cross section for the production of black holes is significantly larger than the Standard Model cross sections [36]. Since neutrinos interact with almost equal probability at any point in the atmosphere, there may be quasi-horizontal showers in the volume of air immediately above the detector, stemming from the light descendants of the black hole [41]. Also, neutrinos that freely propagate through the atmosphere may produce black holes through interactions in the ice or water [39].

Anchordoqui et al. considered the energy loss in black hole creation [41] , which until

then was not accounted for. Based on work presented in [42] they produced the cross section for $\nu N \to BH$ and found:

$$\sigma(E_\nu, x_{min}, n, M_D) \equiv \int_0^1 2zdz \int_{\frac{(x_{min}M_D)^2}{y^2 s}}^1 dx F(n)\pi r_s^2(\sqrt{\hat{s}}, n, M_D)\Sigma f_i(x, Q), \qquad (2.62)$$

where $\hat{s} = 2xm_N E_\nu$ and the $f_i(x, Q)$ are parton distribution functions [43].

Planck mass bounds

As soon as the papers [24, 25] proposing a low scale gravity came out, there was an effort to place strict bounds on the Planck mass. Since the energy scales are testable, it makes sense to try and confine the Planck mass as much as possible. In fact such an effort is presented in chapter 3. We will list here bounds on the Planck mass produced from phenomenology related to the Large Hadron Collider, astrophysical considerations and cosmic rays.

In theories of large extra dimensions the Kaluza-Klein modes of the graviton imply deviations from Newton's law for gravity. These would take the form:

$$V(r) = -G_N \frac{m_1 m_2}{r}[1 + \alpha e^{-r/\lambda}]. \qquad (2.63)$$

Tests on the deviation of Newton's law find a bound for the D-dimensional Planck mass $M_D > 3.6$ TeV [44]. This result is for two extra dimensions. Kaluza-Klein gravitons could also be produced in stars. If we require the graviton luminosity to be consistent with observations (so quite low) we can produce bounds on the Planck mass. The study of the supernova SN1987A gives $M_D > 27$ TeV and $M_D > 2.4$ TeV for two and three extra dimensions respectively [45]. Another bound is produced by requiring that neutron stars are not excessively heated by Kaluza-Klein decays into photons. We get a bound $M_D > 1700$ TeV for two extra dimensions and $M_D > 76$ TeV for three extra dimensions [46]. We can also derive bounds from cosmological considerations. For example, in order to avoid overclosure of the universe by relic gravitons the Planck mass has to be $M_D > 7$ TeV in the case of two extra dimensions [47]. Also relic Kaluza-Klein gravitons decaying into photons will contribute to the cosmic diffuse radiation, from which we get the bound $M_D > 100$ TeV again in scenarios with two extra dimensions [47]. We should mention that these bounds are not absolute and depend on a number of factors. We saw how the number of extra dimensions changes the results. Arguments concerning the geometry of the extra

dimensions can also influence the bounds. Lastly, these numbers would be different if we assumed that the Kaluza-Klein gravitons decay into other states than photons.

Results from particle colliders such as the Large Electron-Positron Collider, the Tevatron and of course the Large Hadron Collider have produced a host of bounds for the Planck mass, too numerous to list. They all are in the range of a few TeV however, which is quite encouraging. For a summary of results see [48].

Finally for theories with a large hidden sector [26, 27] bounds on the Planck mass have also been produced from cosmic rays experiments. Specifically, the non observation of small black holes by the Akeno Giant Air Shower Array implies $M_P > 488$ GeV [49].

Chapter 3

The flavor of quantum gravity

3.1 Introduction

Having given a brief overview of the theoretical background we used as a basis for our work, it is now time to see how it can be used to expand on our current knowledge and produce something useful. The first such project was undertaken under the supervision of Xavier Calmet in collaboration with Nina Gausmann, and resulted in the paper "The flavor of quantum gravity" [50] . Although limited to simplistic examples of quantum black holes and their interactions with particles of the Standard Model, it is nevertheless maybe the most important project since here we develop our methodology for treating quantum black holes in an effective way, in order to probe phenomenological applications and gain insight into a full theory of quantum gravity. After we create a model for the quantum black hole, we calculate the production cross section. Then, we proceed in considering flavor physics within the realm of non-thermal small black holes. Our efforts are in the direction of producing bounds for the Planck scale, the energy scale at which quantum gravity effects become important by using data on the anomalous magnetic moment of the muon, low energy experiments searching for violation of lepton flavor conservation and bounds on a neutron electric dipole moment. Finally we obtain a bound from proton decay.

3.2 Basics of quantum electrodynamics

In our approach towards developing our methodology we will be employing tools from quantum electrodynamics. The theory of quantum electrodynamics is the first quantum field theory to be developed and can be thought of as a unification of electromagnetism, quantum mechanics and special relativity. It deals with the interactions of light and matter, specifically between charged particles and the electromagnetic field. Therefore, it primarily deals with the interactions of photons and electrons. Working in a quantum mechanical environment the theory makes use of Feynman propagators [51], which represent the probability amplitude for a particle to travel from one point to another. They are beautifully illustrated in Feynman diagrams [51], which have become one of the most common tools of particle physics. Quantum mechanics dictate that there is no specific path for a particle to follow and we have to consider all possible paths. Feynman diagrams provide an elegant way of picturing this requirement. The starting equation for quantum electrodynamics describing the interaction of a spin-1/2 field with the electromagnetic field is the Lagrangian [52]:

$$L_{QED} = \bar{\psi}(i\gamma^{\mu}D_{\mu} - m)\psi - \frac{1}{4}F_{\mu\nu}F^{\mu\nu}, \tag{3.1}$$

where ψ is the bispinor field of spin-1/2 particles, $\bar{\psi}$ is the Dirac adjoint, γ^{μ} are the Dirac matrices, D_{μ} is the gauge covariant derivative and $F_{\mu\nu}$ is the electromagnetic field tensor. D_{μ} is given by:

$$D_{\mu} = \partial_{\mu} + ieA_{\mu} + ieB_{\mu}, \tag{3.2}$$

where e is the coupling constant, A_{μ} is the covariant four-potential of the electromagnetic field and B_{μ} is the external field. If we substitute in the previous expression the Lagrangian takes the form:

$$L = i\bar{\psi}\gamma^{\mu}\partial_{\mu}\psi - e\bar{\psi}\gamma_{\mu}(A^{\mu} + B^{\mu})\psi - m\bar{\psi}\psi - \frac{1}{4}F_{\mu\nu}F^{\mu\nu}. \tag{3.3}$$

From this Lagrangian we can determine the field equations of quantum electrodynamics:

$$i\gamma^{\mu}\partial_{\mu}\psi - m\psi = e\gamma_{\mu}(A^{\mu} + B^{\mu})\psi, \tag{3.4}$$

which is nothing more than the Dirac equation along with the electromagnetic field interaction. We also find [52]:

$$\partial_\nu F^{\nu\mu} = e\bar{\psi}\gamma^\mu\psi, \tag{3.5}$$

which under the condition:

$$\partial_\mu A^\mu = 0 \tag{3.6}$$

gives:

$$\Box A^\mu = e\bar{\psi}\gamma^\mu\psi. \tag{3.7}$$

The last equation can be thought of as the quantum field theory equivalent to the Maxwell equations. The usual process when working on a qunatum electrodynamics interaction is to draw the Feynman diagrams and using the Feynman rules for the particles and vertices proceed to calculate the cross section.

Quantum electrodynamics was the first theory to utilize renormalization techniques to cure divergences when calculating integrals. Since perturbation techniques are used in calculations, higher order terms, represented by loops in Feynman diagrams give rise to divergences. Renormalization fixes the various constants and parameters in the Lagrangian in such a way as to be in accordance with experimental results. Experimentally the theory of quantum electrodynamics has met with great success, providing very accurate predictions like for the anomalous magnetic moment of the electron [53].

Although quantum black holes have little to do with the realm of quantum electrodynamics, they still interact with the same particles, electrons and photons. Thus, in our treatment of quantum black holes and their interactions as an effective field theory, we use the same tools in an intuitive manner in order to be able to calculate cross sections and whatever else we may need.

3.3 Methodology

From a theoretical point of view we combine two important aspects of particle physics. First, we already know that collider physics is extremely useful in producing new particles and in validating or dismissing current theories. Even more so now with the experiments

at the Large Hadron Collider that managed to detect what appears to be the Higgs boson [54, 55]. While this is considered the pinnacle of particle physics, there is another approach that can yield useful results. Specifically, high precision low energy measurements can lead to the discovery of new physics efffects. In other words, we can test physics we already know with high accuracy and see if we can detect a hint of something beyond the Standard Model or give more accurate constraints of where and how new physics phenomena might take place. The other aspect of particle physics we are concerned with is the value of the Planck scale. As we discussed before, it can be anywhere between a few TeV and 10^{18}GeV if there are large extra dimensions [24, 25] or a large hidden sector [26, 27] . In our effort to determine a more accurate bound for the Planck scale, seeing that a desert of 10^{15}GeV is not very helpful, we will deal with maybe the most exciting consequence of low scale quantum gravity scenarions, quantum black holes. As we mentioned earlier quantum black holes, i.e., non-thermal small black holes with masses of the order of the Planck scale could be produced abundantly [28, 29]. The first experimental papers setting limits on the masses of these holes have started to appear, see e.g. [56]. The most recent results can be found in [57]. Combining these two approaches, we will produce limits on the Planck scale from quantum black holes processes involved in low energy high precision measurements. To do that we must come up with an "effective" way to work with quantum black holes.

Non-thermal quantum black holes can be thought of as states which are created and decay almost instantly, we will thus treat them as short-lived gravitational states. We can model these states using quantum fields and their interactions using the language of effective field theories. This is natural since these holes only couple to a few particles. At this point we should note a distinction that holds true for the entirety of this thesis. While we use the term "effective field theory", this is not the same as typical effective field theories. Our methodology is different and focuses on finding a way to "effectively" describe a black hole and its behaviour. We use the term somewhat freely since it is the term that makes the most sense, but it shouldn't be confused with the usual effective field theories.

Before we start discussing the interactions of quantum black holes with elementary particles of the Standard Model, let us discuss our assumptions concerning the black holes themselves. A black hole can be uniquely determined by its mass, spin and charge. Also, any consistent theory of quantum gravity should preserve the gauge symmetries of the Standard Model of particle physics. This implies that gauge quantum numbers must be preserved by quantum gravitational interactions including non-thermal quantum black

holes. On the other hand, global symmetries can be violated by quantum gravitational interactions. Examples of Lorentz violating vacua are known in string theory [58]. Lorentz violation effects typically lead to very tight bounds on the scale of quantum gravity. Here we shall assume that Lorentz invariance is not violated and focus on violation of flavor symmetry and CP violation induced by quantum black hole processes. From that point of view, the idea of describing a black hole by a massive quantum field carrying a spin and a charge is reasonable. However, there are some subtleties in the case of quantum black holes. First of all, if they were created in collisions of quarks or gluons, one would expect them to carry a QCD color charge as well since this gauge quantum number cannot be violated. Furthermore, it is not obvious whether their mass spectrum is continuous or discrete. These points will both be analyzed in the following chapters. We should also note Bekenstein's proof that classical black holes do not have baryon number [79].

The first step in our formalism is to write an effective Lagrangian, modelling the quantum black hole with a particle field charged under the gauge quantum numbers of the Standard Model. Such a Lagrangian contains a parameter c which will be determined retroactively. This is done by calculating the production cross section $\sigma(particle1 + particle2 \to QBH)$ and equating it to the cross section of the semiclassical case, namely $\sigma = \pi r_s^2$, where r_s is the Schwarzschild radius. From there we calculate c and plug it in the Lagrangian to get a full expression. From then on we can calculate whatever we need since we have a way to describe quantum black hole processes. This methodology can be better understood with the use of a simple example.

3.4 Quantum black hole as a scalar field

3.4.1 Effective Lagrangian

It is logical to start with the simplest case in order to establish our paradigm. We posit the following Lagrangian for a spinless and neutral quantum black hole ϕ:

$$L_4 = \frac{1}{2}\partial_\mu\phi\partial^\mu\phi - \frac{1}{2}M_{BH}^2\phi^2. \tag{3.8}$$

One expects the first quantum black mass to be of the order of the Planck mass. If the spectrum is discrete, one can consider a collection of scalar fields. On the other hand, if the mass spectrum was continuous, the mass of the quantum black hole would increase with the energy of the process. Note that the latter case resembles very much an unparticle field. In the following we assume a discrete mass spectrum and focus on the

lightest quantum black hole, but this will not impact our results which could be trivially extended to describe a continuous mass spectrum.

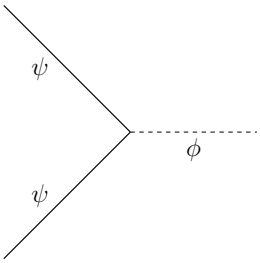

Figure 3.1: Vertex generated by the effective Lagrangian (3.9) which describes the annihilation of two fermions into a quantum black hole.

Let us start from the effective Lagrangian

$$L_6 = \frac{c}{\bar{M}_P^2}\,\partial_\mu\partial^\mu\phi\bar{\psi}_1\psi_2 + h.c. \tag{3.9}$$

where c is the parameter which will be adjusted to yield the correct cross section, $\bar{M}_P$ is the reduced Planck mass, ϕ is a scalar field describing the non-thermal quantum black hole, ψ_i is a fermion field which could be any fermion of the Standard Model. We shall assume here that ϕ is neutral. The gauge charges of ψ_1 must thus be matched by those of ψ_2. We start with dimension 6 operators since in 4-dimensions the cross section for black hole production goes as M_P^{-4}.

3.4.2 Calculation of the cross section

We have our effective Lagrangian and the Feynman diagram describing the production of a quantum black hole from the annihilation of two fermions. In order to calculate the cross section we will use standard QED Feynman rules. We are able to do that because we have incorporated all the "strange" stuff in the parameter c. We treat the black hole as a scalar field, therefore we don't have to consider anything else apart from a very simple Standard Model process with only a slight modification. The amplitude for the Feynman diagram is given by:

$$\mathcal{A} = q^2\frac{c}{\bar{M}_P^2}\bar{v}(p_2)u(p_1), \tag{3.10}$$

where p_1 and p_2 are the momenta of the two fermions and q is the momentum of the black hole. We need the squared amplitude therefore we write the complex-conjugate of the

amplitude:

$$\mathcal{A}^* = q^2 \frac{c}{\bar{M}_P^2} \bar{u}(p_1) v(p_2), \tag{3.11}$$

which together give:

$$|\mathcal{A}|^2 = \left(q^2 \frac{c}{\bar{M}_P^2} \bar{v}(p_2) u(p_1) \right) \left(q^2 \frac{c}{\bar{M}_P^2} \bar{u}(p_1) v(p_2) \right). \tag{3.12}$$

We can rearrange this and sum over spins using the completeness relations:

$$\Sigma u(p) \bar{u}(p) = \not{p} + m \tag{3.13}$$

$$\Sigma v(p) \bar{v}(p) = \not{p} - m \tag{3.14}$$

With no gamma matrices to begin with, rearranging is trivial. We get:

$$\frac{1}{4} \Sigma |\mathcal{A}|^2 = \frac{1}{4} q^4 \frac{c^2}{\bar{M}_P^4} (u(p_1) \bar{u}(p_1))(v(p_2) \bar{v}(p_2)) \tag{3.15}$$

which reduces to:

$$\frac{1}{4} \Sigma |\mathcal{A}|^2 = \frac{1}{4} q^4 \frac{c^2}{\bar{M}_P^4} trace[(\not{p}_1 + m_1)(\not{p}_2 - m_2)]. \tag{3.16}$$

Using standard trace technology, the fact that $q = p_1 + p_2$ and the typical definition of the Mandelstam variable $s = (p_1 + p_2)^2$ we get

$$|\mathcal{A}|^2 = \frac{s^2 c^2}{\bar{M}_P^4} [s - (m_1 + m_2)^2], \tag{3.17}$$

which we can plug in the typical expression for the cross section [5]:

$$\sigma(2\psi \to \phi) = \frac{\pi}{s} |\mathcal{A}|^2 \delta(s - M_{BH}^2) \tag{3.18}$$

to get:

$$\sigma(2\psi \to \phi) = \pi \frac{s c^2}{\bar{M}_P^4} [s - (m_1 + m_2)^2] \delta(s - M_{BH}^2), \tag{3.19}$$

where m_1 and m_2 are the masses of the fermions ψ_1 and ψ_2.

3.4.3 Calculation of the parameter

We have now calculated the cross section for our effective Lagrangian. As expected the result includes our parameter c. We will now equate our result for the cross section with the cross section for the production of a black hole in the semiclassical case, essentially assuming they are the same. This way we can determine c and plug it in the Lagrangian to get a complete expression. The semiclassical cross section is given by:

$$\sigma = \pi r_s^2, \tag{3.20}$$

where the four-dimensional Schwarzschild radius is given by

$$r_s\left(s, 0, \bar{M}_P\right) = \frac{\sqrt{s}}{4\pi \bar{M}_P^2}, \tag{3.21}$$

where $\bar{M}_P$ is the reduced Planck mass.

For the delta function we use the representation:

$$\delta(s - M_{BH}^2) = \frac{\Gamma}{4\pi\sqrt{s}\left[\left(\sqrt{s} - M_{BH}\right)^2 + \frac{\Gamma^2}{4}\right]}, \tag{3.22}$$

where Γ is the decay width of ϕ. The above expression is finite width approximation in the sense that it is a representation of the delta-function in the limit $\Gamma \to 0$.

Finally for c we get:

$$c^2 = \frac{1}{4\pi\left[(p_1+p_2)^2 - (m_1+m_2)^2\right]} \frac{\sqrt{(p_1+p_2)^2}\left[\left(\sqrt{(p_1+p_2)^2} - M_{BH}\right)^2 + \frac{\Gamma^2}{4}\right]}{\Gamma} \tag{3.23}$$

At the time of this project, the width Γ was estimated to be:

$$\Gamma(QBH \to \psi_1 + \psi_2) \sim \frac{M_{BH}}{64\pi^2}, \tag{3.24}$$

since there are about 100 degrees of freedom in the Standard Model, the total width is about a hundred times larger. In the subsequent project, dealing with quantum black holes with spin and color, the decay width is properly calculated to be:

$$\Gamma = \frac{c^2 M_{BH}^5}{8\pi M_P^4}. \tag{3.25}$$

3.5 Applications

The previous analysis has resulted in finding a way to effectively describe a quantum black hole and its interactions with Standard Model particles. Of course this is only an approximation, but it can serve as a guideline for further insight. For that to happen we have to put it to the test, and see how we can use our effective theory in phenomenological applications. One thing we can do is use the effective Lagrangian to estimate bounds for the Planck scale and see how they compare with bounds from other sources. We introduce a γ_5 in the effective Lagrangian describing the coupling of the quantum black hole to the fermions

$$L_{6,CP} = \frac{c}{\bar{M}_P^2}\,\partial_\mu\partial^\mu\phi\bar{\psi}_1 i\gamma_5\psi_2 + h.c. \tag{3.26}$$

It is easy to estimate the one loop induced effective Lagrangian (Figure 3.2) in the low energy regime. Obviously the effective theory is not renormalizable, but we can use power counting arguments. We find

$$L_{eff} = \frac{e}{2}\frac{1}{16\pi^2}\sum_{ij}\frac{m_i}{\bar{M}_P^2}\bar{\psi}_i(A_{ij} + B_{ij}\gamma_5)\sigma_{\mu\nu}\psi_j F^{\mu\nu}, \tag{3.27}$$

where m_i is the mass of the heaviest of the two fermions, $A_{ij} = A$ and $B_{ij} = B$ are numerical coefficients which are found to be of order 1. These coefficients are used in the following applications with a typical value of 1 as in [59]. We took the momentum cutoff of the loop integral to be of the order of the reduced Planck mass. Note that we have carefully considered the Dirac structure of the loop diagram. This led to the chiral suppression factor $m_i/\bar{M}_P$. We should also point out that the Lagrangian we end up with as well as the following analysis is similar to [59]. Instead of writing an effective Lagrangian to describe contributions to the magnetic moment of the muon beyond the Standard Model, we now write a similar effective Lagrangian to describe black hole effects which again exceed the Standard Model. The reasoning and the production of the Lagrangian closely follow the work presented in [59].

3.5.1 Anomalous magnetic moment of the muon

The Dirac equation predicts a muon magnetic moment:

$$\vec{M} = g_\mu\frac{e}{2m_\mu}\vec{S}, \tag{3.28}$$

with gyromagnetic ratio $g_\mu = 2$. Quantum loop effects lead to a small calculable deviation from $g_\mu = 2$, parameterized by the anomalous magnetic moment

$$a_\mu \equiv \frac{g_\mu - 2}{2}. \tag{3.29}$$

This is a quantity that has the advantage of being able to be measured and calculated with high precision. Therefore it is a very useful tool in testing the Standard Model and looking for new physics effects. The latest values for a_μ come from the E821 experiment at Brookhaven National Lab, where the precession of μ^+ and μ^- in a constant external magnetic field was measured as the muons circulated in a confining storage ring. The results were [60]:

$$a_{\mu+}^{exp} = 11659204(6)(5) \times 10^{-10} \tag{3.30}$$

$$a_{\mu-}^{exp} = 11659215(8)(3) \times 10^{-10}. \tag{3.31}$$

We notice two errors in the results, the first is statistical and the second systematic. In order to calculate their average, we have to assume CPT invariance and consider correlations between systematic errors. The average result is [60]:

$$a_{\mu}^{exp} = 11659208.9(5.4)(3.3) \times 10^{-10}. \tag{3.32}$$

The Standard Model prediction for the anomalous magnetic moment of the muon is the sum of three Feynman diagrams. Specifically:

$$a_\mu^{SM} = a_\mu^{QED} + a_\mu^{EW} + a_\mu^{Had}, \tag{3.33}$$

where a_μ^{QED} represents the contributions from the photon and lepton loops, a_μ^{EW} represents the W boson and Z boson loops and a_μ^{Had} represents hadron loops. The first and second part can be calculated from first principles. The third part has to be determined experimentally. For the first part the calculation yields [61]:

$$a_\mu^{QED} = 116584718.09(0.15) \times 10^{-11}. \tag{3.34}$$

For the second part we get [62]:

$$a_\mu^{EW} = 154(1)(2) \times 10^{-11}. \tag{3.35}$$

As we mentioned earlier, hadronic loops can't be currently calculated from theory. Therefore this part contributes most to the uncertainty regarding the anomalous magnetic moment of the muon. The contribution of the hadronic loops from experimental data is split into two parts that give respectively [63]:

$$a_\mu^{Had} = 6923(42)(3) \times 10^{-11}, \tag{3.36}$$

where the first error is experimental and the second due to perturbative quantum chromodynamics and [64]

$$a_\mu^{Had} = 7(26) \times 10^{-11}, \tag{3.37}$$

where the error stems from hadronic light-by-light uncertainties. Adding all these values we get for the anomalous magnetic moment of the muon:

$$a_\mu^{SM} = 116591802(2)(42)(26) \times 10^{-11}, \tag{3.38}$$

where the errors are from the electroweak, lowest-order hadronic and higher-order hadronic parts respectively. The difference between theory and experiment is found to be [65]:

$$\Delta a_\mu = a_\mu^{exp} - a_\mu^{SM} = 287(63)(49) \times 10^{-11}. \tag{3.39}$$

If we use the well known result [59]

$$\Delta a = \frac{1}{16\pi^2} \frac{m_\mu^2}{\bar{M}_P^2} A. \tag{3.40}$$

where A is of order 1 and $\Delta a \sim 10^{-9}$ [66] we obtain:

$$\bar{M}_P \quad > \quad 266\,\text{GeV}. \tag{3.41}$$

as a lower bound for the reduced Planck mass. Note that this bound is obtained with very few assumptions, we only assumed that quantum black holes can be treated as virtual objects which couple to low energy modes. It is surprisingly weak and indicates that quantum black holes could very well be relevant for LHC physics.

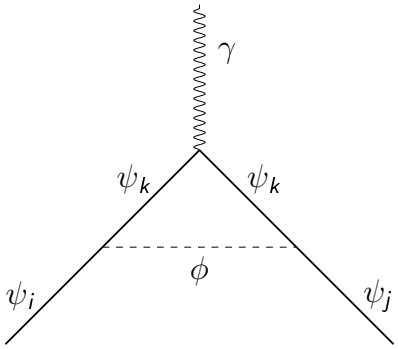

Figure 3.2: Quantum black hole contribution to the anomalous magnetic moment of the muon, rare decays of leptons or the EDM of the fermions of the Standard Model.

3.5.2 Lepton Flavor violation

Lepton Flavor violation in charged lepton decays is a typical probe for new physics effects, beyond the Standard Model. Among the flavor quantum numbers we look for processes that don't preserve the lepton mumber given by the usual formula:

$$L = n_l - n_{\bar{l}} \tag{3.42}$$

where n_l and $n_{\bar{l}}$ are the numbers of leptons and antileptons respectively. The Standard Model depends on the conservation of lepton number. In each particle interaction the lepton mumber is expected to stay the same. A simple example is beta decay:

$$n \to p + e^- + \bar{\nu_e}, \tag{3.43}$$

where the neutron has lepton number 0 since it is a baryon. After the reaction the proton lepton number is 0, the electron lepton number is obviously 1 and the antineutrino has lepton number -1. Therefore, the total lepton number is again 0. Demanding the conservation of lepton number defines the lepton family numbers L_e,L_μ and L_τ, for the electron, the muon and the tau respectively [67]. Each of these numbers has to be conserved.

Actually, in order to preserve lepton family numbers we require the neutrinos to be massless. We know from the observation of neutrino oscillations that neutrinos have a very small non-zero mass. Strictly speaking, that means that the conservation of lepton

numbers is violated [67], albeit to a very small degree due to the very small value of neutrino mass. This doesn't prove to be problematic since the total lepton number conservation law still holds. This makes interactions like the following possible:

$$\mu^- \to e^- + \nu_e + \bar{\nu_\mu}, \tag{3.44}$$

which is a rare muon decay, where we see that although L_e and L_μ are not conserved the total number is.

Unless the lepton mumber is gauged, quantum black hole processes are expected to lead to transitions that do not preserve lepton number. Starting from

$$\Gamma(\mu \to e\gamma) \quad = \quad e^2 \frac{A^2}{1024\pi^5} \frac{m_\mu^5}{\bar{M}_P^4} \tag{3.45}$$

$$\Gamma(\tau \to e\gamma) = \Gamma(\tau \to \mu\gamma) \quad = \quad e^2 \frac{A^2}{1024\pi^5} \frac{m_\tau^5}{\bar{M}_P^4}, \tag{3.46}$$

and using the current experimental limits for the decay of the muon into an electron and a photon, as well as the decay of the tau into a muon and a photon [66] :

$$Br(\mu \to e\gamma) < 1.2 \times 10^{-11} \tag{3.47}$$

$$Br(\tau \to \mu\gamma) < 4.4 \times 10^{-8} \tag{3.48}$$

we find the following limits on the reduced Planck mass

$$\bar{M}_P \quad > \quad 3 \times 10^4 \,\mathrm{GeV} \tag{3.49}$$

using the bound on the transition $\mu \to e\gamma$ and

$$\bar{M}_P \quad > \quad 3 \times 10^3 \,\mathrm{GeV} \tag{3.50}$$

using the bound on the transition $\tau \to \mu\gamma$.

3.5.3 Electric dipole moment

Another effort of probing for new physics consists of the precise measurement of the electric dipole moment of fundamental and composite particles. Electric dipole moments violate P and T symmetries. Assuming that CPT symmetry is still conserved, measurements of the electric dipole moments are very sensitive probes for CP violating processes [68].

If CP is violated by quantum black hole processes, the effective Lagrangian also gives a contribution to the electric dipole moment of leptons and quarks of the Standard Model. The Lagrangian yields the following electric dipole moment of the electron:

$$d(e) = \frac{eB}{16\pi^2}\frac{m_e}{\bar{M}_P^2}. \tag{3.51}$$

Using the current experimental constraint [66]

$$d(e) = (0.07 \pm 0.07) \times 10^{-26} \mathrm{e\,cm}, \tag{3.52}$$

we find a bound on the reduced Planck mass:

$$\bar{M}_P \quad > \quad 1 \times 10^4\,\mathrm{GeV} \tag{3.53}$$

while using the bound for the muon [66],

$$d(\mu) = (-0.1 \pm 0.9) \times 10^{-19} \mathrm{e\,cm}, \tag{3.54}$$

we find:

$$\bar{M}_P \quad > \quad 36\,\mathrm{GeV}. \tag{3.55}$$

Finally, there is also a contribution to the electric dipole moment of the neutron. The current bound on the neutron electric dipole moment is $d(n) = 0.29 \times 10^{-25} \mathrm{e\,cm}$ [66]. One finds

$$d(n) = \frac{4}{3}d(d) - \frac{1}{3}d(u) = \frac{eB}{16\pi^2\bar{M}_P}\left(\frac{4}{3}\frac{m_d}{\bar{M}_P} - \frac{1}{3}\frac{m_u}{\bar{M}_P}\right) \tag{3.56}$$

and a bound on the reduced Planck mass of

$$\bar{M}_P > 5 \times 10^3\,\mathrm{GeV} \tag{3.57}$$

where we took $B \sim 1$, which followed from our estimate.

3.5.4 Proton Decay

Proton decay is the process where a proton decays into lighter particles like the neutral pion and a positron:

$$p^+ \to e^+ + \pi^0, \tag{3.58}$$

with the pion immediately decaying into photons:

$$\pi^0 \to 2\gamma. \tag{3.59}$$

Proton decay has never been observed experimentally. The stability of the proton is attributed to the conservation of the baryon number. Certain theories of grand unification, such as the Georgi-Glashow model require the decay of the proton and predict a half-time of about 10^{36}years [69]. The typical dimension-6 operators for proton decay are [69]

$$\frac{qqql}{\Lambda^2}, \tag{3.60}$$

$$\frac{d^c d^c u^c e^c}{\Lambda^2}, \tag{3.61}$$

$$\frac{\overline{e^c u^c} qq}{\Lambda^2}, \tag{3.62}$$

$$\frac{\overline{d^c u^c} ql}{\Lambda^2}, \tag{3.63}$$

where Λ is the cutoff scale for the Standard Model. There are also dimension-4 and dimension-5 operators for proton decay from supersymmetric models [69].

Quantum black holes could also mediate proton decay. For processes at energies well below the first quantum back hole mass, one can integrate out the fields ϕ and find dimension six operators:

$$\mathcal{L} = \frac{c^2}{\bar{M}_P^4} \frac{s^2}{M_{BH}^2} \bar{\psi}\psi\bar{\psi}\psi \tag{3.64}$$

for $M_{BH}^2 \gg s$. These operators can be used to describe non-thermal quantum black hole production in the collisions of quarks at collider. A treatment for collisions of quarks and gluons appears in chapter 5.

Dimension 6 operators similar to those discussed above can be generated by the exchange of a quantum black hole field which violates the baryon and lepton numbers. These operators mediate proton decay. For the lifetime of the proton we find:

$$\tau = \frac{\bar{M}_P^{12}}{m_p^5 c^4 \Lambda_{QCD}^8} \sim \frac{10^4}{(16\pi)^2} \frac{\bar{M}_P^{10}}{m_p^5 \Lambda_{QCD}^6} \tag{3.65}$$

where Λ_{QCD} is the typical energy of the quarks in the proton. Using $\tau > 5 \times 10^{33} y$ [66], we find $M_P > 1 \times 10^6$ GeV. If low scale quantum gravity is the solution to the weak hierarchy problem, the proton decay problem must be addressed. An obvious solution is to gauge the baryon or lepton number.

3.6 Conclusion

The possibility of lowering the Planck scale to a few TeV [24], [25], [26] has opened up a new world of possibilities. Quantum gravity effects previously thought to be observable at extreme energy scales could be relevant to our current technological capabilities. Quantum black holes could be observed at the Large Hadron Collider or cosmic rays observations, so we need a way to describe them and predict their behaviour. To that end we produced this project as a first step in that direction.

In this chapter we have presented the main methodology of our work. In essence, we have developed a way to effectively describe a quantum black hole and its interactions with particles of the Standard Model. This was done by writing a Lagrangian that contains the interacting fields as well as a parameter c which is determined retroactively. Following the work of [6] and [15] we assume that the cross section for the production of a quantum black hole can be matched to the cross section of the semiclassical case. With that in mind, the Lagrangian is given explicitly and it can be used to probe phenomenological applications.

In order to make some sense of quantum black holes, which can be thought as one of the most intriguing aspects of theoretical physics, we treat them with the usual particle physics language. They are described as short lived gravitationally bound states that decay into a small number of particles. They have the usual characteristics like mass, spin and charge and they preserve the gauge symmetries of the Standard Model. However, global symmetries like Lorentz invariance could be violated. Depending on the particles that created the quantum black hole we effectively treat it as a standard field, in the simplest case a scalar field. In our first example we assume a discrete mass spectrum. A more detailed analysis, regarding a discrete and continuous mass spectrum, follows in the next chapter.

After calculating the cross section and determing c we estimated the one loop induced effective Lagrangian. This was used to derive bounds on the Planck mass from the consideration of the anomalous magnetic moment of the muon, lepton flavor violation, electric dipole moment and proton decay. The bound from the anomalous magnetic moment was found to be of the order of 266 GeV. In the case of the violation of discrete symmetries such as lepton number or CP we produced even tighter bounds of the order of 10^4 GeV and 10^3 GeV respectively. The limit from proton decay was determined to be of the order of 10^6 GeV, but this decomposition could be forbidden. The main result is that unless quantum gravity violates CP or baryon mumber quantum black holes could be accessible

at the Large Hadron Collider.

This project serves as a first example of our methodology. It will be expanded to consider quantum black holes with spin and color produced from quarks and gluons for a more accurate picture. Nevertheless, though the expansion to realistic quantum black holes and later on quantum black holes that produce supersymmetric particles is more complicated, the basis of our methodology will remain the same. We will always be describing quantum black holes in a field theory language to be able to probe their behavior.

Chapter 4

Minimal length and the mass spectrum of a quantum black hole

4.1 Introduction

In this chapter we address the question of whether the quantum black holes we discuss have a discrete or continuous mass spectrum. This is a fundamental question in modern physics and a definite answer would shape the way we produce new physics. The way to approach this topic is to investigate the existence of a minimal length and its consequences. We will give a brief review of the literature on the matter [71], [72, 73], [77], which is the reasoning behind the work presented in [70]. This paper, "Non thermal small black holes", was developed in collaboration with Nina Gausmann under the supervision of Xavier Calmet. Then we will show how the cross section changes from the continuous to the discrete mass spectrum.

4.2 The existence of a minimal length

In order to produce a theory of quantum gravity, one has to consider quantum mechanics and general relativity in the same context. It is well known that this is extremely difficult and that a full theory of quantum gravity remains elusive. When trying to unify these two great theories a small consideration arises which implies the existence of a minimal length. In other words, there is no operational procedure in which we can measure a distance smaller than this minimal length. This is a result of two important aspects, one from each theory. Specifically the uncertainty principle from quantum mechanics and gravitational collapse from general relativity.

As we discussed earlier, the hoop conjecture [22] states that the formation of a black hole is a direct result of an amount of energy E being confined to a ball of size R, where $R < E$. This conjecture along with the uncertainty principle imply the existence of a minimal length l_P. The authors of [72] present this idea in the following way. If we consider a particle of energy E, which is not a black hole then we can write the following relation about its size [72]:

$$r \gtrsim \mathbf{max}[1/E, E], \tag{4.1}$$

where $1/E \sim \lambda_c$ is its Compton wavelength. If we try to minimize with respect to E we get $r \sim l_P$. On the other hand, if the particle is a black hole, then its radius grows with mass: $r \sim E$. This implies that any process trying to measure distances l shorter than l_P will, in the presence of gravity, only be able to measure up to a $1/l$ factor of accuracy [72].

We assume that the position operator $\hat{x}$ has discrete eigenvalues x_i, where the distance between eigenvalues is of order l_P or smaller. We should note that a quantized position does not necessarily mean a quantized momentum and vice versa. If we attempt to measure the spectrum of $\hat{x}(0)$ in time of flight experiments we should be able to determine a discrete spectrum, if we ignore gravitational effects. This is problematic though, since measuring the discreteness of $\hat{x}(0)$ deals with wavelengths comparable to the eigenvalue spacing. With a spacing of l_P or smaller gravitational effects have to be taken into account, because in that regime minimal balls or black holes are produced of size l_P. Thus, a direct measurement with an accuracy better than l_P is impossible [72].

One could consider a different experiment to overcome these difficulties, namely one containing an interferometer, which is capable of measuring distances smaller than the size of any of its components. We will show that even in that case a measurement of eigenvalue

spacing with very high accuracy is again not possible.

We will perform the following simple thought experiment. First we consider a free particle and measure its position at times $t = 0$ and t. If we use the Heisenberg operators for position $\hat{x}(t)$ and momentum $\hat{p}(t)$ we get [72]:

$$\hat{x}(t) = \hat{x}(0) + \hat{p}(0)\frac{t}{M}, \tag{4.2}$$

where t is the time over which the measurement is taken and M is the mass of the particle of which we measure the postion.

The commutator between $\hat{x}(0)$ and $\hat{x}(t)$ is:

$$[\hat{x}(0), \hat{x}(t)] = i\frac{t}{M}. \tag{4.3}$$

If we use the expression:

$$(\Delta A)^2(\Delta B)^2 \geq -\frac{1}{4}(< [\hat{A}, \hat{B}] >)^2, \tag{4.4}$$

we arrive at:

$$|\Delta x(0)||\Delta x(t)| \geq \frac{t}{2M}. \tag{4.5}$$

Since measurement of the discreteness of $\hat{x}(0)$ requires two position measurements it is limited by the greater value between $\Delta x(0)$ and $\Delta x(t)$, which have to be larger than $\sqrt{t/M}$.

$$\Delta x \equiv \mathbf{max}[\Delta x(0), \Delta x(t)] \geq \sqrt{\frac{t}{2M}} \tag{4.6}$$

If we want to lower Δx below l_P we have to increase M. This way we are in danger of creating a gravitational collapse. To prevent that, we also have to increase the size of our measuring device R in such a way so as to have $R > M$. Causality arguments prevent R from exceeding t, otherwise our experiment is not meaningful if we have parts that can't causally communicate. Therefore, following [72] we write

$$t > R > M, \tag{4.7}$$

which combined with our previous expression gives:

$$\Delta x > l_P. \tag{4.8}$$

The above relation implies the existence of a minimal length. If no process exists which can measure a distance smaller than l_P we are lead to believe that we are dealing with a discrete spectrum. For a more detailed analysis see [72, 73].

4.3 Quantized black hole mass

One would think that a minimal length, which implies discretization of space, automatically leads to a discrete mass spectrum for a black hole. While this intuition proves correct there are subtleties that need to be examined. There is extensive literature regarding the quantization of black hole mass and we will present a short overview in order to justify our reasoning in considering a discrete spectrum for the black holes mass.

In their work outlined in [74] the authors argue that the existence of a minimal length leads to a quantization for the mass of the black hole. Working in theories of gravity with extra dimensions, they consider the compactification of a D-dimensional spacetime to the direct product of 4-dimensional Minkowski spacetime and of a d-dimensional compact torus of volume V_d. Following their line of thought we start from:

$$\frac{1}{L_D^{2+d}} \int R\sqrt{-g} d^{4+d}x = \frac{V_d}{L_D^{2+d}} \int R\sqrt{-g} d^4x = \frac{1}{L_{Pl}^2} \int R\sqrt{-g} d^4x, \tag{4.9}$$

where L_{Pl} and L_D are the respective 4-dimensional and D-dimensional Planck lengths. These are connected as such:

$$L_D = (V_d/L_D^d)^{\frac{1}{2}} L_{Pl}, \tag{4.10}$$

where the ratio

$$(V_d/L_D^d) = N \tag{4.11}$$

counts the total number of Kaluza-Klein modes with masses not exceeding L_D^{-1} [75]. The main relation for the quantization is for the area of a D-dimensional black hole:

$$A_D = nL_D^{D-2}. \tag{4.12}$$

If we write the mass of the black hole in terms of the surface area we get:

$$M = M_D^{2+d} A^{\frac{1+d}{2+d}}, \tag{4.13}$$

which implies the quantization of the mass:

$$M_n = M_D n^{\frac{1+d}{2+d}} \tag{4.14}$$

The authors revisit the mass quantization issue in a following paper [71], where they once again argue in favor of a disctrete mass spectrum. Their proof is based on Poincare-invariance of the asymptotic background and is not affected by the geometry of black holes or other short distance considerations. A side effect of their analysis is the fact that small black holes don't decay via Hawking radiation.

A somewhat different approach is presented in [77] where the author uses a Generalized Uncertainty Principle proposed in [76] to reach the same conclusion, that the mass of a black hole is quantized.

A Generalized Uncertainty Principle (sometimes referred as modified uncertainty principle) is motivated by the existence of a minimal length. The modified commutators are given by [76]:

$$[x_i, p_j] = i\hbar \left[\delta_{ij} - \alpha \left(p\delta_{ij} + \frac{p_i p_j}{p}\right) + \alpha^2 (p^2 \delta_{ij} + 3p_i p_j)\right], \tag{4.15}$$

where $\alpha = \alpha_0 l_{Pl}/\hbar$. The modified uncertainty principle takes the form [76]:

$$\Delta x \Delta p \geq \frac{\hbar}{2}[1 - 2\alpha < p > +4\alpha^2 < p^2 >] \geq \left[1 + \left(\frac{\alpha}{\sqrt{< p^2 >}} + 4\alpha^2\right) \Delta p^2 + 4\alpha^2 < p^2 > -2\alpha\sqrt{< p^2 >}\right], \tag{4.16}$$

which implies:

$$\Delta x \geq (\Delta x)_{min} \approx \alpha_0 l_{Pl} \tag{4.17}$$

$$\Delta p \leq (\Delta p)_{max} \approx \frac{M_{Pl}c}{\alpha_0}. \tag{4.18}$$

The author starts with a simple Hamiltonian for the black hole of the form:

$$H = \frac{p^2}{2\alpha} + \frac{\alpha}{2} \tag{4.19}$$

where p is momentum canonically conjugate to α and takes the Wheeler-DeWitt equation for a black holes written as [78]:

$$\alpha^{-s-1}\frac{\partial}{\partial\alpha}\left(\alpha^s\frac{\partial}{\partial\alpha}\psi(\alpha)\right) = (\alpha - 2M)\psi(\alpha). \tag{4.20}$$

Choosing $s = 2$, $R_s = 2M$ and applying the transformation $\psi(\alpha) = U/\alpha$ with $x = \alpha - R_s/2$ we get:

$$-\frac{\partial^2 U}{\partial x^2} + x^2 U = \frac{R_s^2}{4}U, \tag{4.21}$$

which is the equation for a quantum harmonic oscillator with energy levels:

$$\frac{R_s^2}{4} = (2n + 1). \tag{4.22}$$

The last expression implies for the mass of a black hole:

$$M^2(n) = 2(n + 1/2). \tag{4.23}$$

Based on the modified uncertainty principle presented above, the author posits the following commutation relation:

$$[x, p] = i(1 - \alpha p), \alpha > 0 \tag{4.24}$$

where the operators act as:

$$p\psi(p) = p\psi(p) \tag{4.25}$$

$$x\psi(p) = i\left[(1-\alpha p)\frac{\partial}{\partial p}\right]\psi(p). \tag{4.26}$$

With that in mind the Wheeler-DeWitt is modified as such:

$$(1-\alpha p)^2\frac{\partial^2\psi(p)}{\partial p^2} - \alpha(1-\alpha p)\frac{\partial\psi(p)}{\partial p} - (p^2 - M^2)\psi(p) = 0, \tag{4.27}$$

which after a bit of algebra gives for the black hole mass:

$$M^2(n) = 2\left(n+\frac{1}{2}\right) - \alpha^2\left[n^2+n+\frac{1}{4}\right]. \tag{4.28}$$

This result is in accordance with Bekenstein's proposal for the black hole mass [79]. Finally the author argues that through the use of the deformed algebra of Kempf et al. [80] the mass of a black hole in quantum gravity is proportional to n.

4.4 Continuous and discrete mass spectrum

As we just showed, the matter of a discrete continuous spectrum for the position is unequivocally linked to a discrete or continuous spectrum for the mass of a quantum black hole. Most studies so far are assuming that quantum black holes have a continuous mass spectrum despite some recent warnings that the quantum black hole masses ought to be quantized [71]. We shall now describe the production cross section of quantum black holes at the Large Hadron Collider. We shall first discuss the continuous mass spectrum and then the discrete mass spectrum. In both cases, we shall assume that the cross sections can be extrapolated from the cross section obtained for semiclassical black holes, i.e. the geometrical cross section πr_s^2 where r_s is the Schwarzschild radius.

Continuous mass spectrum

In that case, the LHC production cross section for quantum black holes with a continuous mass spectrum is assumed to be of the form

$$\begin{aligned}\sigma^{pp}(s, x_{min}, n, M_D) &= \int_0^1 2zdz \int_{\frac{(x_{min}M_D)^2}{y(z)^2 s}}^1 du \int_u^1 \frac{dv}{v} \\ &\times F(n)\pi r_s^2(us, n, M_D)\sum_{i,j} f_i(v,Q)f_j(u/v,Q)\end{aligned} \tag{4.29}$$

where M_D is the n dimensional reduced Planck mass, $z = b/b_{max}$, $x_{min} = M_{BH,min}/M_D$, n is the number of extra-dimensions, $F(n)$ and $y(z)$ are the factors introduced by Eardley

and Giddings and by Yoshino and Nambu [81]. The n dimensional Schwarzschild radius is given by:

$$r_s(us, n, M_D) = k(n) M_D^{-1} [\sqrt{us}/M_D]^{1/(1+n)} \tag{4.30}$$

where

$$k(n) = \left[2^n \sqrt{\pi}^{n-3} \frac{\Gamma((3+n)/2)}{2+n} \right]^{1/(1+n)}. \tag{4.31}$$

Discrete mass spectrum

We now consider the discrete mass spectrum case. The cross section is given by

$$\begin{aligned} \sigma^{pp}_{QBH}(s, M_{QBH}, n, M_D) &= \pi r_s^2(M_{QBH}, n, M_D) \int_0^1 2z dz \int_{\frac{(M_{QBH})^2}{y(z)^2 s}}^1 du \int_u^1 \frac{dv}{v} \\ &\times F(n) \sum_{i,j} f_i(v, Q) f_j(u/v, Q) \end{aligned} \tag{4.32}$$

with the constant Schwarzschild radius given by

$$r_s(M^2_{QBH}, n, M_D) = k(n) M_D^{-1} [\sqrt{M^2_{QBH}}/M_D]^{1/(1+n)} \tag{4.33}$$

where as previously

$$k(n) = \left[2^n \sqrt{\pi}^{n-3} \frac{\Gamma((3+n)/2)}{2+n} \right]^{1/(1+n)}. \tag{4.34}$$

Note that the parton level cross section is constant in that case. The physics of quantum black holes with a discrete mass spectrum is very different from the continuous case. They are expected to behave as heavy resonances that will decay to a few particles. The total cross section is given by the sum of the individual production cross sections:

$$\sigma^{pp}_{tot}(s, n, M_D) = \sum_i \sigma^{pp}_{QBH}(s, M^i_{QBH}, n, M_D). \tag{4.35}$$

We expect that the mass spectrum is quantized in terms of the Planck mass because of the existence of a minimal length [72, 73] in models incorporating quantum mechanics and general relativity.

To illustrate our point we present an example for the production cross-section of a QBH_1^0 given by [29]

$$\begin{aligned}\sigma^{pp}(s, x_{min}, n, M_D) &= \int_0^1 2zdz \int_{\frac{(x_{min}M_D)^2}{y(z)^2 s}}^1 du \int_u^1 \frac{dv}{v} \\ &\times F(n)\pi r_s^2(us, n, M_D) \\ &\left(\frac{1}{9}\sum_{i,j=q,\bar{q}} f_i(v,Q) f_{\bar{j}}(u/v,Q) + \frac{1}{64} f_g(v,Q) f_g(u/v,Q)\right)\end{aligned} \tag{4.36}$$

where i, j runs over all the quarks and anti-quarks subject to the constraint of QED charge neutrality, and f_q, f_g are the quark and gluon parton distribution functions. For the production of a specific member (i.e., with specified color) of the octet QBH_8^0, one finds the same expression. In case of a discrete mass spectrum us in r_s should be replaced by M_{QBH}^2. The details of the final states have been considered elsewhere [29] and apply to the discrete mass spectrum case as well.

4.5 Conclusion

In this chapter we reviewed part of the literature concerning the existence of a minimal length and the quantization of the mass spectrum. We gave cross sections for the production of a black hole for a continuous and discrete mass spectrum. Obviously, the literature that deals with the discreteness of space and mass is extensive and it was not our intent to review it all. The point of the basic exercise presented here was to justify our reasoning in questioning the nature of space. We followed a simple thought experiment that indicates the existence of a minimal length. This means that there is a lower limit in what we can measure. Since this is connected to the mass spectrum of a quantum black hole we are interested in examining it. We then gave the production cross sections for quantum black holes at the Large Hadron Collider, which are extrapolated from the semiclassical case. Despite arguments for the discreteness of space and any personal preferences we present both cases, a continuous and a discrete spectrum.

Chapter 5

Quantum black holes with spin and color

5.1 Introduction

We have given an overview of our methodogy for the study of quantum black holes. Up to this point our examples have been rather simplistic and their main purpose was to illustrate the logic behind our model building process. This consists of writing an effective Lagrangian in order to describe the interactions of a quantum black hole with particles of the Standard Model, calculating the production cross section and equating it to the semiclassical cross section to fully determine the parameters in the Lagrangian. Due to theories of extra dimensions [24, 25] or a large hidden sector [26, 27], we expect the Planck scale to be as low as of the order of a few TeV. This would make the detection of quantum black holes in collider events a realistic possibility. Therefore we are inclined to examine more realistic particle interactions. In a proton-proton collider, quantum black holes would be produced from the collisions of quarks and gluons. We are thus particularly interested in the quantum black holes carrying QCD and QED quantum numbers and with spins 0, 1/2 and 1 since these should be the lowest lying states. In this chapter we will present three distinct examples. A black hole created from the collision of two quarks, a quark and a gluon and finally a gluon and a gluon. We will give the detailed calculation of the production cross section and the decay width for each case.

5.2 Basics of quantum chromodynamics

Similarly to our treatment of quantum black hole as a scalar field with the tools of quantum electrodynamics in chapter 3, we will be employing quantum chromodynamics methods for the description of quantum black holes created from the collisions of quarks and gluons. Quantum chromodynamics is the quantum field theory that deals with the strong interaction, the force between quarks and gluons. Unlike quantum electrodynamics, which is an abelian gauge theory with the symmetry group $U(1)$, quantum chromodynamics is a non-abelian gauge theory with the symmetry group $SU(3)_c$ [82].

Quarks are color-charged fermions that interact through the exchange of gluons much like charged particles interact through the exchange of photons in quantum electrodynamics. In this case however gluons also carry color charge, therefore they not only mediate the strong interaction but they participate as well. Quarks have never been observed isolated. Instead they band together in mesons (quark-antiquark pair) and baryons (three quarks) like protons and neutrons. Mesons and baryons are collectively called hadrons and they represent the most detailed level of quark analysis we can achieve. This is due to confinement, a property of quantum chromodynamics that dictates that the force between quarks doesn't diminish as the distance between them increases. It is currently believed that confinement is a result of gluons carrying a color charge as well. Quarks and gluons also exhibit asymptotic freedom [82], meaning that at high energies they interact weakly. Confinement and asymptotic freedom don't operate in the same energy scale. Specifically, confinement is dominant in low energy scales and asymptotic freedom in higher ones.

The Lagrangian that produces the dynamics of quantum chromodynamics is [83]:

$$L_{QCD} = \bar{\psi}_i(i(\gamma^\mu D_\mu)_{ij} - m\delta_{ij})\psi_j - \frac{1}{4}G^a_{\mu\nu}G^{\mu\nu}_a, \tag{5.1}$$

where ψ_i is the quark field, m controls the quark mass, the indices i, j differentiate between the different quarks and $G^a_{\mu\nu}$ is the gauge invariant field strength tensor given by [83]:

$$G^a_{\mu\nu} = \partial_\mu G^a_\nu - \partial_\nu G^a_\mu + g f^{abc} G^b_\mu G^c_\nu, \tag{5.2}$$

where g is the coupling constant and f^{abc} are the structure constants of $SU(3)_c$. The resulting dynamics for quantum chromodynamics produce three sets of interactions. The emission or absorption of a gluon by a quark, the emission or absorption of a gluon by a gluon and the direct interaction of two gluons. It is evident that the color charge of the gluon plays a significant role in these interactions.

Quantum chromodynamics is a much more complicated theory than quantum electrodynamics and it required the development of various techniques to produce results. These include the perturbative approach to quantum chromodynamics, which is based on asymptotic freedom, lattice chromodynamics, which introduces a discretization of spacetime, the $1/N$ expansion approach and many others [84], [85]. Due to the complexity of the theory computational methods are often employed to help with calculations that would otherwise be impossible. Quantum chromodynamics enjoys its share of experimental evidence, such as the discovery of the top quark and the gluon [86],[87].

Once again, as in chapter 3 we will use Feynman rules from a well established quantum field theory to calculate cross sections for the production of quantum black holes. It is the main core of our methodology of treating the exotic quantum black holes with an effective field theory in order to produce results that can help grant insight for a full quantum gravity theory.

5.3 Collisions of two fermions

This example is similar to the one presented in chapter 3, albeit more refined. The colliding fermions could be quarks, with the appropriate color factor, or in the simplest case leptons. The color factor in the quark case is what introduces the extra numerical factors. We will discuss both cases. We start with the Lagrangian:

$$L_{fermion+fermion} = \frac{c}{\bar{M}_p^2}\partial_\mu\partial^\mu\phi\bar{\psi}_1\psi_2 + h.c. \tag{5.3}$$

where c is the (non-local) parameter we will use to match the semiclassical cross section, $\bar{M}_p$ is the reduced Planck mass, ϕ is a scalar field representing the quantum black hole, and ψ_i is a fermion field. In this case the black hole is spinless. The cross section for ϕ production is:

$$\sigma(2\psi \to \phi) = \frac{\pi}{s}\,|A|^2\,\delta(s - M_{BH}^2), \tag{5.4}$$

where M_{BH} is the mass of the black hole, $s = (p_1 + p_2)^2$ and p_1,p_2 are the four-momenta of ψ_1 ψ_2. Depending on whether the incoming particles are quarks or leptons we get a slightly different amplitude, specifically:

$$|A|^2 = s^2\frac{c^2}{4\bar{M}_p^4}[s - (m_1 + m_2)^2], \tag{5.5}$$

for leptons and

$$|A|^2 = s^2 \frac{c^2}{36\bar{M}_p^4}[s - (m_1 + m_2)^2], \tag{5.6}$$

for quarks, where m_1 and m_2 are the masses of the fermions ψ_1 and ψ_2.

We now compare this cross section with the geometrical cross section. We use the representation for the delta-function:

$$\delta(s - M_{BH}^2) = \frac{\Gamma}{4\pi\sqrt{s}[(\sqrt{s} - M_{BH})^2 + \frac{\Gamma^2}{4}]} \tag{5.7}$$

where Γ is the decay width of ϕ. Γ can be calculated using the Lagrangian (5.3) as:

$$\Gamma = \frac{1}{2M} \int \frac{d\Omega}{16\pi^2} \frac{k}{E_{cm}} |A|^2. \tag{5.8}$$

where we integrate over spherical coordinates with k being the momentum for the initial state.

The matrix element used in the calculation of Γ has to do with the decay of the black hole instead of the production. Therefore instead of averaging over initial states we need to sum over final states. This modifies the amplitude accordingly:

$$|A|^2 = s^2 \frac{2c^2}{\bar{M}_p^4}[s - (m_1 + m_2)^2], \tag{5.9}$$

for leptons and

$$|A|^2 = s^2 \frac{6c^2}{\bar{M}_p^4}[s - (m_1 + m_2)^2], \tag{5.10}$$

for quarks. This gives us

$$\Gamma = \frac{c^2 M_{BH}^3 [s - (m_1 + m_2)^2]}{8\pi \overline{M}_P^4}. \tag{5.11}$$

for leptons and

$$\Gamma = \frac{6c^2 M_{BH}^3 [s - (m_1 + m_2)^2]}{16\pi \overline{M}_P^4}. \tag{5.12}$$

for quarks. We can thus find an expression for our non-local parameter c:

$$c = 4\left(\frac{\pi^2 M_P^8(s^{\frac{3}{2}} - 2sM_{BH} + \sqrt{s}M_{BH}^2)}{M_{BH}^3[s-(m_1+m_2)^2]^2(128\pi^2 M_P^4 - \sqrt{s}M_{BH}^3)}\right)^{\frac{1}{4}} \tag{5.13}$$

for leptons and

$$c = 4\left(\frac{\pi^2 M_P^8(s^{\frac{3}{2}} - 2sM_{BH} + \sqrt{s}M_{BH}^2)}{3M_{BH}^3[s-(m_1+m_2)^2]^2(128\pi^2 M_P^4 - 3\sqrt{s}M_{BH}^3)}\right)^{\frac{1}{4}} \tag{5.14}$$

for quarks. If we plug our expressions for c back in the Lagrangian it is fully determined and contains no unknown terms or parameters. For the derivation of the previous equations we used the exact same methodology as in 3, with the only difference being that we now took into account color factors for quarks, hence the double set of results.

5.4 Collisions of a quark and a gluon

This is a more realistic example of a collision for the production of a quantum black hole and more relevant to events at the Large Hadron Collider. The colliding particles have spin and color and instead of producing a black hole that resembles a scalar field they will produce something akin to a quark. The analysis of this example is a bit more complicated but the principles remain the same. Let us start from the Lagrangian:

$$L = \frac{c}{\Lambda}\bar{\Psi}_1\sigma^{\mu\nu}\Psi_2 G_{\mu\nu}, \tag{5.15}$$

where $G_{\mu\nu}$is the gluon field strength tensor, Ψ_1 is the initial quark, Ψ_2 represents the quantum black hole and $\sigma^{\mu\nu}$ is simply the commutator of the gamma matrices. Our Lagrangian once again contains our parameter c and Λ is a scale parameter.

The amplitude for this diagram is derived from the Feynman rules for QCD with ϵ_ν being the polarization vector:

$$A = \bar{u}\frac{c}{\Lambda}i\sigma^{\mu\nu}k_\mu\epsilon_\nu u \tag{5.16}$$

Working in the same way as in chapter 3, with the same completeness relations, we get for the squared amplitude:

$$|A|^2 = Tr(\not{p_1} + m_1)i\sigma^{\mu\nu}k_\mu\epsilon_\nu(\not{p_2} + m_2)(-i)\sigma^{\alpha\beta}k_a\epsilon_\beta \tag{5.17}$$

Another useful relation we will use in our calculation is:

$$\Sigma\epsilon_\nu\epsilon_\beta = \left(-g_{\nu\beta} + \frac{\eta_\nu k_\beta + k_\nu\eta_\beta}{\eta\cdot k} - \frac{\eta^2 k^\nu k^\beta}{(\eta\cdot k)^2}\right), \tag{5.18}$$

which is the sum over polarizations, where ν and k represent the two gluons and η is an auxiliary vector.

In order to simplify the calculation, we will break it down and show that the last two parts of the above expression don't contribute to the cross section.

$$(\not{p}_1 + m_1)\sigma^{\mu\nu}k_\mu(\not{p}_2 + m_2)\sigma^{\alpha\beta}k_\alpha\left(\frac{\eta_\nu k_\beta + k_\nu\eta_\beta}{\eta\cdot k}\right) = \tag{5.19}$$

$$\frac{i}{4\eta\cdot k}(\not{p}_1 + m_1)\sigma^{\mu\nu}k_\mu(\not{p}_2 + m_2)(\gamma^\alpha\gamma^\beta - \gamma^\beta\gamma^\alpha)k_\alpha k_\beta + \frac{i}{4\eta\cdot k}(\not{p}_1 + m_1)(\gamma^\mu\gamma^\nu - \gamma^\nu\gamma^\mu)k_\mu k_\nu(\not{p}_2 + m_2)\sigma^{\alpha\beta}k_\alpha\eta_\beta = 0 \tag{5.20}$$

which is justified because

$$(\gamma^\alpha\gamma^\beta - \gamma^\beta\gamma^\alpha)k_\alpha k_\beta = 0 \tag{5.21}$$

and also

$$(\gamma^\mu\gamma^\nu - \gamma^\nu\gamma^\mu)k_\mu k_\nu = 0 \tag{5.22}$$

Using the same logic the third part disappears as well

$$(\not{p}_1 + m_1)i\sigma^{\mu\nu}k_\mu(\not{p}_2 + m_2)(-i)\sigma^{\alpha\beta}k_\alpha\left(\frac{-\eta^2 k^\nu k^\beta}{(\eta\cdot k)^2}\right) = 0 \tag{5.23}$$

Now the first part doesn't disappear and is a bit complicated but nevertheless by using various tricks and standard Dirac algebra it boils down to a somewhat simpler expression.

$$(\not{p}_1 + m_1)i\sigma^{\mu\nu}k_\mu(\not{p}_2 + m_2)(-i)\sigma^{\alpha\beta}k_a(-g_{\nu\beta}) = \frac{-1}{16}(\not{p}_1 + m_1)(\gamma^\mu\gamma^\nu - \gamma^\nu\gamma^\mu)k_\mu(\not{p}_2 + m_2)(\gamma^\alpha\gamma^\beta - \gamma^\beta\gamma^\alpha)k_\alpha(-g_{\nu\beta}) \propto \tag{5.24}$$

$$(\not{p}_1 + m_1)(\gamma^\mu\gamma^\nu - \gamma^\nu\gamma^\mu)k_\mu(\not{p}_2 + m_2)(\gamma^\alpha\gamma^\nu - \gamma^\nu\gamma^\alpha)k_\alpha, \tag{5.25}$$

where we omit all numerical factors, which will be added at the end.

In order to save ourselves some tedious algebra, we do a quick count of the number of gamma matrices in each term. As we know from trace technology any term with an odd number of gamma matrices disappears, so there is no reason to calculate them explicitly and we can just get rid of them now. Applying this we get:

$$\begin{aligned}(\not{p}_1 + m_1)(\gamma^\mu\gamma^\nu - \gamma^\nu\gamma^\mu)k_\mu(\not{p}_2 + m_2)(\gamma^\alpha\gamma^\nu - \gamma^\nu\gamma^\alpha)k_\alpha = \\ \not{p}_1(\gamma^\mu\gamma^\nu - \gamma^\nu\gamma^\mu)k_\mu\not{p}_2(\gamma^\alpha k_\alpha\gamma_\nu - \gamma_\nu\gamma^\alpha k_\alpha) + \\ m_1m_2(\gamma^\mu\gamma^\nu - \gamma^\nu\gamma^\mu)k_\mu(\gamma^\alpha k_\alpha\gamma_\nu - \gamma_\nu\gamma^\alpha k_\alpha)\end{aligned} \tag{5.26}$$

The above expression can be split in two for simplicity. We will start with the mass term

$$m_1m_2(\gamma^\mu\gamma^\nu\gamma^\alpha\gamma_\nu k_\mu k_\alpha - \gamma^\mu\gamma^\nu\gamma_\nu\gamma^\alpha k_\mu k_\alpha - \gamma^\nu\gamma^\mu\gamma^\alpha\gamma_\nu k_\mu k_\alpha + \gamma^\nu\gamma^\mu\gamma_\nu\gamma^\alpha k_\mu k_\alpha) \tag{5.27}$$

which looks rather difficult but is simplified tremendously using the following formulae

$$\gamma^\nu\gamma^\alpha\gamma_\nu = -2\gamma^\alpha \tag{5.28}$$

$$\gamma^\nu\gamma_\nu = 4I \tag{5.29}$$

$$\gamma^\nu\gamma^\mu\gamma^\alpha\gamma_\nu = 4g^{\mu\alpha} \tag{5.30}$$

$$\gamma^\nu\gamma^\mu\gamma^\alpha\gamma_\nu = -2g^{\mu\alpha} \tag{5.31}$$

and finally gives

$$m_1m_2(-2\gamma^\mu\gamma^\alpha k_\mu k_\alpha - 4\gamma^\mu\gamma^\alpha k_\mu k_\alpha - 4g^{\mu\alpha}k_\mu k_\alpha - 2\gamma^\mu\gamma^\alpha k_\mu k_\alpha) = -48k^2m_1m_2 \tag{5.32}$$

The first term is more difficult in principle but substantially easier after the treatment of the second term. We write every gamma matrix explicitly and thus get the following expression:

$$\gamma^\rho p_{1\rho}(\gamma^\mu\gamma^\nu - \gamma^\nu\gamma^\mu)k_\mu\gamma^\sigma p_{2\sigma}(\gamma^\alpha\gamma_\nu - \gamma_\nu\gamma^\alpha)k_\alpha =$$

$$p_{1\rho}p_{2\sigma}(\gamma^\rho\gamma^\mu\gamma^\nu\gamma^\sigma\gamma^\alpha\gamma_\nu - \gamma^\rho\gamma^\mu\gamma^\nu\gamma^\sigma\gamma_\sigma\gamma^\alpha - \gamma^\rho\gamma^\nu\gamma^\mu\gamma^\sigma\gamma^\alpha\gamma_\nu + \gamma^\rho\gamma^\nu\gamma^\mu\gamma^\sigma\gamma_\nu\gamma^\alpha)k_\mu k_\alpha \quad (5.33)$$

Once again we come up with something terrifying at first look that simplifies when we use the same formulae as before, We get:

$$p_{1\rho}p_{2\sigma}(4\gamma^\rho\gamma^\mu g^{\sigma\alpha} - \gamma^\rho\gamma^\mu(-2\gamma^\sigma)\gamma^\alpha - \gamma^\rho(-2\gamma^\mu\gamma^\sigma\gamma^\alpha) + 4\gamma^\rho g^{\mu\sigma}\gamma^\alpha)k_\mu k_\alpha = \quad (5.34)$$

$$4(\not{p}_1\not{k})(p_2k) + 2(\not{p}_1\not{k})(\not{p}_2\not{k}) + 2(\not{p}_1\not{k})(\not{p}_2\not{k}) + 4\not{p}_1(kp_2)\not{k}. \quad (5.35)$$

The trace of that finally gives

$$96(p_1 \cdot k)(p_2 \cdot k). \quad (5.36)$$

Bringing everything together the total trace is:

$$2(p_1k)(p_2k) - k^2m_1m_2 \quad (5.37)$$

We substitute this in the cross section formula and with a bit of rearranging we get

$$\sigma = \frac{\pi}{4s}\frac{c^2}{\Lambda^2}(s - m_1^2)(-u + M_{BH}^2)\delta(s - M_{BH}^2), \quad (5.38)$$

where s and u are the Mandelstam variables (s is the square of the initial momenta and u is the squared difference of final and initial momenta).

We can see that the field that represents the black hole carries the same quantum numbers as a quark. Again comparing to the geometrical cross section

$$\sigma = \pi r_s^2, \quad (5.39)$$

where r_s is the four-dimensional Schwarzschild radius:

$$r_s(s, \bar{M}_P) = \frac{\sqrt{s}}{4\pi\bar{M}_P^2} \quad (5.40)$$

we find:

$$c^2 = \frac{\Lambda^2(4s^{\frac{7}{2}} - 8s^3 M_{BH} + 4s^{\frac{5}{2}} M_{BH}^2 + s^{\frac{5}{2}}\Gamma^2)}{4\overline{M}_P^4 \pi\Gamma[(s - m_1^2)(-u + M_{BH}^2)]}, \tag{5.41}$$

with the decay width given by:

$$\Gamma = c^2 \frac{M_{BH}^3}{\pi\Lambda^2}. \tag{5.42}$$

which enables us to find a representation for c:

$$c = \left(\frac{4\Lambda^4\pi^2(s^{\frac{7}{2}} - 2s^3 M_{BH} + s^{\frac{5}{2}} M_{BH}^2)}{M_{BH}^3(4\pi^2\overline{M}_P^4(s - m_1^2)(-u + M_{BH}^2) - s^{\frac{5}{2}} M_{BH}^3)} \right)^{\frac{1}{4}}. \tag{5.43}$$

Collecting our results we now have a fully determined Lagrangian, the production cross section for a quantum black hole and the decay width. All this information can be used almost directly to examine the phenomenology of quantum black holes at the Large Hadron Collider.

5.5 Collisions of two gluons

It is evident that our methodogy, although it takes some liberties in writing down a Lagrangian, consists of nothing more than typical QED and QCD calculations. There are no exotic terms and no mountain of divergences to be cured. At first glance this feels rather strange especially when we are dealing with objects such as quantum black holes. We introduce our parameter c which absorbs all the factors pertaining to quantum gravity, that we would otherwise be unable to analyze. This pattern of work has another, not so obvious advantage. We can browse through the literature for similar calculations in order to verify our own or to get a result immediately. This has been done in several steps until now. In chapter 3 we compared our analysis to work done in [59]. In the previous calculation, which was rather tedious, we used [88] to verify our result since the calculation has certain similarities. This is also what we plan to do in the gluon-gluon example.

In this case the intermediate state (the black hole) again resembles a scalar field. We start from the Lagrangian:

$$L = \frac{c}{M_P} \Phi G^{\mu\nu} G_{\mu\nu}, \tag{5.44}$$

where c is our usual parameter, Φ describes the black hole and $G_{\mu\nu}$ is the gluon field strength tensor. We immediately observe it looks quite similar to a Lagrangian describing gluon fusion. We start from two gluons and produce something akin to a scalar field. In our methodology, for all intents and purposes the black hole is a scalar field. It carries the same information and interacts with particles of the Standard Model in the same way. We model the quantum black hole as a field and thus treat it as such. If we follow the work in [89] and simplify for 4 dimensions the calculation is exactly the same and we obtain the cross section:

$$\sigma = \frac{c^2 M_{BH}^2}{4\pi \overline{M}_P^2} \delta(s - M_{BH}^2) \tag{5.45}$$

As in the two previous cases c is given by

$$c^2 = \frac{\pi(4s^{\frac{5}{2}} - 8s^2 M_{BH} + 4s^{\frac{3}{2}} M_{BH}^2 + s^{\frac{3}{2}}\Gamma^2)}{4\Gamma M_{BH}^2 \overline{M}_P^2} \tag{5.46}$$

and the decay width is calculated as

$$\Gamma = \frac{2c^2}{\pi M_P^2} M_{BH}^3. \tag{5.47}$$

We thus find

$$c = \left(\frac{\pi^2 \overline{M}_P^4 (s^{\frac{5}{2}} - 2s^2 M_{BH} + s^{\frac{3}{2}} M_{BH}^2)}{M_{BH}^5 (2\overline{M}_P^4 - M_{BH} s^{\frac{3}{2}})} \right)^{\frac{1}{4}}. \tag{5.48}$$

Once again we have come full circle and determined the value of our parameter c.

5.6 Conclusion

In this chapter we have expanded our formalism, initially developed in chapter 3 for the treatment of quantum black holes. We have given three significant examples where a black hole can be produced from the collision of particles like quarks and gluons. First we revisited the case where a quantum black hole is formed from the collision of two fermions and differentiated between leptons and quarks. Then, we considered the collision of a quark and a gluon where the calculation of the cross section is presented explicitly. Although a bit complicated at certain points, it is still a quantum field theory calculation and the usual techniques are employed to simplify it and reach a result. Finally, we considered the production of a quantum black hole from the collision of two gluons. Having written a Lagrangian almost identical to Higgs production via gluon fusion we examined the results presented in [89] to calculate the cross section. In each case we calculated the cross section for the production of a quantum black hole, compared it to the geometrical case and found an expression for our parameter c. Then it was just a matter of calculating the decay width to complete the analysis, as outlined in section 5.3.

We demonstrated the advantages of our methodology. We showed that even though we examine very exotic objects, quantum black holes, all we need to work with them is well formulated quantum field theories. Quantum electrodynamics and quantum chromodynamics are considered working theories and as such they provide us with the necessary tools to calculate cross sections and decay widths. Our formalism also allows us to approach other subjects of particle physics, in order to probe for quantum gravity effects. Such an effort is presented in the following chapter where we visit the realm of supersymmetry.

We expect that this formalism to treat quantum black holes can be helpful when trying to implement quantum black hole processes in event generators. We emphasize that the Lagrangian we are proposing to describe the interactions of quantum black holes with particles of the Standard Model should not be regarded as an effective theory in the usual sense, it is rather an effective manner to describe the interactions of these black holes with usual particles. In this, more detailed, analysis it becomes clear that the idea of treating quantum black holes as fields gives us a way of approaching a quantum gravity object with physics of the Standard Model. Although this is at best an approximation it can still yield useful results especially if theories that lower the Planck scale to the TeV range prove to be true. The analysis presented in this chapter can serve as the basis for realistic phenomenology, meaning that the theoretical calculations presented here are not too far from what programs such as CalcHep [90] require. In fact, a few trivial considerations can

make the work presented here ready to apply in any computational event generator. For instance, we would have to consider the total decay width, instead of the one we calculated. This can be easily derived as 57 times the decay width of the theoretical calculation. It is our hope that the results presented here will provide the necessary theoretical background for more experimentally driven projects.

Chapter 6

Enhancement of supersymmetric particles production via quantum black holes

6.1 Introduction

So far we have considered quantum black holes and how they can be created from the collisions of Standard Model particles. We have discussed about their quick decay into a few particles, which until now have also been Standard Model particles. In this chapter we consider what other particles we could get as decay products of a quantum black hole. We argue that even if supersymmetry is broken at the Planck scale, the superpartners of the Standard Model particles must couple gravitationally to their Standard Model partners. Quantum black holes are thus a portal into the supersymmetric world. We will show that in models with low scale quantum gravity, supersymmetric particles could be produced with sizable cross sections at the 14 TeV Large Hadron Collider.

Since we are now entering the realm of supersymmetry we need to adjust our pool of data to include all supersymmetric particles. First we calculate the branching ratios for the decomposition of black holes created by the same initial state particles. This is nothing more than the ratio of the number of possible states for each interaction divided with the total number of states. The number of possible states is counted using the Clebsh-Gordan coefficients. As expected, if we add all the branching ratios for each table we get 1, meaning all states have been considered. The resulting branching ratios were then plugged in a Monte Carlo integration algorithm developed by Nina Gausmann to produce the coresponding cross sections.

6.2 Basics of Supersymmetry

Supersymmetry is a proposed extension to the Standard Model that transforms fermions into bosons and vice versa. As the name suggests, it is an expansion of the spacetime symmetries of quantum field theory, specifically the Poincare symmetry [91]. Supersymmetry introduces a host of new particles, the superpartners of the Standard Model particles, that have the same quantum numbers as their partners except spin, which differs by a half-integer. It is considered a spontaneously broken symmetry, since no supersymmetric particles have yet been observed. It is one of the main candidates for theories beyond the Standard Model and if proven correct would address a number of open issues in particle physics.

Motivation for supersymmetry

Supersymmetry is at a strange stage at the moment. The lack of observations that would validate the theory, in particle accelerators like the Large Hadron Collider, is alarming, yet it is a heavily motivated theory that would solve several problems. One of the main motivations for supersymmetry is the hierarchy problem, particularly why is the Higgs boson so much lighter than the Planck mass. Quantum corrections are supposed to make the mass very large and an extreme fine-tuning is required to bring it back in line. The corrections are a result of the Higgs boson splitting into a quark-antiquark pair and are given by [92]:

$$m_{H^0}^2 = 2m^2 + c(\tilde{\alpha}/4\pi)\Lambda^2, \tag{6.1}$$

where m_{H^0} is the observed Higgs mass, m is the bare Higgs mass parameter, $\tilde{\alpha}$ is the coupling constant c is a constant and Λ is the cut-off energy. Λ has to be of the same order as the electroweak scale. Since the mass of the $W^{\pm}$ boson is connected to the Higgs mass, when Λ grows so should m_{H^0} and $m_{W^{\pm}}$, but experimental results suggest that this is not the case. That makes it impossible for the Higgs mass to be as large as the quantum corrections would require. A not so popular way to address this issue is to fine-tune the problem. One could choose an extremely specific value for the bare mass in order to cancel out the large corrections. Although technically correct this practice is doubtful, since a precision fix of the order of 10^{-24} just doesn't look very physical. Other motivations for supersymmetry include [92, 93] that it provides a candidate particle for dark matter, a mechanism for electroweak symmetry breaking and beautifully unifies the weak, strong

and electromagentic interactions. It is also a requirement for superstring theory, making it that much more desirable. Lastly it allows us to circumvent the Coleman-Mandula theorem which states that [94]"spacetime and internal symmetries cannot be combined in any but a trivial way". The resulting Haag-Lopuszanski-Sohnius theorem [95] shows how supersymmetry allows spacetime and internal symmetries to be consistently combined.

The Minimal Supersymmetric Standard Model

The simplest supersymmetric extension to the Standard Model is the Minimal Supersymmetric Standard Model. It dictates that the number of fermionic degrees of freedom must be equal to the number of bosonic degrees of freedom. It introduces a plethora of new particles, the superpartners of the typical Standard Model particles [92]. The superpartners of the quarks and leptons are the squarks and sleptons, which are scalar particles with spin 0. The superpartners of the gluons are the gluinos with spin 1/2 and the superpartners of the $W^{\pm}$ Z^0 and γ bosons are the gauginos with spin 1/2. The Higgsinos, with spin 1/2, are also introduced as the superpartners of the Higgs sector in the Minimal Supersymmetric Standard Model. Linear combinations of Higgsinos and gauginos produce two charginos ($\tilde{X}_1^{\pm}, \tilde{X}_2^{\pm}$) and four neutralinos ($\tilde{X}_1^0, \tilde{X}_2^0, \tilde{X}_3^0$ and $\tilde{X}_4^0$).

Supersymmetry allows a new quantum number called R-parity. As a symmetry, acting on the Minimal Supersymmetric Standard Model, it forbids the couplings that would violate lepton and baryon number. It is defined as [92]:

$$P_R = (-1)^{2s+3B+L}, \tag{6.2}$$

where s is the spin, B is the baryon number and L is the lepton number. Standard Model particles have R-parity 1 and supersymmetric particles have R-parity -1. If R-parity is conserved supersymmetric particles can only be produced in pairs and the lightest particle (LSP) cannot decay [96]. This lightest particle is one of the candidates for dark matter. It interacts only through gravity and the weak interaction and is commonly called a weakly interacting massive particle (WIMP) [96].

Supersymmetry breaking

If supersymmetry was unbroken the superpartners would have been observed by now. Therefore we assume that supersymmetry is a broken symmetry. A great deal of effort is dedicated to discovering how is supersymmetry broken, while retaining its useful properties such as the cancellation of the quadratic divergences in the Higgs mass. This

requirement gives the name soft supersymmetry breaking [96]. In broken supersymmetric models the divergences don't disappear completely but are, instead of quadratic, logarithmic and proportional to the mass difference between the particles of a supersymmetry multiplet [96]. This has as a result that the squark masses cannot be much larger than 1 TeV and consequently should be observed at the Large Hadron Collider. The most popular mechanisms for soft supersymmetry breaking are the gravity-mediated supersymmetry breaking [96], which communicates supersymmetry breaking to the supersymmetric Standard Model through gravitational interactions and gauge mediated supersymmetry breaking [96], which communicates supersymmetry breaking to the supersymmetric Standard Model through gauge interactions.

Cross sections for the production of supersymmetric particles

We list a few supersymmetry production cross sections, some of which we will use to compare with the cross section for the production of supersymmetric particles via a quantum black hole. The quantity t which appears frequently in the following expressions is the Mandelstam variable defined as the squared difference of initial and final momenta. We start with gluino pair production from two gluons [97]:

$$\frac{d\sigma}{dt}(gg \to \tilde{g}\tilde{g}) = \frac{9\pi\alpha_s^2}{4s^2}\{\frac{2(m_{\tilde{g}}^2 - t)(m_{\tilde{g}}^2 - u)}{s^2} + \frac{(m_{\tilde{g}}^2 - t)(m_{\tilde{g}}^2 - u) - 2m_{\tilde{g}}^2(m_{\tilde{g}}^2 + t)}{(m_{\tilde{g}}^2)^2} + \frac{(m_{\tilde{g}}^2 - t)(m_{\tilde{g}}^2 - u) - 2m_{\tilde{g}}^2(m_{\tilde{g}}^2 + u)}{(m_{\tilde{g}}^2)^2} + \frac{m_{\tilde{g}}^2(s - 4m_{\tilde{g}}^2)}{(m_{\tilde{g}}^2 - t)(m_{\tilde{g}}^2 - u)} - \frac{(m_{\tilde{g}}^2 - t)(m_{\tilde{g}}^2 - u) + m_{\tilde{g}}^2(u - t)}{s(m_{\tilde{g}}^2 - t)} - \frac{(m_{\tilde{g}}^2 - t)(m_{\tilde{g}}^2 - u) + m_{\tilde{g}}^2(t - u)}{s(m_{\tilde{g}}^2 - u)}\}, \tag{6.3}$$

where s,t,u are the Mandelstam variables and α_s is the strong fine structure constant. Gluino pairs can also be produced from a quark-antiquark interaction [97]:

$$\frac{d\sigma}{dt}(q\bar{q} \to \tilde{g}\tilde{g}) = \frac{8\pi\alpha_s^2}{9s^2}\{\frac{4}{3}\left(\frac{m_{\tilde{g}}^2 - t}{m_{\tilde{q}}^2 - t}\right)^2 + \frac{4}{3}\left(\frac{m_{\tilde{g}}^2 - u}{m_{\tilde{q}}^2 - u}\right)^2 + \frac{3}{s^2}[(m_{\tilde{g}}^2 - t)^2 + (m_{\tilde{g}}^2 - u)^2 + 2m_{\tilde{g}}^2 s] - 3\frac{[(m_{\tilde{g}}^2 - t)^2 + m_{\tilde{g}}^2 s]}{s(m_{\tilde{q}}^2 - t)} - 3\frac{[(m_{\tilde{g}}^2 - u)^2 + m_{\tilde{g}}^2 s]}{s(m_{\tilde{q}}^2 - u)} + \frac{1}{3}\frac{m_{\tilde{g}}^2 s}{(m_{\tilde{q}}^2 - t)(m_{\tilde{q}}^2 - u)}\}. \tag{6.4}$$

Finally, gluinos can be produced in association with squarks [97]:

$$\frac{d\sigma}{dt}(gq \to \tilde{g}\tilde{q}_i) = \frac{\pi\alpha_s^2}{24s^2}\frac{\left[\frac{16}{3}(s^2+(m_{\tilde{q}_i}^2-u)^2)+\frac{4}{3}s(m_{\tilde{q}_i}^2-u)\right]}{s(m_{\tilde{g}}^2-t)(m_{\tilde{q}_i}^2-u)^2}\times \left((m_{\tilde{g}}^2-u)^2+(m_{\tilde{q}_i}^2-m_{\tilde{g}}^2)^2+\frac{2sm_{\tilde{g}}^2(m_{\tilde{q}_i}^2-m_{\tilde{g}}^2)}{m_{\tilde{g}}^2-t}\right). \tag{6.5}$$

Moving on to the production of squarks there are several cross sections depending on the various squark types [97]. We start with the production of a squark-antisquark pair from two gluons:

$$\frac{d\sigma}{dt}(gg \to \tilde{q}_i\bar{\tilde{q}}_i) = \frac{\pi\alpha_s^2}{4s^2}\{\frac{1}{3}\left(\frac{m_{\tilde{q}}^2+t}{m_{\tilde{q}}^2-t}\right)^2+\frac{1}{3}\left(\frac{m_{\tilde{q}}^2+u}{m_{\tilde{q}}^2-u}\right)^2+ \frac{3}{32s^2}(8s(4m_{\tilde{q}}^2-s)+4(u-t)^2)+\frac{7}{12}-\frac{1}{48}\frac{(4m_{\tilde{q}}^2-s)^2}{(m_{\tilde{q}}^2-t)(m_{\tilde{q}}^2-u)}+ \frac{3}{32}\frac{[(u-t)(4m_{\tilde{q}}^2+4t-s)-2(m_{\tilde{q}}^2-u)(6m_{\tilde{q}}^2+2t-s)]}{s(m_{\tilde{q}}^2-t)}+ \frac{3}{32}\frac{[(t-u)(4m_{\tilde{q}}^2+4u-s)-2(m_{\tilde{q}}^2-t)(6m_{\tilde{q}}^2+2u-s)]}{s(m_{\tilde{q}}^2-u)}+ \frac{7}{96}\frac{(4m_{\tilde{q}}^2+4t-s)}{m_{\tilde{q}}^2-t}+\frac{7}{96}\frac{4m_{\tilde{q}}^2+4u-s}{m_{\tilde{q}}^2-u}\}. \tag{6.6}$$

Squarks are also produced from quark-antiquark pairs. There are several different cross sections depending on factors like flavor and type [97]. If the initial and final state flavors are the same, the cross section is:

$$\frac{d\sigma}{dt}(q\bar{q} \to \tilde{q}_i\bar{\tilde{q}}_i) = \frac{2\pi\alpha_s^2}{9s^2}\left(\frac{1}{(t-m_{\tilde{g}}^2)^2}+\frac{2}{s^2}-\frac{2/3}{s(t-m_{\tilde{g}}^2)}\right)\times[-st-(t-m_{\tilde{q}_i}^2)^2]. \tag{6.7}$$

If initial and final state flavors are different, the cross section is:

$$\frac{d\sigma}{dt}(q\bar{q} \to \tilde{q_i'}\bar{\tilde{q_i'}}) = \frac{4\pi\alpha_s^2}{9s^4}[-st-(t-m_{\tilde{q_i'}}^2)^2]. \tag{6.8}$$

If the two initial state quarks are of different flavors then the cross section is:

$$\frac{d\sigma}{dt}(q\bar{q'} \to \tilde{q}_i\bar{\tilde{q}_i'}) = \frac{2\pi\alpha_s^2}{9s^2}\frac{[-st-(t-m_{\tilde{q}_i}^2)^2]}{(t-m_{\tilde{g}}^2)^2}. \tag{6.9}$$

If the initial quarks are of different flavor and the final state squarks are of different type, the cross section is:

$$\frac{d\sigma}{dt}(q\bar{q'} \to \tilde{q_i}\bar{\tilde{q_j'}}) = \frac{2\pi\alpha_s^2}{9s^2}\frac{m_{\tilde{g}}^2 s}{(t-m_{\tilde{g}}^2)^2}. \tag{6.10}$$

If the initial state quarks have the same flavor and final state quarks are of different type, the cross section is:

$$\frac{d\sigma}{dt}(q\bar{q} \to \tilde{q_i}\bar{\tilde{q_j}}) = \frac{2\pi\alpha_s^2}{9s^2}\frac{m_{\tilde{g}}^2 s}{(t-m_{\tilde{g}}^2)^2}. \tag{6.11}$$

Finally, quark-quark annihilation can lead to squark pairs. If the initial state quarks have the same flavor and the final state squarks have the same flavor and type, the cross section is:

$$\frac{d\sigma}{dt}(qq \to \tilde{q_i}\tilde{q_i}) = \frac{\pi\alpha_s^2}{9s^2}m_{\tilde{g}}^2 s\left(\frac{1}{(t-m_{\tilde{g}}^2)^2} + \frac{1}{(u-m_{\tilde{g}}^2)^2} - \frac{2/3}{(t-m_{\tilde{g}}^2)(u-m_{\tilde{g}}^2)}\right). \tag{6.12}$$

If the initial state quarks have the same flavor and the final state squarks are of different type, the cross section is:

$$\frac{d\sigma}{dt}(qq \to \tilde{q_i}\tilde{q_j}) = \frac{2\pi\alpha_s^2}{9s^2}\left(\frac{[-st-(t-m_{\tilde{q}_i}^2)(t-m_{\tilde{q}_j}^2)]}{(t-m_{\tilde{g}}^2)} + \frac{[-su-(u-m_{\tilde{q}_i}^2)(u-m_{\tilde{q}_j}^2)]}{u-m_{\tilde{g}}^2}\right) \tag{6.13}$$

If the initial and final state quarks have different flavors but the final state squarks are of the same type, the cross section is:

$$\frac{d\sigma}{dt}(qq' \to \tilde{q_i}\tilde{q_i'}) = \frac{2\pi\alpha_s^2}{9s^2}\frac{m_{\tilde{g}}^2 s}{(t-m_{\tilde{g}}^2)^2}. \tag{6.14}$$

Lastly, if the initial state quark flavors are different and the final state squarks are of different types, the cross section is:

$$\frac{d\sigma}{dt}(qq' \to \tilde{q_i}\tilde{q_j'}) = \frac{2\pi\alpha_s^2}{9s^2}\frac{[-st-(t-m_{\tilde{q}_i}^2)(t-m_{\tilde{q}_j}^2)]}{(t-m_{\tilde{g}}^2)^2}. \tag{6.15}$$

There are many more processes with their corresponding cross sections, but we chose to list the most basic ones. They can serve as a basis for comparison to the production of superparticles through quantum black holes.

Experimental status

Supersymmetry is a theory with a very active experimental search effort. It is constrained by, and at the same time looked for, in low energy experiments as well as high energy particle interactions taking place at colliders. These include measurements of precision electroweak observables such as [98] the anomalous magnetic moment of the muon and limits on rare B-meson and K-meson decays, limits on electric dipole moments and limits on proton decay. Supersymmetric particles were looked for at the Large Electron-Positron Collider, the Tevatron and the Large Hadron Collider with no detection so far [98]. We also get constraints on supersymmetry models from astronomical observations like dark matter density measurements [98]. While supersymmetry hasn't been ruled out yet with current experimental constraints, a number of results hint that a revision may soon be required [98]. The value for the mass of the Higgs boson, recently discovered at the Large Hadron Collider, is considered too large for supersymmetry and requires specific circumstances to be allowed. Also deviations of Higgs couplings, especially in their gamma-gamma final state could prove problematic for supersymmetry models. It is hoped that the newest results from the Large Hadron Collider, which will operate at higher energies, or experiments from the proposed Super Large Hadron Collider will provide a clear answer one way or another.

6.3 Methodology

The Large Hadron Collider is accumulating data at an impressive pace but unfortunately, as we mentioned earlier, there is so far no indication of physics beyond the Standard Model. On the contrary, the discovery of a Higgs boson at 125 GeV would fit very nicely with the Standard Model and may be an indication that the hierarchy problem was not the correct principle to guide us towards physics beyond the Standard Model. While time will tell whether it is a fatal one, the lack of observation at the Large Hadron Collider of new particles beyond the Standard Model ones is a blow to models designed to stabilize the value of the Higgs mass at the weak scale. It is particularly serious for supersymmetric models whose raison d'etre is precisely to stabilize the Higgs potential which comes at the expense of introducing a plethora of new particles and some peculiar model building to break supersymmetry.

One could argue that supersymmetry is useful to unify the gauge couplings of the Standard Model and give up the hierarchy problem as suggested in [99, 100] but it has

been demonstrated recently that threshold corrections, whether they are due to quantum gravitational physics or strong dynamics above the unification scale, can account very nicely for the numerical unification of these couplings without having to introduce new particles below the grand unification scale [101].

While supersymmetry may not be relevant at the weak scale, it has been recently emphasized that this symmetry is important for quantum gravity [102]. However, below the Planck scale, this symmetry could be broken, as jokingly suggested in the supersplit supersymmetry paper [103].

In this chapter we advocate that even if supersymmetry is broken at a very high energy scale and even in a supersplit scenario, the particles of that sector must interact gravitationally with the particles of the Standard Model. In particular, quantum black holes must be able to mediate transitions from our sector, i.e. the Standard Model, to the hidden supersector. In order to illustrate our point, we shall consider the Minimal Supersymmetric Standard Model with all supersymmetric particles, extra Higgs boson as well, having masses of the order of the Planck scale. Actually, quantum black holes could be a gateway to any hidden sector that interacts only gravitationally with the particles of the Standard Model. Of course, if supersymmetry is restored at the Planck scale, then besides being produced via quantum black holes, superpartners of the Standard Model particles will be produced via the well studied processes. Quantum black holes will lead to an enhancement of the cross sections and allow the expansion of the search for superpartners beyond the expected reach of the Large Hadron Collider in traditional supersymmetric searches. The black hole production cross section is given, as we shall see below, by the geometric cross section and is thus much larger than any usual particle physics cross section.

While models with low scale quantum gravity [24, 25, 26, 27] have been introduced to address the hierarchy problem, the real value in these ideas was to show that we do not know from first principles the energy scale at which quantum gravitational effects become strong. Indeed, the Planck scale could be anywhere between a few TeV and the traditional 10^{18} GeV.

If the Planck scale is low, and accessible to the Large Hadron Collider, supersymmetric particles must be produced in quantum black hole processes as well. By quantum black holes we understand non-thermal small black holes with masses close to the Planck scale. While it is now well understood that semi-classical black holes, with masses 5 to 20 times larger than the Planck scale, cannot be produced at the LHC because this collider is not

energetic enough even if the Planck mass is at a few TeVs [28], the possibility remains to produce non-thermal quantum black holes [29].

Most of the time the black holes which are created carry a $SU(3)_c$ charge and come in different representations of $SU(3)_c$ as well as QED charges. This allows to predict how they will be produced or decay.

We assume that the production cross section can be extrapolated from the semi-classical one:

$$\begin{aligned}\sigma^{pp}(s, x_{min}, n, M_D) &= \int_0^1 2zdz \int_{\frac{(x_{min}M_D)^2}{y(z)^2 s}}^1 du \int_u^1 \frac{dv}{v} \\ &\times F(n)\pi r_s^2(us, n, M_D) \sum_{i,j} f_i(v, Q) f_j(u/v, Q)\end{aligned} \tag{6.16}$$

where M_D is the n dimensional reduced Planck mass, $z = b/b_{max}$, $x_{min} = M_{BH,min}/M_D$, n is the number of extra-dimensions, $F(n)$ and $y(z)$ are the factors introduced by Eardley and Giddings [6] and by Yoshino and Nambu [81]. The n dimensional Schwarzschild radius is given by

$$r_s(us, n, M_D) = k(n) M_D^{-1} [\sqrt{us}/M_D]^{1/(1+n)} \tag{6.17}$$

where

$$k(n) = \left[2^n \sqrt{\pi}^{n-3} \frac{\Gamma((3+n)/2)}{2+n} \right]^{1/(1+n)} . \tag{6.18}$$

The fact that quantum black holes are non-thermal is reflected in the assumption that they decay only to a few particles immediately after their creation.

The production cross sections will be as in [29] and are given in Table (6.1) for a Planck mass of 3 TeV and a 14 TeV LHC assuming that the first quantum black hole has a mass of 3 TeV. On the other hand, the particle spectrum of supersymmetric theories is much richer than in the Standard Model and the branching ratios calculated in [29, 104] have to be revisited. Note that here we are not using the term branching ratio in its usual sense since we use it to describe the decomposition of a collection of black holes created by the same initial state particles.

Assuming that the particle spectrum at the Planck scale is that of the Minimal Supersymmetric Standard Model, we obtain the branching ratios which can be found in Tables (6.3) to (6.10). Obviously, the branching ratios are strongly dependent on the symmetries

Models	RS	ADD $n = 5$	ADD $n = 6$	ADD $n = 7$	4 dim
σ(p+p $\to$ any QBH) in fb	4.41×10^2	7.94×10^3	1.06×10^4	1.35×10^4	16.83

Table 6.1: LHC Cross sections for the production of quantum black holes for a center of mass energy of 14 TeV [29]. We took a reduced Planck scale of 3 TeV for illustration purposes.

which are preserved by quantum gravity. Here we are as conservative as possible and assume that gauge symmetries, flavor symmetries, B-L number and Lorentz invariance are conserved.

When considering spin addition and conservation we take all particles to be massless, which justifies the Clebsh-Gordan coefficients we have used. In a collision of two fermions $(1/2 \times 1/2)$, the spin-1 state is three times more likely to form than the spin-0 state. If a boson collides with a fermion, the spin-1/2 state is just half as likely to form compared to the spin-3/2 state and for two gluons the spin state ratio for the spin-0, spin-1 and spin-2 is 2:3:7. All spin factors are displayed in Table 6.2.

Table 6.2: **Spin factors** for massless particles, determined by Clebsch-Gordon-coefficients

	0	1/2	1
0	0	1/2	1
1/2		0 , 1 1 : 3	1/2 , 3/2 1 : 2
1			0 , 1 , 2 2 : 3 : 7

The cross section for a specific final state is obtained by summing over the production cross sections of the contributing quantum black holes which have been multiplied with the desired branching ratio (cf. Tables 6.3-6.10):

$$\sigma_{\text{QBH}\to\text{final state}} = \sum_{\substack{\text{average}\\ \text{initial states}}} \sigma_{\text{initial state}\to\text{QBH}} \times \text{BR}_{\text{final state}} \,.$$

Each cross section for a specific initial state was calculated via equation (6.16) using a Monte Carlo integration algorithm. We then multiply the result by the suitable branching ratios. The desired cross section for the chosen final state is given by taking the average over all initial state contributions. We considered an ADD brane world model with 5,6 and

7 extra dimensions [24], the Randall Sundrum model [25] with one warped extra dimension and for a four dimensional model with TeV quantum gravity model presented in [26].

We also consider quantum black holes with discrete masses. In that case the cross section is given by [70, 104]:

$$\sigma^{pp}_{tot}(s,n,M_D) \;=\; \sum_i \sigma^{pp}_{QBH}(s,M^i_{QBH},n,M_D)\,. \tag{6.19}$$

Each individual production cross section in the discrete case has the following form:

$$\begin{aligned}\sigma^{pp}_{QBH}(s,M_{QBH},n,M_D) \;=\; & \pi r_s^2(M^2_{QBH},n,M_D)\int_0^1 2zdz\int_{\frac{(M_{QBH})^2}{y(z)^2 s}}^1 du\int_u^1\frac{dv}{v} \\ & \times F(n)\sum_{i,j} f_i(v,Q)f_j(u/v,Q)\end{aligned} \tag{6.20}$$

where M_{QBH} is the mass of the black hole, respectively. For the Schwarzschild radius, we take

$$r_s(M^2_{QBH},n,M_D) = k(n)M_D^{-1}[M_{QBH}/M_D]^{1/(1+n)} \tag{6.21}$$

and $k(n)$ remains the same as in the continuous case. Assuming that space-time is quantized at short distances and that there is a minimal length [72], the mass distribution is expected to be partitioned in terms of the Planck mass. As before, the cross section for a specific final state is obtained by summing over the production cross sections of the contributing quantum black holes which have been multiplied with the desired branching ratio Tables (6.3) to (6.10):

$$\sigma_{\text{QBH}\to\text{final state}} = \sum_{\substack{\text{average}\\ \text{initial states}}}\sum_{\text{masses}} \sigma_{\text{initial state}\to\text{QBH}_{\text{mass}}}\times \text{BR}_{\text{final state,model}}\,.$$

For the sake of illustration we take a Planck mass of 3 TeV and a center of mass energy of 14 TeV. The minimal quantum black hole mass is 3 TeV and we set all the Yoshino and Nambu functions to one. We find that if the reduced Planck scale is in the TeV region, the cross section for the production of superpartners could be quite large even in a supersplit scenario, indeed they are typically large at least for the continuous black hole mass scenario. The production cross section for each decay mode is obtained by multiplying the production cross section for quantum black holes in a given model and multiplying it by the appropriate branching ratio. Note that the conservation laws we

have chosen allow transitions of the type $uu \to \tilde{u}\tilde{u}$ which look like a symmetry violating operator. One should, however, keep in mind that these operators are only relevant for energies $\sqrt{s} \sim M_P$ since there is a threshold energy for the production of quantum black holes. These effective operators could, however, become problematic if inserted into loops. Since very little is known about quantum gravity and the physics of these most quantum black holes, we choose not to worry about it. It could be that these holes do not couple to long wavelength and highly off-shell perturbative modes are suppressed or that B is conserved in these processes. In the latter case, quantum black holes formed by two quarks would always decay back to two quarks, while quantum black holes formed by a gluon and a (anti-) quark, two gluons or a quark and and anti-quark would still be allowed to decay into the superpartners of Standard Model particles. The numerical cross sections for the different final states allowed in our model can be found in the tables in the following section. The continuous mass case cross sections in Tables (6.11) to (6.14) are obviously larger than the one obtained for a discrete mass spectrum (see Tables (6.15) to (6.18)).

Note that if the supersymmetric particles all have masses equal to the Planck scale, i.e. 3 TeV in the value we took to illustrate our framework, the signature for supersymmetric particles would be quite different from usual ones. While they will be produced via the well studied typical supersymmetric production mechanism, they will principally be produced via quantum black hole processes. Note that quantum black holes with masses smaller than twice the Planck scale would not decay into the supersymmetric sector as there is no phase space available. For heavier black holes, in our example heavier than 6 TeV, they would be able to decay to two supersymmetric objects which would decay quickly to two standard model particles and an extra supersymmetric one via the usual supersymmetric decay channels. This production mechanism is very different from the standard ones and dedicated searches should be considered.

6.4 Enhancement of the cross section

In this section we will explicitly calculate and compare the cross sections for the production of supersymmetric particles via normal processes and via a quantum black hole. We will use a simple example to illustrate our point. If we consider the interaction of two quarks with the same flavor, the cross section for final state squarks of different type is [97]:

$$\frac{d\sigma}{dt}(q\bar{q} \to \tilde{q}_i\bar{\tilde{q}}_j) = \frac{2\pi\alpha_s^2}{9s^2}\frac{m_{\tilde{g}}^2 s}{(t-m_{\tilde{g}}^2)^2}, \tag{6.22}$$

where α_s is the strong fine structure constant with a value of 0.089, $m_{\tilde{g}} = 3\text{TeV}$ and $\sqrt{s} = 14\text{TeV}$. If we integrate for t we get:

$$\sigma_1 - \sigma_0 = \left[-\frac{2}{9} \frac{\pi \alpha_s^2 m_{\tilde{g}}^2}{s(t - m_{\tilde{g}}^2)} \right]_{t_0}^{t_1}. \tag{6.23}$$

For the limits of the integral we use the expression for t in the center-of-mass frame [105]:

$$t = (E_{1cm} - E_{3cm})^2 - (p_{1cm} - p_{3cm})^2 - 4p_{1cm}p_{3cm}sin^2(\theta_{cm}/2) = \\ t_0 - 4p_{1cm}p_{3cm}sin^2(\theta_{cm}/2), \tag{6.24}$$

where particle 1 and particle 2 represent the initial states and paricle and particle 4 the final states. θ_{cm} is the angle between particle 1 and particle 3. To produce the limits we need for our integral we calculate the values t_0 for $\theta_{cm} = 0$ and t_1 for $\theta_{cm} = \pi$. We find:

$$t_0 = \left[\frac{m_1^2 - m_3^2 - m_2^2 + m_4^2}{2\sqrt{s}} \right]^2 - (p_{1cm} - p_{3cm})^2 \tag{6.25}$$

$$t_1 = \left[\frac{m_1^2 - m_3^2 - m_2^2 + m_4^2}{2\sqrt{s}} \right]^2 - (p_{1cm} + p_{3cm})^2 \tag{6.26}$$

The center-of-mass energy for all particles is derived from the following expressions [105]:

$$E_{1cm} = \frac{s + m_1^2 - m_2^2}{2\sqrt{s}}, \tag{6.27}$$

$$E_{2cm} = \frac{s + m_2^2 - m_1^2}{2\sqrt{s}}, \tag{6.28}$$

$$E_{3cm} = \frac{s + m_3^2 - m_4^2}{2\sqrt{s}}, \tag{6.29}$$

$$E_{4cm} = \frac{s + m_4^2 - m_3^2}{2\sqrt{s}}, \tag{6.30}$$

while for the momenta [105]:

$$p_{icm} = \sqrt{E_{icm}^2 - m_i^2}. \tag{6.31}$$

If we substitute all the numbers we find the following values for the cross section:

$$\sigma = 0.27 \times 10^{-4} fb \tag{6.32}$$

Now we do the same calculation for the same supersymmetric particles created from the decay of a quantum black hole. As in chapter 3 we use the geometrical cross section:

$$\sigma_{QBH} = \pi r_s^2 \times (BR), \tag{6.33}$$

where:

$$r_s = \frac{\sqrt{s}}{4\pi M_P^2} \tag{6.34}$$

is the Schwarzschild radius and we have also input the relevant branching ratio since we are examining a specific set of interactions. Substituting all the numbers we find:

$$\sigma_{QBH} = 0.97 \times 10^{-2} fb \tag{6.35}$$

We notice that there is an enhancement of at least order 100. The enhancement is even larger when one considers all the possible interactions. It shouldn't be surprising as a result since the method of breaching the hidden sector of supersymmetry in this manner is quite different from the usual methods supersymmetry searches use.

6.5 Conclusion

In this chapter we discussed supersymmetric particles as decay products of a quantum black hole and argued that they must couple gravitationally to their Standard Model partners, even if supersymmetry is broken below the Planck scale. Thus, we considered quantum black holes as an indirect route to any hidden sector that interacts only gravitationally with Standard Model particles. In fact, our methodology leads to an enhancement in the cross sections relevant to the detection of supersymmetric particles. We extrapolated the cross section from the semiclassical case and calculated a series of branching ratios describing the decay of a collection of black holes created by the same initial particles. We took a rather conservative approach, conserving all major symmetries and considered both a continuous and discrete mass spectrum for the black holes and came up with a larger cross section for the continuous case. Completing our analysis we reached the result that supersymmetric particles could be produced with large cross sections at the 14 TeV Large Hadron Collider, albeit with different signatures from standard supersymmetric searches.

6.6 Tables

Table 6.3: **QBH** (u, u, 4/3)

Particle 1	Particle 2	Branching Ratios
u	u	80%
$\tilde{u}$	$\tilde{u}$	20%

Table 6.4: **QBH** (d, d, -2/3)

Particle 1	Particle 2	Branching Ratios
d	d	80%
$\tilde{d}$	$\tilde{d}$	20%

Table 6.5: **QBH** (u, d, 1/3)

Particle 1	Particle 2	Branching Ratios
u	d	80%
$\tilde{u}$	$\tilde{d}$	20%

Table 6.6: **QBH** (u, $\bar{d}$, 1)

Particle 1	Particle 2	Branching Ratios
u	$\bar{d}$	80%
$\tilde{u}$	$\tilde{\bar{d}}$	20%

Table 6.7: **QBH** (u, g, 2/3)

Particle 1	Particle 2	Branching Ratios
u	g	54.55%
u	γ	6.82%
u	Z^0	6.82%
u	H	1.52%
u	G	3.03%
$\tilde{u}$	$\tilde{g}$	18.18%
$\tilde{u}$	$\tilde{\gamma}$	2.27%
$\tilde{u}$	$\tilde{Z^0}$	2.27%
$\tilde{u}$	$\tilde{H}$	1.52%
$\tilde{u}$	$\tilde{G}$	3.03%

Table 6.8: **QBH** (q_i, $\bar{q_i}$, 0)

Particle 1	Particle 2	Branching Ratio	Particle 1	Particle 2	Branching Ratios
u	$\bar{u}$	20.52%	$\tilde{u}$	$\tilde{\bar{u}}$	5.13%
d	$\bar{d}$	20.52%	$\tilde{d}$	$\tilde{\bar{d}}$	5.13%
l^-	l^+	2.28%	$\tilde{l^-}$	$\tilde{l^+}$	0.57%
ν	$\bar{\nu}$	2.28%	$\tilde{\nu}$	$\tilde{\bar{\nu}}$	0.57%
g	g	4.28%	$\tilde{g}$	$\tilde{g}$	4.28
g	γ	3.8%	$\tilde{g}$	$\tilde{\gamma}$	3.8%
g	Z^0	3.8%	$\tilde{g}$	$\tilde{Z^0}$	3.8%
g	H	2.85%	$\tilde{g}$	$\tilde{H}$	2.85%
g	G	3.26%	$\tilde{g}$	$\tilde{G}$	2.44%
γ	γ	0.48%	$\tilde{\gamma}$	$\tilde{\gamma}$	0.48%
γ	Z^0	0.48%	$\tilde{\gamma}$	$\tilde{Z^0}$	0.48%
γ	H	0.36%	$\tilde{\gamma}$	$\tilde{H}$	0.36%
γ	G	0.4%	$\tilde{\gamma}$	$\tilde{G}$	0.3%
Z^0	Z^0	0.43%	$\tilde{Z^0}$	$\tilde{Z^0}$	0.48%
Z^0	H	0.36%	$\tilde{Z^0}$	$\tilde{H}$	0.36%
Z^0	G	0.4%	$\tilde{Z^0}$	$\tilde{G}$	0.3%
H	H	0.12%	$\tilde{H}$	$\tilde{H}$	0.12%
G	G	0.76%	$\tilde{G}$	$\tilde{G}$	0.19%
W^-	W^+	0.48%	$\tilde{W^-}$	$\tilde{W^+}$	0.48%

Table 6.9: **QBH** (q_i, $\bar{q_j}$, 0)

Particle 1	Particle 2	Branching Ratios
q_i	$\bar{q_j}$	80%
$\tilde{q_i}$	$\tilde{\bar{q_j}}$	20%

Table 6.10: **QBH** (g, g, 0)

Particle 1	Particle 2	Branching Ratio	Particle 1	Particle 2	Branching Ratios
q_i	$\bar{q}_i$	17.32%	$\tilde{q}_i$	$\tilde{\bar{q}}_i$	11.54%
l^-	l^+	0.51%	$\tilde{l^-}$	$\tilde{l^+}$	0.34%
ν	$\bar{\nu}$	0.51%	$\tilde{\nu}$	$\tilde{\bar{\nu}}$	0.34%
g	g	25.35%	$\tilde{g}$	$\tilde{g}$	18.11%
g	γ	6.34%	$\tilde{g}$	$\tilde{\gamma}$	4.53%
g	Z^0	6.34%	$\tilde{g}$	$\tilde{Z^0}$	4.53%
γ	γ	0.4%	$\tilde{\gamma}$	$\tilde{\gamma}$	0.28%
γ	Z^0	0.4%	$\tilde{\gamma}$	$\tilde{Z^0}$	0.28%
Z^0	Z^0	0.4%	$\tilde{Z^0}$	$\tilde{Z^0}$	0.28%
Z^0	H	0.1%	$\tilde{Z^0}$	$\tilde{H}$	0.07%
Z^0	G	0.09%	$\tilde{Z^0}$	$\tilde{G}$	0.48%
H	H	0.06%	$\tilde{H}$	$\tilde{H}$	0.05%
G	G	0.57%	$\tilde{G}$	$\tilde{G}$	0.11%
W^-	W^+	0.4%	$\tilde{W^-}$	$\tilde{W^+}$	0.28%

Particle 1	Particle 2	4 dim	ADD n=5	ADD n=6	ADD n=7	RS
u	u	6.69×10^{0}	3.02×10^{3}	4.03×10^{3}	5.11×10^{3}	1.70×10^{2}
u	$\bar{u}$	1.97×10^{-1}	1.00×10^{2}	1.35×10^{2}	1.71×10^{2}	5.42×10^{0}
u	d	2.65×10^{0}	1.25×10^{3}	1.68×10^{3}	2.13×10^{3}	6.96×10^{1}
u	$\bar{d}$	4.69×10^{-1}	2.41×10^{2}	3.23×10^{2}	4.10×10^{2}	1.30×10^{1}
$\bar{u}$	d	1.11×10^{-1}	5.75×10^{1}	7.70×10^{1}	9.78×10^{1}	3.09×10^{0}
$\bar{u}$	$\bar{d}$	1.49×10^{-2}	8.06×10^{0}	1.08×10^{1}	1.37×10^{1}	4.26×10^{-1}
d	d	9.20×10^{-1}	4.50×10^{2}	6.02×10^{2}	7.64×10^{2}	2.47×10^{1}
d	$\bar{d}$	1.75×10^{-1}	9.07×10^{1}	1.22×10^{2}	1.54×10^{2}	4.87×10^{0}
$\bar{u}$	$\bar{u}$	8.90×10^{-3}	4.75×10^{0}	6.37×10^{0}	8.09×10^{0}	2.52×10^{-1}
$\bar{d}$	$\bar{d}$	1.35×10^{-2}	7.45×10^{0}	1.00×10^{1}	1.27×10^{1}	3.91×10^{-1}
u	g	4.82×10^{-1}	2.42×10^{0}	3.24×10^{2}	4.11×10^{2}	1.31×10^{1}
u	γ	1.61×10^{-1}	8.06×10^{1}	1.08×10^{2}	1.37×10^{2}	4.38×10^{0}
u	Z^0	1.61×10^{-1}	8.06×10^{1}	1.08×10^{2}	1.37×10^{2}	4.38×10^{0}
u	H	5.35×10^{-2}	2.69×10^{1}	3.60×10^{1}	4.57×10^{1}	1.46×10^{0}
u	G	1.07×10^{-1}	5.37×10^{1}	7.19×10^{1}	9.13×10^{1}	2.92×10^{0}
d	g	1.66×10^{-1}	8.53×10^{1}	1.14×10^{2}	1.45×10^{2}	4.59×10^{0}
d	γ	5.52×10^{-2}	2.84×10^{1}	3.81×10^{1}	4.84×10^{1}	1.53×10^{0}
d	Z^0	5.52×10^{-2}	2.84×10^{1}	3.81×10^{1}	4.84×10^{1}	1.53×10^{0}
d	H	1.84×10^{-2}	9.47×10^{0}	1.27×10^{1}	1.61×10^{1}	5.10×10^{-1}
d	G	3.68×10^{-2}	1.89×10^{1}	2.54×10^{1}	3.22×10^{1}	1.02×10^{0}
$\bar{u}$	g	1.67×10^{-2}	8.90×10^{0}	1.19×10^{1}	1.52×10^{1}	4.74×10^{-1}
$\bar{u}$	γ	5.58×10^{-3}	2.97×10^{0}	3.98×10^{0}	5.06×10^{0}	1.58×10^{-1}
$\bar{u}$	Z^0	5.58×10^{-3}	2.97×10^{0}	3.98×10^{0}	5.06×10^{0}	1.58×10^{-1}
$\bar{u}$	H	1.86×10^{-3}	9.89×10^{-1}	1.33×10^{0}	1.69×10^{0}	5.26×10^{-2}
$\bar{u}$	G	3.72×10^{-3}	1.98×10^{0}	2.65×10^{0}	3.37×10^{0}	1.05×10^{-1}
$\bar{d}$	g	2.23×10^{-2}	1.21×10^{1}	1.62×10^{1}	2.06×10^{1}	6.38×10^{-1}
$\bar{d}$	γ	7.44×10^{-3}	4.02×10^{0}	5.39×10^{0}	6.85×10^{0}	2.13×10^{-1}
$\bar{d}$	Z^0	7.44×10^{-3}	4.02×10^{0}	5.39×10^{0}	6.85×10^{0}	2.13×10^{-1}
$\bar{d}$	H	2.48×10^{-3}	1.34×10^{0}	1.80×10^{0}	2.28×10^{0}	7.08×10^{-2}
$\bar{d}$	G	4.96×10^{-3}	2.68×10^{0}	3.59×10^{0}	4.57×10^{0}	1.42×10^{-1}

Table 6.11: Continuous mass spectrum black holes. Particle 1 and Particle 2 refer to the particles produced in the decomposition of the black hole. For illustration, we considered a center of mass energy of 14 TeV with a Planck scale of 3 TeV and a minimal black hole mass of 3 TeV. Cross sections are in fb.

Particle 1	Particle 2	4 dim	ADD n=5	ADD n=6	ADD n=7	RS
l^-	l^+	9.48×10^{-3}	4.87×10^{0}	6.53×10^{0}	8.29×10^{0}	2.62×10^{-1}
ν	$\bar{\nu}$	9.48×10^{-3}	4.87×10^{0}	6.53×10^{0}	8.29×10^{0}	2.62×10^{-1}
g	g	2.76×10^{-2}	1.46×10^{1}	1.96×10^{1}	2.49×10^{1}	7.79×10^{-1}
g	γ	1.98×10^{-2}	1.04×10^{1}	1.40×10^{1}	1.78×10^{1}	5.57×10^{-1}
g	Z^0	2.54×10^{-2}	1.33×10^{1}	1.78×10^{1}	2.27×10^{1}	7.11×10^{-1}
g	H	5.62×10^{-3}	2.86×10^{0}	3.83×10^{0}	4.87×10^{0}	1.55×10^{-1}
g	G	5.62×10^{-3}	2.86×10^{0}	3.83×10^{0}	4.87×10^{0}	1.55×10^{-1}
γ	γ	3.61×10^{-3}	1.90×10^{0}	2.55×10^{0}	3.24×10^{0}	1.01×10^{-1}
γ	Z^0	5.48×10^{-3}	2.85×10^{0}	3.82×10^{0}	4.86×10^{0}	1.53×10^{-1}
γ	H	1.87×10^{-3}	9.54×10^{-1}	1.28×10^{0}	1.62×10^{0}	5.16×10^{-2}
γ	G	1.87×10^{-3}	9.54×10^{-1}	1.28×10^{0}	1.62×10^{0}	5.16×10^{-2}
Z^0	Z^0	5.48×10^{-3}	2.85×10^{0}	3.82×10^{0}	4.86×10^{0}	1.53×10^{-1}
Z^0	H	1.87×10^{-3}	9.54×10^{-1}	1.28×10^{0}	1.62×10^{0}	5.16×10^{-2}
Z^0	G	4.19×10^{-3}	2.18×10^{0}	2.93×10^{0}	3.72×10^{0}	1.17×10^{-1}
H	H	1.29×10^{-3}	6.69×10^{-1}	8.97×10^{-1}	1.14×10^{0}	3.59×10^{-2}
H	G	2.32×10^{-3}	1.23×10^{0}	1.65×10^{0}	2.10×10^{0}	6.55×10^{-2}
G	G	4.82×10^{-3}	2.50×10^{0}	3.35×10^{0}	4.26×10^{0}	1.34×10^{-1}
W^-	W^+	5.48×10^{-3}	2.18×10^{0}	3.82×10^{0}	4.86×10^{0}	1.53×10^{-1}

Table 6.12: Continuous mass spectrum black holes. Particle 1 and Particle 2 refer to the particles produced in the decomposition of the black hole. For illustration, we considered a center of mass energy of 14 TeV with a Planck scale of 3 TeV and a minimal black hole mass of 3 TeV. Cross sections are in fb.

Particle 1	Particle 2	4 dim	ADD n=5	ADD n=6	ADD n=7	RS
$\tilde{u}$	$\tilde{u}$	1.67×10^{0}	7.54×10^{2}	1.01×10^{3}	1.28×10^{3}	4.26×10^{1}
$\tilde{u}$	$\tilde{\bar{u}}$	7.45×10^{-2}	3.85×10^{1}	5.17×10^{1}	6.56×10^{1}	2.07×10^{0}
$\tilde{u}$	$\tilde{d}$	6.63×10^{-1}	3.14×10^{2}	4.19×10^{2}	5.32×10^{2}	1.74×10^{1}
$\tilde{u}$	$\tilde{\bar{d}}$	1.17×10^{-1}	6.02×10^{1}	8.07×10^{1}	1.02×10^{2}	3.24×10^{0}
$\tilde{\bar{u}}$	$\tilde{d}$	2.79×10^{-2}	1.44×10^{1}	1.93×10^{1}	2.45×10^{1}	7.73×10^{-1}
$\tilde{\bar{u}}$	$\tilde{\bar{d}}$	3.72×10^{-3}	2.02×10^{0}	2.70×10^{0}	3.44×10^{0}	1.06×10^{-1}
$\tilde{d}$	$\tilde{d}$	2.30×10^{-1}	1.20×10^{2}	1.50×10^{2}	1.91×10^{2}	6.17×10^{-2}
$\tilde{d}$	$\tilde{\bar{d}}$	6.90×10^{-2}	3.61×10^{1}	4.84×10^{1}	6.15×10^{1}	1.93×10^{-0}
$\tilde{\bar{u}}$	$\tilde{\bar{u}}$	2.23×10^{-3}	1.19×10^{0}	1.59×10^{0}	2.02×10^{0}	6.31×10^{-2}
$\tilde{\bar{d}}$	$\tilde{\bar{d}}$	3.30×10^{-3}	1.86×10^{0}	2.50×10^{0}	3.18×10^{0}	9.79×10^{-2}
$\tilde{u}$	$\tilde{g}$	4.28×10^{-1}	2.15×10^{2}	2.88×10^{2}	3.65×10^{2}	1.17×10^{1}
$\tilde{u}$	$\tilde{\gamma}$	5.35×10^{-2}	2.69×10^{1}	3.60×10^{1}	4.57×10^{1}	1.46×10^{0}
$\tilde{u}$	$\tilde{Z^0}$	5.35×10^{-2}	2.69×10^{1}	3.60×10^{1}	4.57×10^{1}	1.46×10^{0}
$\tilde{u}$	$\tilde{H}$	5.35×10^{-2}	2.69×10^{1}	3.60×10^{1}	4.57×10^{1}	1.46×10^{0}
$\tilde{u}$	$\tilde{G}$	1.07×10^{-1}	5.37×10^{1}	7.19×10^{1}	9.13×10^{1}	2.92×10^{0}
$\tilde{d}$	$\tilde{g}$	1.47×10^{-1}	7.58×10^{1}	1.02×10^{2}	1.29×10^{2}	4.08×10^{0}
$\tilde{d}$	$\tilde{\gamma}$	1.84×10^{-2}	9.47×10^{0}	1.27×10^{1}	1.61×10^{1}	5.10×10^{-1}
$\tilde{d}$	$\tilde{Z^0}$	1.84×10^{-2}	9.47×10^{0}	1.27×10^{1}	1.61×10^{1}	5.10×10^{-1}
$\tilde{d}$	$\tilde{H}$	1.84×10^{-2}	9.47×10^{0}	1.27×10^{1}	1.61×10^{1}	5.10×10^{-1}
$\tilde{d}$	$\tilde{G}$	3.68×10^{-2}	1.89×10^{1}	2.54×10^{1}	3.22×10^{1}	1.02×10^{0}
$\tilde{\bar{u}}$	$\tilde{g}$	1.49×10^{-2}	7.91×10^{0}	1.06×10^{1}	1.35×10^{1}	4.21×10^{-1}
$\tilde{\bar{u}}$	$\tilde{\gamma}$	1.86×10^{-3}	9.89×10^{-1}	1.33×10^{0}	1.69×10^{0}	5.26×10^{-2}
$\tilde{\bar{u}}$	$\tilde{Z^0}$	1.86×10^{-3}	9.89×10^{-1}	1.33×10^{0}	1.69×10^{0}	5.26×10^{-2}
$\tilde{\bar{u}}$	$\tilde{H}$	1.86×10^{-3}	9.89×10^{-1}	1.33×10^{0}	1.69×10^{0}	5.26×10^{-2}
$\tilde{\bar{u}}$	$\tilde{G}$	3.72×10^{-3}	1.98×10^{0}	2.65×10^{0}	3.37×10^{0}	1.05×10^{-1}
$\tilde{\bar{d}}$	$\tilde{g}$	1.98×10^{-2}	1.07×10^{1}	1.44×10^{1}	1.83×10^{1}	5.67×10^{-1}
$\tilde{\bar{d}}$	$\tilde{\gamma}$	2.48×10^{-3}	1.34×10^{0}	1.80×10^{0}	2.28×10^{0}	7.08×10^{-2}
$\tilde{\bar{d}}$	$\tilde{Z^0}$	2.48×10^{-3}	1.34×10^{0}	1.80×10^{0}	2.28×10^{0}	7.08×10^{-2}
$\tilde{\bar{d}}$	$\tilde{H}$	2.48×10^{-3}	1.34×10^{0}	1.80×10^{0}	2.28×10^{0}	7.08×10^{-2}
$\tilde{\bar{d}}$	$\tilde{G}$	4.96×10^{-3}	2.68×10^{0}	3.59×10^{0}	4.57×10^{0}	1.42×10^{-1}

Table 6.13: Continuous mass spectrum black holes. Particle 1 and Particle 2 refer to the particles produced in the decomposition of the black hole. For illustration, we considered a center of mass energy of 14 TeV with a Planck scale of 3 TeV and a minimal black hole mass of 3 TeV. Cross sections are in fb.

Particle 1	Particle 2	4 dim	ADD n=5	ADD n=6	ADD n=7	RS
$\tilde{l^-}$	$\tilde{l^+}$	3.86×10^{-3}	2.01×10^{0}	2.69×10^{0}	3.42×10^{0}	1.08×10^{-1}
$\tilde{\nu}$	$\tilde{\bar{\nu}}$	3.86×10^{-3}	2.01×10^{0}	2.69×10^{0}	3.42×10^{0}	1.08×10^{-1}
$\tilde{g}$	$\tilde{g}$	6.49×10^{-2}	3.39×10^{1}	4.55×10^{1}	5.78×10^{1}	1.82×10^{0}
$\tilde{g}$	$\tilde{\gamma}$	3.06×10^{-2}	1.58×10^{1}	2.12×10^{1}	2.69×10^{1}	8.49×10^{-1}
$\tilde{g}$	$\tilde{Z^0}$	3.06×10^{-2}	1.58×10^{1}	2.12×10^{1}	2.69×10^{1}	8.49×10^{-1}
$\tilde{g}$	$\tilde{H}$	2.00×10^{-2}	1.02×10^{1}	1.36×10^{1}	1.73×10^{1}	5.50×10^{-1}
$\tilde{g}$	$\tilde{G}$	1.50×10^{-2}	7.63×10^{0}	1.02×10^{1}	1.30×10^{1}	4.12×10^{-1}
$\tilde{\gamma}$	$\tilde{\gamma}$	3.16×10^{-3}	1.62×10^{0}	2.18×10^{0}	2.76×10^{0}	8.75×10^{-2}
$\tilde{\gamma}$	$\tilde{Z^0}$	3.16×10^{-3}	1.62×10^{0}	2.18×10^{0}	2.76×10^{0}	8.75×10^{-2}
$\tilde{\gamma}$	$\tilde{H}$	2.50×10^{-3}	1.27×10^{0}	1.70×10^{0}	2.16×10^{0}	6.87×10^{-2}
$\tilde{\gamma}$	$\tilde{G}$	1.87×10^{-3}	9.54×10^{-1}	1.28×10^{0}	1.62×10^{0}	5.16×10^{-2}
$\tilde{Z^0}$	$\tilde{Z^0}$	3.16×10^{-3}	1.62×10^{0}	2.18×10^{0}	2.76×10^{0}	8.75×10^{-2}
$\tilde{Z^0}$	$\tilde{H}$	3.16×10^{-3}	1.62×10^{0}	2.18×10^{0}	2.76×10^{0}	8.75×10^{-2}
$\tilde{Z^0}$	$\tilde{G}$	4.19×10^{-3}	2.18×10^{0}	2.93×10^{0}	3.72×10^{0}	1.17×10^{-1}
$\tilde{H}$	$\tilde{H}$	3.16×10^{-3}	1.62×10^{0}	2.18×10^{0}	2.76×10^{0}	8.75×10^{-2}
$\tilde{H}$	$\tilde{G}$	4.19×10^{-3}	2.18×10^{0}	2.93×10^{0}	3.72×10^{0}	1.17×10^{-1}
$\tilde{G}$	$\tilde{G}$	4.82×10^{-3}	2.50×10^{0}	3.35×10^{0}	4.26×10^{0}	1.34×10^{-1}
$\tilde{W^-}$	$\tilde{W^+}$	3.16×10^{-3}	1.62×10^{0}	2.18×10^{0}	2.76×10^{0}	8.75×10^{-2}

Table 6.14: Continuous mass spectrum black holes. Particle 1 and Particle 2 refer to the particles produced in the decomposition of the black hole. For illustration, we considered a center of mass energy of 14 TeV with a Planck scale of 3 TeV and a minimal black hole mass of 3 TeV. Cross sections are in fb.

Particle 1	Particle 2	4 dim	ADD n=5	ADD n=6	ADD n=7	RS
u	u	7.58×10^{0}	4.16×10^{3}	5.59×10^{3}	7.11×10^{3}	2.17×10^{2}
u	$\bar{u}$	1.78×10^{-1}	1.09×10^{2}	1.47×10^{2}	1.88×10^{2}	5.49×10^{0}
u	d	2.86×10^{0}	1.64×10^{3}	2.20×10^{3}	2.81×10^{3}	8.42×10^{1}
u	$\bar{d}$	5.21×10^{-1}	3.20×10^{2}	4.31×10^{2}	5.50×10^{2}	1.61×10^{1}
$\bar{u}$	d	1.10×10^{-1}	6.86×10^{1}	9.24×10^{1}	1.18×10^{2}	3.43×10^{0}
$\bar{u}$	$\bar{d}$	1.55×10^{-2}	9.99×10^{0}	1.35×10^{1}	1.72×10^{1}	4.93×10^{-1}
d	d	9.48×10^{-1}	5.59×10^{2}	7.52×10^{2}	9.58×10^{2}	2.84×10^{1}
d	$\bar{d}$	1.53×10^{-1}	9.49×10^{1}	1.28×10^{2}	1.63×10^{2}	4.75×10^{0}
$\bar{u}$	$\bar{u}$	8.13×10^{-3}	5.22×10^{0}	7.03×10^{0}	8.97×10^{0}	2.58×10^{-1}
$\bar{d}$	$\bar{d}$	1.64×10^{-2}	1.07×10^{1}	1.44×10^{1}	1.83×10^{1}	5.25×10^{-1}
u	g	4.68×10^{-1}	2.84×10^{2}	3.83×10^{2}	4.88×10^{2}	1.43×10^{1}
u	γ	5.84×10^{-2}	3.55×10^{1}	4.79×10^{1}	6.10×10^{1}	1.79×10^{0}
u	Z^0	5.84×10^{-2}	3.55×10^{1}	4.79×10^{1}	6.10×10^{1}	1.79×10^{0}
u	H	1.95×10^{-2}	1.18×10^{1}	1.60×10^{1}	2.03×10^{1}	5.96×10^{-1}
u	G	3.90×10^{-2}	2.37×10^{1}	3.19×10^{1}	4.07×10^{1}	1.19×10^{0}
d	g	1.54×10^{-1}	9.59×10^{1}	1.29×10^{2}	1.65×10^{2}	4.79×10^{0}
d	γ	1.93×10^{-2}	1.20×10^{1}	1.61×10^{1}	2.06×10^{1}	5.99×10^{-1}
d	Z^0	1.93×10^{-2}	1.20×10^{1}	1.61×10^{1}	2.06×10^{1}	5.99×10^{-1}
d	H	6.43×10^{-3}	4.00×10^{0}	5.38×10^{0}	6.86×10^{0}	2.00×10^{-1}
d	G	1.29×10^{-2}	7.99×10^{0}	1.08×10^{1}	1.37×10^{1}	4.00×10^{-1}
$\bar{u}$	g	1.45×10^{-2}	9.28×10^{0}	1.25×10^{1}	1.60×10^{1}	4.59×10^{-1}
$\bar{u}$	γ	1.81×10^{-3}	1.16×10^{0}	1.56×10^{0}	2.00×10^{0}	5.74×10^{-2}
$\bar{u}$	Z^0	1.81×10^{-3}	1.16×10^{0}	1.56×10^{0}	2.00×10^{0}	5.74×10^{-2}
$\bar{u}$	H	6.03×10^{-4}	3.87×10^{-1}	5.21×10^{-1}	6.65×10^{-1}	1.91×10^{-2}
$\bar{u}$	G	1.21×10^{-3}	7.74×10^{-1}	1.04×10^{0}	1.33×10^{0}	3.83×10^{-2}
$\bar{d}$	g	2.17×10^{-2}	1.40×10^{1}	1.89×10^{1}	2.41×10^{0}	6.91×10^{-1}
$\bar{d}$	γ	2.72×10^{-3}	1.75×10^{0}	2.36×10^{0}	3.01×10^{0}	8.64×10^{-2}
$\bar{d}$	Z^0	2.72×10^{-3}	1.75×10^{0}	2.36×10^{0}	3.01×10^{0}	8.64×10^{-2}
$\bar{d}$	H	9.05×10^{-4}	5.84×10^{-1}	7.87×10^{-1}	1.00×10^{0}	2.88×10^{-2}
$\bar{d}$	G	1.81×10^{-3}	1.17×10^{0}	1.57×10^{0}	2.01×10^{0}	5.76×10^{-2}

Table 6.15: Discrete mass spectrum black holes. Particle 1 and Particle 2 refer to the particles produced in the decomposition of the black hole. For illustration, we considered a center of mass energy of 14 TeV with a Planck scale of 3 TeV and a minimal black hole mass of 3 TeV. Cross sections are in fb.

Particle 1	Particle 2	4 dim	ADD n=5	ADD n=6	ADD n=7	RS
l^-	l^+	7.88×10^{-3}	4.84×10^{0}	6.51×10^{0}	8.30×10^{0}	2.43×10^{-1}
ν	$\bar{\nu}$	7.88×10^{-3}	4.84×10^{0}	6.51×10^{0}	8.30×10^{0}	2.43×10^{-1}
g	g	2.75×10^{-2}	1.75×10^{1}	2.35×10^{1}	3.00×10^{1}	8.66×10^{-1}
g	γ	1.05×10^{-2}	6.61×10^{0}	8.91×10^{0}	1.14×10^{1}	3.30×10^{-1}
g	Z^0	2.59×10^{-2}	1.60×10^{1}	2.15×10^{1}	2.75×10^{1}	8.01×10^{-1}
g	H	1.53×10^{-2}	9.38×10^{0}	1.26×10^{1}	1.61×10^{1}	4.71×10^{-1}
g	G	1.53×10^{-2}	9.38×10^{0}	1.26×10^{1}	1.61×10^{1}	4.71×10^{-1}
γ	γ	9.78×10^{-4}	6.09×10^{-1}	8.20×10^{-1}	1.05×10^{0}	3.04×10^{-2}
γ	Z^0	2.89×10^{-3}	1.78×10^{0}	2.40×10^{0}	3.06×10^{0}	8.93×10^{-2}
γ	H	1.91×10^{-3}	1.17×10^{0}	1.58×10^{0}	2.01×10^{0}	5.89×10^{-2}
γ	G	1.91×10^{-3}	1.17×10^{0}	1.58×10^{0}	2.01×10^{0}	5.89×10^{-2}
Z^0	Z^0	2.89×10^{-3}	1.78×10^{0}	2.40×10^{0}	3.06×10^{0}	8.93×10^{-2}
Z^0	H	1.81×10^{-3}	1.17×10^{0}	1.58×10^{0}	2.01×10^{0}	5.89×10^{-2}
Z^0	G	2.18×10^{-3}	1.34×10^{0}	1.81×10^{0}	2.30×10^{0}	6.73×10^{-2}
H	H	7.13×10^{-4}	4.39×10^{-1}	5.92×10^{-1}	7.54×10^{-1}	2.20×10^{-2}
H	G	2.65×10^{-4}	1.69×10^{-1}	2.28×10^{-1}	2.91×10^{-1}	8.38×10^{-3}
G	G	2.82×10^{-3}	1.73×10^{0}	2.33×10^{0}	2.98×10^{-1}	8.69×10^{-2}
W^-	W^+	2.89×10^{-3}	1.78×10^{0}	2.40×10^{0}	3.06×10^{0}	8.93×10^{-2}

Table 6.16: Discrete mass spectrum black holes. Particle 1 and Particle 2 refer to the particles produced in the decomposition of the black hole. For illustration, we considered a center of mass energy of 14 TeV with a Planck scale of 3 TeV and a minimal black hole mass of 3 TeV. Cross sections are in fb.

Particle 1	Particle 2	4 dim	ADD n=5	ADD n=6	ADD n=7	RS
$\tilde{u}$	$\tilde{u}$	1.89×10^{0}	1.04×10^{3}	1.40×10^{3}	1.78×10^{3}	5.42×10^{1}
$\tilde{u}$	$\tilde{\bar{u}}$	4.75×10^{-2}	2.92×10^{1}	3.93×10^{1}	5.01×10^{1}	1.46×10^{0}
$\tilde{u}$	$\tilde{d}$	7.15×10^{-1}	4.10×10^{2}	5.51×10^{2}	7.01×10^{2}	2.11×10^{1}
$\tilde{u}$	$\tilde{\bar{d}}$	1.30×10^{-1}	8.00×10^{1}	1.08×10^{2}	1.37×10^{2}	4.02×10^{0}
$\tilde{\bar{u}}$	$\tilde{d}$	2.76×10^{-2}	1.72×10^{1}	2.31×10^{1}	2.95×10^{1}	8.57×10^{-1}
$\tilde{\bar{u}}$	$\tilde{\bar{d}}$	3.87×10^{-3}	2.50×10^{0}	3.37×10^{0}	4.30×10^{0}	1.23×10^{-1}
$\tilde{d}$	$\tilde{d}$	2.37×10^{-1}	1.40×10^{2}	1.88×10^{2}	2.40×10^{2}	7.11×10^{0}
$\tilde{d}$	$\tilde{\bar{d}}$	4.11×10^{-2}	2.56×10^{1}	3.45×10^{1}	4.39×10^{1}	1.28×10^{0}
$\tilde{\bar{u}}$	$\tilde{\bar{u}}$	2.03×10^{-3}	1.30×10^{0}	1.76×10^{0}	2.24×10^{0}	6.44×10^{-2}
$\tilde{\bar{d}}$	$\tilde{\bar{d}}$	4.03×10^{-3}	2.67×10^{0}	3.59×10^{0}	4.59×10^{0}	1.31×10^{-1}
$\tilde{u}$	$\tilde{g}$	1.56×10^{-1}	9.48×10^{1}	1.28×10^{2}	1.63×10^{2}	4.77×10^{0}
$\tilde{u}$	$\tilde{\gamma}$	1.95×10^{-2}	1.18×10^{1}	1.60×10^{1}	2.03×10^{1}	5.96×10^{-1}
$\tilde{u}$	$\tilde{Z^0}$	1.95×10^{-2}	1.18×10^{1}	1.60×10^{1}	2.03×10^{1}	5.96×10^{-1}
$\tilde{u}$	$\tilde{H}$	1.95×10^{-2}	1.18×10^{1}	1.60×10^{1}	2.03×10^{1}	5.96×10^{-1}
$\tilde{u}$	$\tilde{G}$	3.90×10^{-2}	2.37×10^{1}	3.19×10^{1}	4.07×10^{1}	1.19×10^{0}
$\tilde{d}$	$\tilde{g}$	5.15×10^{-2}	3.20×10^{1}	4.31×10^{1}	5.49×10^{1}	1.60×10^{0}
$\tilde{d}$	$\tilde{\gamma}$	6.43×10^{-3}	4.00×10^{0}	5.38×10^{0}	6.86×10^{0}	2.00×10^{-1}
$\tilde{d}$	$\tilde{Z^0}$	6.43×10^{-3}	4.00×10^{0}	5.38×10^{0}	6.86×10^{0}	2.00×10^{-1}
$\tilde{d}$	$\tilde{H}$	6.43×10^{-3}	4.00×10^{0}	5.38×10^{0}	6.86×10^{0}	2.00×10^{-1}
$\tilde{d}$	$\tilde{G}$	1.29×10^{-2}	7.99×10^{0}	1.08×10^{1}	1.37×10^{1}	4.00×10^{-1}
$\tilde{\bar{u}}$	$\tilde{g}$	4.83×10^{-3}	3.09×10^{0}	4.17×10^{0}	5.32×10^{0}	1.53×10^{-1}
$\tilde{\bar{u}}$	$\tilde{\gamma}$	6.03×10^{-4}	3.87×10^{-1}	5.21×10^{-1}	6.65×10^{-1}	1.91×10^{-2}
$\tilde{\bar{u}}$	$\tilde{Z^0}$	6.03×10^{-4}	3.87×10^{-1}	5.21×10^{-1}	6.65×10^{-1}	1.91×10^{-2}
$\tilde{\bar{u}}$	$\tilde{H}$	6.03×10^{-4}	3.87×10^{-1}	5.21×10^{-1}	6.65×10^{-1}	1.91×10^{-2}
$\tilde{\bar{u}}$	$\tilde{G}$	1.21×10^{-3}	7.74×10^{-1}	1.04×10^{0}	1.33×10^{0}	3.83×10^{-2}
$\tilde{\bar{d}}$	$\tilde{g}$	7.24×10^{-3}	4.67×10^{0}	6.30×10^{0}	8.03×10^{0}	2.30×10^{-1}
$\tilde{\bar{d}}$	$\tilde{\gamma}$	9.05×10^{-4}	5.84×10^{-1}	7.87×10^{-1}	1.00×10^{0}	2.88×10^{-2}
$\tilde{\bar{d}}$	$\tilde{Z^0}$	9.05×10^{-4}	5.84×10^{-1}	7.87×10^{-1}	1.00×10^{0}	2.88×10^{-2}
$\tilde{\bar{d}}$	$\tilde{H}$	9.05×10^{-4}	5.84×10^{-1}	7.87×10^{-1}	1.00×10^{0}	2.88×10^{-2}
$\tilde{\bar{d}}$	$\tilde{G}$	1.81×10^{-3}	1.17×10^{0}	1.57×10^{0}	2.01×10^{0}	5.76×10^{-2}

Table 6.17: Discrete mass spectrum black holes. Particle 1 and Particle 2 refer to the particles produced in the decomposition of the black hole. For illustration, we considered a center of mass energy of 14 TeV with a Planck scale of 3 TeV and a minimal black hole mass of 3 TeV. Cross sections are in fb.

Particle 1	Particle 2	4 dim	ADD n=5	ADD n=6	ADD n=7	RS
$\tilde{l^-}$	$\tilde{l^+}$	2.14×10^{-3}	1.32×10^{0}	1.78×10^{0}	2.26×10^{0}	6.61×10^{-2}
$\tilde{\nu}$	$\tilde{\bar{\nu}}$	2.14×10^{-3}	1.32×10^{0}	1.78×10^{0}	2.26×10^{0}	6.61×10^{-2}
$\tilde{g}$	$\tilde{g}$	2.78×10^{-2}	1.72×10^{1}	2.31×10^{1}	2.95×10^{1}	8.60×10^{-1}
$\tilde{g}$	$\tilde{\gamma}$	2.16×10^{-2}	1.33×10^{1}	1.79×10^{1}	2.28×10^{1}	6.67×10^{-1}
$\tilde{g}$	$\tilde{Z^0}$	2.16×10^{-2}	1.33×10^{1}	1.79×10^{1}	2.28×10^{1}	6.67×10^{-1}
$\tilde{g}$	$\tilde{H}$	2.04×10^{-2}	1.25×10^{1}	1.68×10^{1}	2.15×10^{1}	6.28×10^{-1}
$\tilde{g}$	$\tilde{G}$	1.53×10^{-2}	9.38×10^{0}	1.26×10^{1}	1.61×10^{1}	4.71×10^{-1}
$\tilde{\gamma}$	$\tilde{\gamma}$	2.63×10^{-3}	1.61×10^{0}	2.17×10^{0}	2.77×10^{0}	8.09×10^{-2}
$\tilde{\gamma}$	$\tilde{Z^0}$	2.63×10^{-3}	1.61×10^{0}	2.17×10^{0}	2.77×10^{0}	8.09×10^{-2}
$\tilde{\gamma}$	$\tilde{H}$	2.63×10^{-3}	1.56×10^{0}	2.11×10^{0}	2.68×10^{0}	7.85×10^{-2}
$\tilde{\gamma}$	$\tilde{G}$	1.91×10^{-3}	1.17×10^{0}	1.58×10^{0}	2.01×10^{0}	5.89×10^{-2}
$\tilde{Z^0}$	$\tilde{Z^0}$	2.63×10^{-3}	1.61×10^{0}	2.17×10^{0}	2.77×10^{0}	8.09×10^{-2}
$\tilde{Z^0}$	$\tilde{H}$	2.63×10^{-3}	1.61×10^{0}	2.17×10^{0}	2.77×10^{0}	8.09×10^{-2}
$\tilde{Z^0}$	$\tilde{G}$	2.18×10^{-3}	1.34×10^{0}	1.81×10^{0}	2.30×10^{0}	6.73×10^{-2}
$\tilde{H}$	$\tilde{H}$	2.63×10^{-3}	1.61×10^{0}	2.17×10^{0}	2.77×10^{0}	8.09×10^{-2}
$\tilde{H}$	$\tilde{G}$	2.18×10^{-3}	1.34×10^{0}	1.81×10^{0}	2.30×10^{0}	6.73×10^{-2}
$\tilde{G}$	$\tilde{G}$	2.82×10^{-3}	1.73×10^{0}	2.33×10^{0}	2.98×10^{0}	8.69×10^{-2}
$\tilde{W^-}$	$\tilde{W^+}$	2.63×10^{-3}	1.61×10^{0}	2.17×10^{0}	2.77×10^{0}	8.09×10^{-2}

Table 6.18: Discrete mass spectrum black holes. Particle 1 and Particle 2 refer to the particles produced in the decomposition of the black hole. For illustration, we considered a center of mass energy of 14 TeV with a Planck scale of 3 TeV and a minimal black hole mass of 3 TeV. Cross sections are in fb.

Chapter 7

Conclusion

We can safely say that quantum gravity is at the forefront of interesting problems left to solve in modern physics. Gravity was the first force to be understood and analyzed at a classical level and it seems that it will be the last to be fully explored. General relativity gave us tremendous insight and a strong mathematical background on gravity and the nature of spacetime. It has withstood the test of time, under heavy scrutiny, and has predicted a series of phenomena like black holes and gravitational lensing, that still fascinate scientists. Quantum mechanics, on the other hand, explored the microscopic scale and set the pillars of modern physics with advances such as Schrodinger's equation and Heisenberg's uncertainty prnciple. Quantum gravity is the realm where these two theories are asked to solve the same problem simultaneously. How does gravity behave at the quantum level? The difficulties and obstacles of this endeavour are well documented elsewhere. Suffice it to say we still have a long way to go.

A major problem in this effort is the total lack of any experimental or observational data. For years it was believed that the energy scale where quantum gravity effects become important is of the order of 10^{18} GeV. That sort of value prohibits any work other than pure pen and paper theory building. Without any hints from observations or experiments we are left with the daunting task of accurately describing something we essentially know nothing about. All this could possibly change soon. It all began with the seminal paper [24], which started as an effort to solve the Hierarchy Problem. It effectively found a way to lower the Planck scale to a much more friendly value, a few TeV. While other papers present ways of achieving a similar result [25], [26] the main achievement is the same. Quantum gravity could be accessible with current technology. This breakthrough fueled the fire and physicists strive to discover ways to probe quantum gravity experimentally. In other words, we need to have an idea of what we are looking for in order to find it.

The purpose of the DPhil program that resulted in this thesis is to help towards this goal, by contributing to our understanding of how quantum gravity behaves and how can we expect to detect it.

We focused our efforts on quantum black holes. Black holes are not the easiest object to work with. We still struggle with some aspects of astronomical black holes, quantum microscopic black holes that work under a different set of rules should be impossible to describe. Setting aside their exotic nature, they do have a huge advantage. If theories that lower the Planck scale to a few TeV prove to be true, they are expected to form and decay in the Large Hadron Collider or cosmic rays experiments. With that in mind, we need to find a way to describe them and anticipate their behavior, even approximately.

As with almost every project in physics, our work was based on previous efforts. In chapter 2 we give a short review of the relevant literature. The first step is anticipating the creation of a black hole, something that is achieved via the hoop conjecture [22]. Then, we follow the work of Eardley and Giddings [6], which discussed the classical black hole production from the collision of two high energy particles. The estimate for the cross section is essentially the one we end up using for the quantum treatment of the problem. Stephen D. H. Hsu approached the same problem [15] by introducing a path integral formalism initially developed in [16, 17]. The cross section remained more or less the same. It is the same cross section we use in our methodology and it is considered a good approximation. We list the main properties of semiclassical black holes and how they differ from their quantum analogs. The most important difference is that while semiclassical black holes are expected to follow typical Hawking decay [20], quantum black holes are treated as non-thermal objects that will decay only to a few particles. We also report that it is highly unlikely that semiclassical black holes will be observed at the Large Hadron Collider, something that doesn't hinder us much, since this project focuses on quantum black holes. We then describe the characteristics of a quantum black hole with the most important being that it's not so much a black hole, as it is a short lived gravitationally bound state. This is a significant viewpoint we use on our work. Lastly, we give an overview of the ways to achieve a lower Planck scale, which enables us to develop our theory.

Since quantum gravity effects could be relevant to current technology we are hard pressed to find a way to bridge theory with experiment. To that end, we developed our "effective" theory as described in chapter 3. If a quantum black hole can be understood as a gravitationally bound state, which is the product of a high energy collision, then we argue

that we can treat it effectively as a field that interacts with particles of the Standard Model. Depending on the interaction that created it, the quantum black hole will be similar to what one would expect typically, be it a scalar field or a quark or some other particle. This reduces an exotic problem with an unknown underlying theory to a simple problem of quantum field theory, which we know how to work with. In lack of a complete theory of quantum gravity, we view the problem from a different angle. What goes in must come out and what comes out has to be similar to what we would normally expect. Major symmetries, and a few logical assumptions, can guide us in regard to the properties of a quantum black hole. Just because we lack a full understanding of a process doesn't mean that the rest of physics breaks down. Therefore, we approximate the quantum black hole with a Standard Model field, a process which although is an approximation, should still yield useful information. Our methodology is quite simple. We write an effective Lagrangian to describe the quantum black hole and its interactions with particles of the Standard Model and introduce a parameter c which will incorporate the fact that this is not really simple quantum field theory but contains a quantum black hole. We then calculate the production cross section and equate it to the semiclassical cross section and determine c retroactively. Having a Lagrangian to work with, we produce bounds on the Planck mass by considering phenomena such as the anomalous magnetic moment of the muon, lepton flavor violation, electric dipole moment and proton decay. The bounds we derived indicate that unless quantum gravity violates CP or baryon number quantum black holes could be accessible at the Large Hadron Collider.

During our analysis for [50], we faced the question of the fundamental nature of space and consequently the mass of a quantum black hole. It could be continuous or it could be discrete. There is extensive literature on the subject, but it is beyond the scope of this thesis to review it all. We focus on arguments regarding the existence of a minimal length. The idea of a minimal length is suggested when one tries to reconcile gravitational collapse from general relativity with the uncertainty principle from quantum mechanics. We follow a thought experiment from [72] that concludes with the notion that there is indeed a minimal length. This is irrevocably linked to a discrete mass spectrum for a quantum black hole. While the discussion on the subject is quite interesting, the scientific community has not yet decided on a definite answer to the question and both routes are being explored. Since the Planck scale is the scale where quantum black holes operate and therefore the scale we are concerned with, we are predisposed to consider both possibilities. We produce production cross sections for quantum black holes at the Large Hadron Collider for both

a continuous and discrete mass spectrum, both extrapolated from the cross section of the semiclassical case. While in chapters 3 and 5 we are leaning towards a discrete spectrum in chapter 6 we consider both cases. This way dedicated searches, based on our results, can choose according to their reasoning or even use both lines of thought.

The next logical step after the initial development of our methodology was to expose it to more realistic conditions. In a proton-proton collider, quantum black holes would be produced from the collisions of particles such as quarks and gluons. Building on the formalism developed in chapter 3, we examine three significant examples of processes that could produce a quantum black hole. First we review and refine the production of a black hole from two fermions and examine the distinction between leptons and quarks. Then we consider the result from the collision of a quark and a gluon and finally the result of a collision of two gluons. Following the line of thought presented in chapter 3, we treat the black hole as a scalar field, a quark and again a scalar field respectively. We consider the advantages of our methodology, which proves to hold up well when tested in more complicated situations. The treatment of a quantum black hole with normal quantum field theory is rather straightforward, as long as one is careful when writing the initial Lagrangian. The rest can be calculated and used in other phenomenology projects. There has been some interest expressed in our results, but it would be premature to include it in this thesis.

While our methodology seems to work well so far, we didn't stop thinking about the nature of a quantum black hole, in order to gain insight on what other lines of thought we might pursue to produce useful results. Initially we were preoccupied with the mechanics of creating a quantum black hole. We listed the assumptions and produced cross sections for several cases. Regarding the next stage of evolution of a quantum black hole we described it as a non thermal object that quickly decays into a few particles. These particles were expected to be similar to the particles that created the black hole. After all, symmetries have to be preserved. As is the habit of physicists, we expanded into a realm of physics not directly linked to our project. Specifically, we considered the possibility of a quantum black hole decaying to supersymmetric particles. The reasoning behind this consideration is that supersymmetric particles must couple gravitationally to their Standard Model partners. Using programming tools developed by Nina Gausmann we considered all types of particle interactions that could form a quantum black hole and their possible decay products. Using the cross section of the semiclassical case we produced tables of branching ratios, organized in a more compact form than the raw data.

We preserved all major symmetries and gave results for both types of spectra, continuous and discrete. Our conclusion of this work is that there is an enhancement in the cross sections involved in the detection of supersymmetric particles and that supersymmetric particles could be produced with large cross sections at the Large Hadron Collider.

Summing up the entirety of this thesis, we developed an effective way of describing and working with quantum black holes. We used our methodology on several processes and came up with useful results. Obviously, this work and the ideas presented here can be expanded to consider a broader set of problems. It is a way of working with relatively unknown objects, i.e. quantum black holes, using tools already known to us. As such, our methodology can be applied extensively. In particular, the subject of quantum black holes and their possible detection can use all the refinement and exploration it can get. We hope that the processes and results outlined here can serve the purpose of expanding our understanding of the fundamentals of nature and contribute a small building block towards a theory of quantum gravity.

Bibliography

[1] P. K. Townsend "Black Holes" arxiv:gr-qc/9707012v1
S. Carroll "Spacetime and Geometry: An introduction to General Relativity" ISBN-10: 0805387323
R. M. Wald "General Relativity" ISBN-10: 0226870332
R. M. Wald "Gravitational Collapse and Cosmic Censorship" arxiv:gr-qc/9710068
R. Beig, P. T. Chrusciel "Stationary Black Holes" arxiv:gr-qc/0502041
S. Weinberg "Gravitation and cosmology: Principles and applications of the genereal theory of relativity"
S. M. Carroll "Lecture Notes on General Relativity" arxiv:gr-qc/9712019v1
G. T. Hooft "Introduction to General Relativity"
E. Gallo, D. Marolf "Resource letter BH-2:Black Holes" arxiv:0806.2316
S. A. Hughes "Trust but verify: The case for astrophysical black holes" arxiv:hep-ph/0511217 and others. 4, 5, 6, 7, 8, 9, 10

[2] Wheeler, John A. (1990), A Journey Into Gravity and Spacetime, Scientific American Library, San Francisco: W. H. Freeman, ISBN 0-7167-6034-7 6, 8

[3] Haugen, Mark P.; C. Lmmerzahl (2001). Principles of Equivalence: Their Role in Gravitation Physics and Experiments that Test Them. Springer. arXiv:gr-qc/0103067. ISBN 978-3-540-41236-6 6

[4] Birkhoff, G. D. (1923). Relativity and Modern Physics. Cambridge, MA: Harvard University Press. 8

[5] Feynman, R. P. (1948). "The Space-Time Formulation of Nonrelativistic Quantum Mechanics". "Reviews of Modern Physics" doi:10.1103/RevModPhys.20.367.
An introduction to quantum field theory, by M.E.Peskin and H.D.Schroeder, ISBN 0-201-50397-2
Frank Wilczek (1999) "Quantum field theory", Reviews of Modern Physics 71: S83S95
Luis Alvarez-Gaume, Miguel A. Vazquez-Mozo "Introductory Lectures on Quantum Field Theory" arXiv:hep-th/0510040
S. Weinberg "The quantum theory of fields" ISBN 0521 55001 7 and others. 10, 11, 12, 13, 14, 36

[6] D. M. Eardley and S. B. Giddings, Phys. Rev. D **66**, 044011 (2002) [arXiv:gr-qc/0201034]; 10, 15, 16, 46, 78, 98

[7] R.Penrose *unpublished* (1974). 15

[8] P. D. D'Eath and P. N. Payne, "Gravitational Radiation In High Speed Black Hole Collisions. 1. Perturbation Treatment Of The Axisymmetric Speed Of Light Collision," Phys. Rev. D **46**, 658 (1992). 15

[9] P. D. D'Eath and P. N. Payne, "Gravitational Radiation In High Speed Black Hole Collisions. 2. Reduction To Two Independent Variables And Calculation Of The Second Order News Function," Phys. Rev. D **46**, 675 (1992). 15

[10] P. D. D'Eath and P. N. Payne, "Gravitational Radiation In High Speed Black Hole Collisions. 3. Results And Conclusions," Phys. Rev. D **46**, 694 (1992). 15

[11] P.D. D'Eath, *Black Holes: Gravitational Interactions*, Oxford Science Publications (1996). 15

[12] T. Banks and W. Fischler, "A model for high energy scattering in quantum gravity," arXiv:hep-th/9906038. 15

[13] S. B. Giddings and S. Thomas, "High energy colliders as black hole factories: The end of short distance physics," arXiv:hep-ph/0106219, *Phys. Rev. D.* 15

[14] P. C. Aichelburg and R. U. Sexl, "On The Gravitational Field Of A Massless Particle," Gen. Rel. Grav. **2**, 303 (1971). 16

[15] S. D. H. Hsu, Phys. Lett. B **555**, 92 (2003) [arXiv:hep-ph/0203154]. 17, 18, 46, 98

[16] T. M. Gould, S. D. H. Hsu and E. R. Poppitz, Nucl. Phys. B**437**, 83 (1995), arXiv: hep-ph/9403353. 17, 98

[17] S. D. H. Hsu, "Quantum Scattering and Classical Solutions," in *Sintra '94 NATO ASI Workshop on Electroweak Physics and the Early Universe*, arXiv:hep-ph/9406234. 17, 98

[18] M. Fabbrichesi, R. Pettorino, G. Veneziano and G. A. Vilkovisky, Nucl. Phys. B**419** 147 (1994). 18

[19] P. Kanti, "Black holes in theories with large extra dimensions: a review," *Int. J. Mod. Phys.* A **19**, 4899 (2004) [hep-ph/0402168]; 18

[20] S. W. Hawking, *Commun. Math. Phys.* **43**, 199 (1975). 18, 23, 98

[21] N. Arkani-Hamed, S. Dimopoulos, G. R. Dvali, Phys. Lett. **B429**, 263-272 (1998) [hep-ph/9803315]; 19, 21, 28, 33, 46, 58, 77, 80, 97

[22] K. S. Thorne, in Magic without Magic: John Archbald Wheeler, edited by J.Klauder (Freeman, San Francisco, 1972). 19, 49, 98

[23] L. A. Anchordoqui, J. L. Feng, H. Goldberg and A. D. Shapere, Phys. Lett. B **594**, 363 (2004) [arXiv:hep-ph/0311365]. 24

[24] N. Arkani-Hamed, S. Dimopoulos, G. R. Dvali, Phys. Lett. **B429**, 263-272 (1998) [hep-ph/9803315]; I. Antoniadis, N. Arkani-Hamed, S. Dimopoulos *et al.*, Phys. Lett. **B436**, 257-263 (1998) [hep-ph/9804398]. 19, 21, 28, 33, 46, 58, 77, 80, 97

[25] L. Randall, R. Sundrum, Phys. Rev. Lett. **83**, 3370-3373 (1999) [hep-ph/9905221]. 19, 21, 28, 33, 46, 58, 77, 80, 97

[26] X. Calmet, S. D. H. Hsu, D. Reeb, Phys. Rev. **D77**, 125015 (2008) [arXiv:0803.1836 [hep-th]]. 19, 21, 29, 33, 46, 58, 77, 80, 97

[27] X. Calmet, Mod. Phys. Lett. A **25**, 1553 (2010) [arXiv:1005.1805 [hep-ph]]. 18, 19, 22, 29, 33, 58, 77

[28] P. Meade and L. Randall, JHEP **0805**, 003 (2008) [arXiv:0708.3017 [hep-ph]]. 23, 33, 78

[29] X. Calmet, W. Gong and S. D. H. Hsu, Phys. Lett. B **668**, 20 (2008) [arXiv:0806.4605 [hep-ph]]. viii, 23, 25, 33, 56, 78, 79

[30] J. Calmet, S. Narison, M. Perrottet and E. de Rafael, Rev. Mod. Phys. **49**, 21 (1977) 24

[31] L. A. Anchordoqui, J. L. Feng, H. Goldberg and A. D. Shapere, Phys. Lett. B **594**, 363 (2004) [arXiv:hep-ph/0311365]. 24

[32] X. Calmet, M. Graesser and S. D. H. Hsu, Phys. Rev. Lett. 93, 211101 (2004) [arXiv:hep-th/0405033]. 25

[33] X. Calmet and P. de Aquino, arXiv:0906.0363 [hep-ph].

[34] E. A. Mirabelli, M. Perelstein and M. E. Peskin, Phys. Rev. Lett. **82**, 2236 (1999) [arXiv:hep-ph/9811337];

[35] D. M. Gingrich, "Quantum black holes with charge, colour, and spin at the LHC", arXiv:0912.0826. 27

[36] J. L. Feng and D. Shapere, Phys. Rev. Lett. **88**, 021303 (2001). 27

[37] L. Anchordoqui and H. Goldberg, Phys. Rev. D **65**, 047502 (2002). 27

[38] R. Emparan, M. Masip and R. Rattazzi, Phys. Rev. D **65**, 064023 (2002). 27

[39] M. Kowalski, A. RIngwald and H. Tu, Phys. Lett. B **529**, 1 (2002); J.Alvarez-Muniz, J. L. Feng,F. Halzen, T. Han and D. Hooper, Phys. Rev. D **65**, 124015 (2002); P. Jain, S. Kar, D. W. McKay, S. Panda and J.P. Ralston, Phys. Rev. D **66**, 065018 (2002). 27

[40] S. I. Dutta, M.H. Reno and I. Sarcevic, Phys. Rev. D **66**, 033002 (2002). 27

[41] L. A. Anchordoqui, J. L. Feng, H. Goldberg, and A. D. Shapere, Phys. Rev. D **68**, 104025 (2003). 27

[42] H. Yoshimo and Y. Nambu, Phys. Rev. D **66**, 065004 (2002); **67**, 024009 (2003). 28

[43] L. A. Anchordoqui, J. L. Feng, H. Goldberg, and A. D. Shapere, Phys. Rev. D **65**, 124027 (2002). 28

[44] E.G. Adelberger et al. Prog. Part. Nucl. Phys. **62**, 102 (2009). 28

[45] C. Hanhart et al. Phys. Lett. **B509**, 1 (2001). 28

[46] S. Hannestad and G. G. Raffelt, Phys. Rev. **D67**, 125008 (2003). 28

[47] L. J. Hall and D. Tucker-Smith, Phys. Rev. **D60**, 085008 (1999). 28

[48] J. Parsons and A. Pomarol Particle Data Group "Review on extra Dimensions" (2011) 29

[49] X. Calmet and M. Feliciangeli "Bounds on four-dimensional Planck mass" arxiv:0806.4304v1 29

[50] X. Calmet, D. Fragkakis and N. Gausmann, Eur. Phys. J. C **71**, 1781 (2011) [arXiv:1105.1779 [hep-ph]]; 30, 99

[51] R. Feynman, "QED: The strange theory of light and matter", Princeton University Press, ISBN 978-0-691-12575-6. 31

[52] C. Cohen-Tannoudji, "Photons and Atoms: Introduction to Quantum electrodynamics", Wiley-Interscience, ISBN 978-0-471-18433-1. 31, 32

[53] W. Greiner, J. Reinhardt, "Quantum electrodynamics". 32

[54] The ATLAS Collaboration, Observation of a new particle in the search for the Standard Model Higgs boson with the ATLAS detector at the LHC, arXiv:1207.7214. 33

[55] The CMS Collaboration, Observation of a new boson at a mass of 125 GeV with the CMS experiment at the LHC, arXiv:1207.7235. 33

[56] G. Aad *et al.* [ATLAS Collaboration], arXiv:1103.3864 [hep-ex]. 33

[57] CMS Collaboration, Search for Black Holes in pp Collisions at sqrt(s) = 8 TeV, CMS-PAS-EXO-12-009 33

[58] V. A. Kostelecky, S. Samuel, Phys. Rev. **D39**, 683 (1989). 34

[59] X. Calmet, H. Fritzsch and D. Holtmannspotter, Phys. Rev. D **64**, 037701 (2001) [arXiv:hep-ph/0103012]. 38, 40, 66

[60] G. W. Bennet et al. Phys., Rev. Latt. **89** 101804 (2002) 39

[61] T. Kinoshita and M. Nio, Phys. Rev. **D73**, 013003 (2006) 39

[62] A. Czarnecki et al. Phys. Rev. **D67**, 073006 (2003) 40

[63] M. Davier et al., Phys. J. **C71**, 1515 (2011) 40

[64] J. Prades, E. de Rafael and A. Vainshtein, arxiv:0901.0306 [hep-ph] (2009) 40

[65] A. Hoecker and W. J. Marciano "The muon anomalous magetic moment" Particle data group review (2011) 40

[66] K. Nakamura et al. (Particle Data Group), J. Phys. G **37**, 075021 (2010). 40, 42, 43, 45

[67] P. Tipler, R. Llewellyn, Modern Physics (4th edition) ISBN 0-7167-4345-0 41, 42

[68] M. Jung, "A robust limit for the electric dipole moment of the electron", arxiv:1301.1681v2 43

[69] P. Nath, P. F. Perez, "Proton stabiity in grand unified theories, in strings, and in branes", arxiv:0601023 44

[70] X. Calmet, D. Fragkakis and N. Gausmann, "Non thermal small black holes," to appear in 'Black Holes: Evolution, Theory and Thermodynamics,' to be published by Nova Publishers, arXiv:1201.4463 [hep-ph]. 48, 80

[71] G. Dvali, C. Gomez and S. Mukhanov, arXiv:1106.5894 [hep-ph]. 48, 52, 54

[72] L. J. Garay, Int. J. Mod. Phys. A **10**, (1995) 145 [arXiv:gr-qc/9403008]; C. A. Mead, Phys. Rev. **135**, (1964) B849; T. Padmanabhan, Class. Quant. Grav. **4**, (1987) L107. 48, 49, 50, 51, 55, 80, 99

[73] X. Calmet, M. Graesser and S. D. H. Hsu, Phys. Rev. Lett. **93**, (2004) 211101 [arXiv:hep-th/0405033]; Int. J. Mod. Phys. D **14** (2005) 2195 [arXiv:hep-th/0505144]; X. Calmet, Eur. Phys. J. C **54**, 501 (2008) [hep-th/0701073]. 48, 51, 55

[74] G. Dvali, C. Gomez and S. Mukhanov, "Probing Quantum Geometry at LHC", arxiv:1006.2466v1. 51

[75] G. Dvali, "Black Holes and Large N Species Solution to the Hierarchy Problem", arxiv:0706.2050. 51

[76] A. F. Ali, S. Das, E. C. Vagenas, "Discreteness of Space from the Generalized Uncertainty Principle", arxiv:0906.5396v1. 52

[77] B. Majumder, "Quantum Black Hole and the Modified Uncertainty Principle", arxiv:1105.5314v2. 48, 52

[78] J. Makela and P. Repo, Phys. Rev. D (57) 4899 (1998). 53

[79] J. D. Bekenstein, Phys. Rev. D **7** 2333 (1973) J. D. Bekenstein, Phys. Rev. D **9** 3292 (1974). 34, 54

[80] A. Kempf, G. Mangano, R. B. Mann, Phys. Rev. D **52** (1995) 1108; A. Kempf, J. Phys. A **30** (1997) 2093. 54

[81] H. Yoshino and Y. Nambu, Phys. Rev. D **67**, 024009 (2003) [arXiv:gr-qc/0209003]. Improved results have been obtained in H. Yoshino and V. S. Rychkov, Phys. Rev. D **71**, 104028 (2005) [Erratum-ibid. D **77**, 089905 (2008)] [arXiv:hep-th/0503171]. 55, 78

[82] A. Pich, "Quantum chromodynamics", arxiv:hep-ph/9505231. 59

[83] Greiner, Walter, Schfer, Andreas (1994) "Quantum Chromodynamics", Springer, ISBN 0-387-57103-5. 59

[84] Halzen, Francis; Martin, Alan (1984) "Quarks and Leptons: An Introductory Course in Modern Particle Physics", John Wiley and Sons, ISBN 0-471-88741-2. 60

[85] Creutz, Michael (1985) "Quarks, Gluons and Lattices", Cambridge University Press. ISBN 978-0-521-31535-7. 60

[86] P. Soding and G. Wolf, "Experimental Evidence on QCD", DOI:10.1146/annurev.ns.31.12081.001311. 60

[87] F. Fiedler, "Top quark production and properties at the Tevatron", arxiv:hep-ex/0506005. 60

[88] H. Fritzsch and D. Holtmannspotter Phys. Lett. B 457, 186 (1999). 66

[89] S.Dawson Nuclear Physics B359 (1991) 283-300. 67, 68

[90] Alexander Belyaev, Neil D. Christensen, Alexander Pukhov, CalcHEP 3.4 for collider physics within and beyond the Standard Model, arXiv:1207.6082 68

[91] S. Weinberg, "The quantum theory of fields, Volume 3: Supersymmetry", Cambridge University Press, Cambridge, (1999). ISBN 0-521-66000-9. 71

[92] S. P. Martin, "A Supersymmetry Primer", arxiv:hep-ph/9709356. 71, 72

[93] J. L. Feng, "Naturalness and the Status of Supersymmetry", arxiv:hep-ph/1302.6587. 71

[94] Sidney Coleman and Jeffrey Mandula (1967). "All Possible Symmetries of the S Matrix". Physical Review 159 (5): 12511256. Bibcode:1967PhRv..159.1251C. doi:10.1103/PhysRev.159.1251 72

[95] R. Haag, Sohnius, Martin, Lopuszanski, Jan T. (1975), "All possible generators of supersymmetries of the S-matrix", Muclear Physics. B **88**, 257-274. 72

[96] H. E. Haber, "RPP review: Supersymmetry, part I (Theory)". 72, 73

[97] H. Baer, R. N. Cahn, "RPP Review cross section formulae" (2012). 73, 74, 81

[98] O. Buchmueller, P. de Jong, "RPP review: Supersymmetry, part II (Experiment)". 76

[99] G. F. Giudice and A. Romanino, Nucl. Phys. B **699**, 65 (2004) [Erratum-ibid. B **706**, 65 (2005)] [hep-ph/0406088]. 76

[100] N. Arkani-Hamed and S. Dimopoulos, JHEP **0506**, 073 (2005) [hep-th/0405159]. 76

[101] X. Calmet, S. D. H. Hsu and D. Reeb, Phys. Rev. Lett. **101**, 171802 (2008) [arXiv:0805.0145 [hep-ph]]; AIP Conf. Proc. **1078**, 432 (2009) [arXiv:0809.3953 [hep-ph]]; Phys. Rev. D **81**, 035007 (2010) [arXiv:0911.0415 [hep-ph]]; X. Calmet and T. -C. Yang, Phys. Rev. D **84**, 037701 (2011) [arXiv:1105.0424 [hep-ph]]. 77

[102] S. Ferrara and A. Marrani, "Quantum Gravity Needs Supersymmetry," Contribution to the Proceedings of the International School of Subnuclear Physics, 49th Course: 'Searching for the Unexpected at LHC and Status of Our Knowledge', Erice, Italy, June 24 - July 3, 2011, arXiv:1201.4328 [hep-th]. 77

[103] P. J. Fox, D. E. Kaplan, E. Katz, E. Poppitz, V. Sanz, M. Schmaltz, M. D. Schwartz and N. Weiner, hep-th/0503249. 77

[104] X. Calmet and N. Gausmann, arXiv:1209.4618 [hep-ph]. 78, 80

[105] J. D. Jackson, D. R. Tovey "RPP Review Kinematics" (2012). 82

[106] C. G. Wohl, "RPP Review Young diagrams" (2012). x, 107, 108

Appendix A

SU(n) Multiplets

In this appendix we will briefly present the methodology for coupling multiplets, in order to write possible interactions. This was done for the possible transitions in a proton collider presented in chapter 2.

In general, an SU(n) multiplet can be identified by a set of $n-1$ nonnegative integers [106], called the label. These numbers can sometimes be derived from the geometry of the multiplet or found in the literature. For example in SU(3) an octet is labeled as (1,1) and a decuplet as (3,0). Two multiplets are conjugate to each other when their labels satisfy the relation [106] $(\alpha, \beta, \dots) \leftrightarrow (\dots, \beta, \alpha)$.

The label of a multiplet can be used to determine the number of particles through the following relations [106]:

In SU(2), $N = N(\alpha)$

$$N = \frac{(\alpha+1)}{1} \tag{A.1}$$

In SU(3) ,$N = N(\alpha, \beta)$

$$N = \frac{(\alpha+1)}{1}\frac{(\beta+1)}{1}\frac{(\alpha+\beta+2)}{2} \tag{A.2}$$

In SU(4), $N = N(\alpha, \beta, \gamma)$

$$N = \frac{(\alpha+1)}{1}\frac{(\beta+1)}{1}\frac{(\gamma+1)}{1}\frac{(\alpha+\beta+2)}{2}\frac{(\beta+\gamma+2)}{2}\frac{(\alpha+\beta+\gamma+3)}{3} \tag{A.3}$$

and so on. We notice that the numbers appear in consecutive order with no cyclicity.

In order to couple multiplets we need to introduce Young diagrams. These diagrams are schematic representations and they follow a few simple rules. They are drawn as a set of boxes arranged in rows, where each row has to be at least as long as the one beneath it. We present a label in a Young diagram in the following way [106]: the top row expands α boxes to the right past the end of the second row, the second row expands β boxes past the end of the third row and so on. For an SU(n) multiplet there will be at most n rows. Some examples for the multiplets (1,0),(0,1),(0,0),(1,1) and (3,0) are presented in figure A.1.

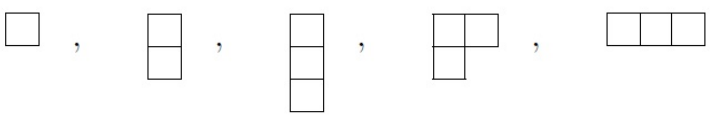

Figure A.1: Examples of Young diagrams [106].

We use Young diagrams to couple multiplets and determine what multiplets are produced. We first draw the Young diagrams for the two multiplets we want to couple, but in one of the diagrams we replace the boxes with the label numbers. For the first row α, for the second β and so on. Then we add the label numbers from the lettered diagram to the other one in any way possible as to not have more than one of each label number in each column. We do this first for the α's then the β's until we have exhausted the label numbers. This will probably give us too many diagrams. We get rid of any diagrams where the full sequence of letters formed by reading right to left in each row is not admissible. A sequence of letters a,b,c,... is admissible if "at any point in the sequence at least as many a's have occured as b's, at least as many b's have occured as c's etc" [106]. An example for two SU(3) octets is presented in figure A.2.

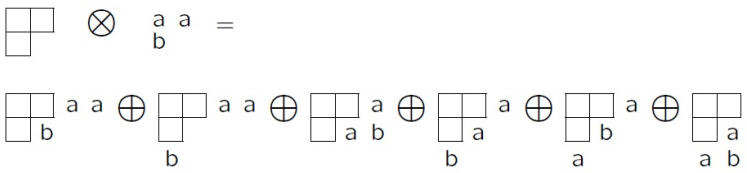

Figure A.2: Young diagrams for the coupling of two SU(3) octets [106].

The Young diagrams in figure A.2 represent the possible multiplet labels which are;

$$(1,1) \otimes (1,1) = (2,2) \oplus (3,0) \oplus (0,3) \oplus (1,1) \oplus (1,1) \oplus (0,0), \tag{A.4}$$

or as presented in chapter 2 in number of particles:

$$\mathbf{8} \otimes \mathbf{8} = \mathbf{27} \oplus \mathbf{10} \oplus \overline{\mathbf{10}} \oplus \mathbf{8} \oplus \mathbf{8} \oplus \mathbf{1}. \tag{A.5}$$